From Department of Neuroscience
Karolinska Institutet, Stockholm, Sweden

# ON STRIATUM IN SILICO

Johanna Frost Nylén

Stockholm 2023

# On striatum *in silico*

## Thesis for Doctoral Degree (Ph.D.)

By

## Johanna Frost Nylén

The thesis will be defended in public in Eva & Georg Klein lecture room at Solnavägen 9, Karolinska Institutet, on Monday, June 19th, 2023, at 9.30.

**Principal Supervisor:**
Professor Sten Grillner
Karolinska Institutet
Department of Neuroscience

**Co-supervisor(s):**
Professor Jeanette Hellgren Kotaleski
Royal Institute of Technology
School of Computer Science
and Communication
&
Karolinska Institutet
Department of Neuroscience

Professor Gilad Silberberg
Karolinska Institutet
Department of Neuroscience

**Opponent:**
Professor Dieter Jaeger
Emory University
Department of Biology

**Examination Board:**
Associate Professor Karima Chergui
Karolinska Institutet
Department of Physiology and Pharmacology

Professor Åsa Mackenzie
Uppsala Universitet
Department of Organismal Biology

Professor Per Petersson
Umeå Universitet
Department of Integrative Medical Biology

"Du ska alltid tänka:

Jag är här på jorden denna enda gång!

Jag kan aldrig komma hit igen!

Och detsamma sa Sigfrid till sig själv:

Tag vara på ditt liv!

Akta det väl!

Slarva inte bort det!

För nu är det din stund på jorden"


Från "Din stund på jorden"

av Vilhelm Moberg


Till mamma, pappa och Julia,

# ABSTRACT

The basal ganglia are a collection of subcortical nuclei involved in movement and action selection. The striatum is the main input nucleus with extensive projections from the cortex and thalamus, and dopaminergic projections from SNc and VTA. The two main cell types are the striatal projection neurons (SPNs), which are divided into the direct (dSPN) and indirect (iSPN) pathways, based on the downstream projections and the expression of dopamine D1 and D2 receptors, respectively. The remaining 5% consists mainly of GABAergic interneurons, such as parvalbumin-expressing fast-spiking interneurons (FS) and low threshold spiking interneurons (LTS). The cholinergic interneuron (ChIN) is spontaneously active and unlike the other interneurons releases acetylcholine. This thesis is focused on investigating the function of the striatum and the role of SPNs and the striatal interneurons. This is achieved by building a platform, tools, and a database of multi-compartmental models of SPN, FS, ChIN, and LTS; and through simulations systematically uncovering the roles of these striatal neuron types and external input and, more specifically, the role of neuromodulation and intrastriatal inhibition.

In Paper I, *Snudda,* a platform for simulating large-scale networks, is developed and includes multi-compartmental models of dSPN, iSPN, FS, LTS, and ChIN. The tools include methods to generate external input from the cortex and thalamus; and dopaminergic modulation from SNc. Paper II investigates the relationship between ChIN and LTS. The ChIN releases ACh, which activates both nicotinic and muscarinic receptors within the striatum. The dominating effect on LTS is inhibition caused by muscarinic M4 receptors. LTS, on the other hand, releases NO which excites ChINs. Paper II showed that the interaction between these neuromodulators could control the activity of ChIN and LTS, which are generally spontaneously active. In the subsequent Paper III, *Snudda* was complemented with the neuromodulation package called *Neuromodcell*, a Python Package, for creating models of neuromodulation, which can be included in large-scale network simulations in *Snudda.* The method of simulating neuromodulators in *Snudda* was expanded to include multiple simultaneously active modulators. This resulted in several simulations with simultaneous ACh pause with DA burst as well as an ACh burst with a DA burst. In Paper IV, the effect of intrastriatal surround inhibition on striatal activity was investigated by utilizing ablations, clustered input, dopaminergic modulation, and other features in *Snudda.* These simulations demonstrated that shunting inhibition could reduce the amplitude of corticostriatal input onto SPNs. The surround inhibition can further modulate the plateau potentials in SPNs, which is dependent on the GABA reversal. Lastly, the competition between populations of SPNs can be modified by varying the strength, size, and positions of populations. Furthermore, dopaminergic modulation can enhance the effect of dSPNs, while increasing the inhibition onto iSPNs. Overall, this thesis provides an analysis of the striatal microcircuit and a tool for further investigations of the striatum *in silico*; and demonstrates the importance to consider the different components of the striatal microcircuit and how neuromodulators can reshape microcircuits on both single neuron and network levels.

# LIST OF SCIENTIFIC PAPERS

I.  Hjorth JJJ, Kozlov A, Carannante I, **Frost Nylén J**, Lindroos R, Johansson Y, Tokarska A, Dorst MC, Suryanarayana SM, Silberberg G, Hellgren Kotaleski J, Grillner S. The microcircuits of striatum in silico. Proc Natl Acad Sci U S A. 2020 Apr 28;117(17):9554-9565. doi: 10.1073/pnas.2000671117. Epub 2020 Apr 22. PMID: 32321828; PMCID: PMC7197017.

II. **Frost Nylén J,** Carannante I, Grillner S, Hellgren Kotaleski J. Reciprocal interaction between striatal cholinergic and low-threshold spiking interneurons - A computational study. Eur J Neurosci. 2021 Apr;53(7):2135-2148. doi: 10.1111/ejn.14854. Epub 2020 Jun 26. PMID: 32511809.

III. **Frost Nylén J**, Hjorth JJJ, Grillner S, Hellgren Kotaleski J. Dopaminergic and Cholinergic Modulation of Large Scale Networks *in silico* Using *Snudda*. Front Neural Circuits. 2021 Oct 21;15:748989. doi: 10.3389/fncir.2021.748989. PMID: 34744638; PMCID: PMC8568057.

IV. **Frost Nylén J**, Hjorth JJJ, Kozlov A, Carannante I, Hellgren Kotaleski J, Grillner S. The roles of surround inhibition for the intrinsic function of the striatum, analyzed *in silico* (Manuscript)

# LIST OF SCIENTIFIC PAPERS NOT INCLUDED IN THE THESIS

- Comley, L. H., Nijssen, J., Frost-Nylen, J., & Hedlund, E. (2016). Cross-disease comparison of amyotrophic lateral sclerosis and spinal muscular atrophy reveals conservation of selective vulnerability but differential neuromuscular junction pathology. *The Journal of comparative neurology*, *524*(7), 1424–1442. https://doi.org/10.1002/cne.23917

- de la Torre-Martínez, R., Chia, Z., Tokarska, A., Frost-Nylén, J., Augustine, G. J., & Silberberg, G. (2023). Presynaptic and Postsynaptic Determinants of the Functional Connectivity Between the Claustrum and Anterior Cingulate Cortex. *BioRxiv*, 2023.03.23.533767. https://doi.org/10.1101/2023.03.23.533767

- Frost Nylén, J., Thompson, WS., Robertson. B., and Grillner. S. (in press). The basal ganglia downstream control of action – an evolutionarily conserved strategy. *Current Neuropharmacology*

# Contents

# LIST OF ABBREVIATIONS

ACh       acetylcholine

AChE      acetylcholine esterase

ChIN      cholinergic interneuron

DA        dopamine

DLS       dorsolateral striatum

DMS       dorsomedial striatum

dSPN      direct pathway striatal projection neuron

FS        fast-spiking interneuron

GABA      γ-aminobutyric acid

GPe       globus pallidus externa

GPi       globus pallidus interna

iSPN      indirect pathway striatal projection neuron

IT        intratelencephalic

LTD       long-term depression

LTP       long-term potentiation

LTS       low threshold spiking interneuron

NGF       neurogliaform

NO        nitric oxide

NOS       nitric oxide synthase

NPY       neuropeptide Y

PD        Parkinson's disease

PPN       pedunculopontine nucleus

PT        pyramidal tract

PV        parvalbumin

SABI      spontaneously active bursty interneurons

SNc       substantia nigra pars compacta

SNr       substantia nigra pars reticulata

SOM       somatostatin

TAN       tonically active neuron

ThIN      tyrosine-hydroxylase releasing interneuron

VTA       ventral tegmental area

# 1 INTRODUCTION

One of the most influential textbooks in Neuroscience is the "Principles of Neural Science", an essential and comprehensive guide for anyone studying the nervous system. On the first page of the 5th edition, there is an image of an ancient Egyptian papyrus from the 17th century BCE (Kandel et al., 2012). During this period, Ancient Egypt was ruled by the dynasties of the Middle Kingdom, which lasted between 2040 - 1640 BCE. The papyrus is called "Edwin Smith Surgical Papyrus" after Edwin Smith who bought the papyrus in Luxor in 1862 (Stiefel et al., 2006). It consists of a collection of ancient medical and surgical texts describing 48 cases, including several spinal injuries and skull fractures. The specific section in "Principles of Neural Science" describes the medical procedure following a skull fracture. The author mentions the "brain" or  (skull-organ), eight times within the text (Kandel et al., 2012; Minagar et al., 2003; Wickens, 2014) and it is the earliest reference to the brain in human history.

Today, Neuroscience is an interdisciplinary field that incorporates several academic disciplines including biology, psychology, chemistry, mathematics, engineering, and computer science. During the 1960s, the first "Departments of Neuroscience" were established at various universities including Harvard and the University of California, Irvine (as the Department of Neurobiology and Department of Neurobiology and Behavior). The aim was to gather scientists from different departments, such as Biochemistry, Anatomy, and Physiology who worked with different aspects of the nervous system. This led to many important discoveries such as critical periods during development and the first demonstration of peptidergic transmission. In 1969, the Society of Neuroscience was created and gave researchers in Neuroscience a new arena to share and develop their thoughts and ideas.

Although, the field of Neuroscience was not coined until the 1960s; many of the important contributors to Neuroscience had made their discoveries hundreds of years earlier. Galen was a Greek physician (129-210 CE) who performed dissections on various animals and non-human primates, particularly Barbary macaques, as he considered these most like human brains (Finger, 1994). His dissections included the corpus callosum, fornix, cranial nerves, ventricles, and the spinal cord. His anatomical descriptions and writings influenced the early history of Neuroscience. Galen severely criticized earlier theories on the brain, like the Aristotelian theory that the brain was a radiator for the heart, because according to Galen, if:

*"the encephalon was formed for the sake of the heat of the heart, to cool it and to bring it to a moderate temperament, is utterly absurd, since in that case Nature would not have placed the encephalon so far from the heart."*

(Burn, 2013)

The commonly held view is that the writings of Galen dominated, unchallenged, until Andreas Vesalius published "The Fabric of the Human Body" in 1543. Although, most of Galen's writings were adopted during the Middle Ages and later. Certain important contributions were made by Islamic scholars, during the Islamic Golden Age. Scholars such as Avicenna agreed with Galen but also gave important criticism on the nature of nerves and tendons and the partial crossing of the optic nerve (optic chiasma) (Sadeghi et al., 2020).

In the 1660s, Jan Swammerdam a Dutch natural scientist created the first neuromuscular preparation with a frog leg (Verkhratsky et al., 2006). Through "irritation", Swammerdam caused the muscle to contract, which was monitored via the movement of needles. However, the experimental support for the

electrical nature of nerve impulses did not arrive until 1791 when Luigi Galvani published "De Viribus Electricitatis in Motu Musculari Commentarius" (Piccolino, 1998). An important step in the history of Neuroscience and the birth of the field of electrophysiology.

Another important contribution to the field of Neuroscience came with the development and usage of microscopes. Early pioneers in the field were James Hooke (1653-1703) and Antony van Leeuwenhoek (1632-1723), the father of the microscope (Whitaker et al., 2007). The invention of the Golgi stain by Camillo Golgi in 1837 furthered the field and enabled the visualization of individual neurons in their entirety (Bentivoglio et al., 2019). Ramon y Cajal applied and refined the Golgi method and could show that neurons are separate entities. These findings became the basis for what is known as the neuron doctrine (Jones, 1999). In 1906, Golgi and Ramón y Cajal shared the Nobel Prize in Physiology or Medicine "in recognition of their work on the structure of the nervous system". This was a fundamental discovery and is one of the most important concepts in the field of Neuroscience.

These discoveries provide a short summary of the numerous contributions to the field of Neuroscience. But it is apparent that, at the start of the 20th century, it had already included techniques and concepts from a long list of disciplines including physics, anatomy, physiology, microscopy, and philosophy, demonstrating the interdisciplinary nature of the field.

## 1.1   THE HISTORY OF THE BASAL GANGLIA

One of the most serious disorders associated with the basal ganglia is Parkinson's disease (PD). The first treatments for PD became available for patients in the 1970s. A great scientific accomplishment that was dependent on several important observations and discoveries including the discovery of dopamine in the 1950s. The disease received its name from James Parkinson, who published his observations of PD in "An Essay on the Shaking Palsy" in 1817 (Parkinson, 1817). Since the identification of PD as a clinical entity occurred during the industrial revolution, the cause of PD was hypothesized, among others, to be environmental. The combination of possible environmental and genetic factors in PD is still being investigated (Ball et al., 2019), with its causes probably being a combination of both factors contributing to disease progression.

In "Did parkinsonism occur before 1817?", Stern (1989) discusses the contribution of genetic and environmental factors by investigating diseases of ancient societies. As noted by Stern, it is difficult to know if the motor deficits, which are now associated with PD, are the same as those described in the historical sources. In any case, this section will adopt a similar approach and look at "the History of the Basal Ganglia" through the lens of PD.

The available records of what ancient civilizations observed in terms of neurological disorders are, of course, limited by the discovery of the written script. In Ancient Mesopotamia, the cradle of civilization, the earliest medical texts date to the Ur III period (2112-2004 BCE) (Scurlock & Andersen, 2005). In "Diagnoses in Assyrian and Babylonian Medicine: Ancient Sources, Translations, and Modern Medical Analyses" by Scurlock and Andersen (2005), the authors analyzed ancient clay tablets dealing with medical diagnosis and prognosis. The collection of clay tablets describes the work of the *asipu*, the Babylonian doctor, and was written by the Borsippian scholar, Esgail-kin-apli during the period (1068-1047 BCE). The following passage, on Clay Tablet III, was concluded to be one of the earliest references and prognosis of PD:

*"If his head trembles, his neck and spine are bent, but he cannot stick out his tongue, his saliva flows from his mouth, his hands, legs, and feet all tremble at once and when he walks, he falls forwards, he will not get well."*

In "Did parkinsonism occur before 1817", Stern mentions other contributions from both Ancient Egypt and India. A papyrus from the 19th dynasty describes the condition of an old king:

*"A divine old age had slackened his mouth. He cast his spitle upon the ground and spat it out."*

This could be an early description of the Parkinsonian symptom of excessive drooling (Stern, 1989). Another example comes from Ayurvedic medicine. In the *Charakasamhita* compiled by Agnivesh (circa 2500 BCE), the chapter entitled *Vepathu* contains descriptions of different forms of tremor (Stern, 1989). These descriptions demonstrate that diseases such as PD and its severity were known by ancient scholars and societies, although they were not equipped to understand the causes of the disease or its treatment.

The road toward the treatment of PD was long. Milestones in this scientific journey were the identification and description of the basal ganglia, the discovery of dopamine, and the development and refinement of the L-DOPA treatment for patients.

The description of the basal ganglia as a collection of subcortical nuclei began with Galen, but the first extensive characterization was performed by Andreas Vesalius in 1543, in "De Humani Corporis Fabrica". Following Vesalius, several scientists contributed to the description of the basal ganglia nuclei including Thomas Willis (1621–1675), Niels Stensen (1638-1686), Félix Vicq d'Azyr (1748–1794), and Christian Reil (1759–1813) (Bogousslavsky & Tatu, 2017; Parent, 2012; Steiner & Tseng, 2016). In 1819-1826, Karl Friedrich Burdach published a three-part volume entitled "Vom Baue und Leben des Gehirns". In this volume, Burdach describes the dark nucleus situated caudally to the basal ganglia within the mesencephalon, the substantia nigra pars compacta (SNc); although he gave credit to Félix Vicq d'Azyr for the discovery (Parent, 2012). During the same time, James Parkinson was making his observations and attempts to understand shaking palsy. Burdach and Félix Vicq d'Azyr had already described the anatomical structure, which through neurodegeneration, leads to the symptoms of PD. But the idea of neurotransmitters and neuromodulators was still far in the future. About 100 years later, Otto Loewi discovered how nerve impulses are transmitted via chemical messengers; and identified the first neurotransmitter, acetylcholine (ACh) (McCoy and Tan, 2014). Following the discovery of ACh, the field of neurotransmitters and neuromodulators exploded (Figure 1).

The 10th discovery concerned the neuromodulator Dopamine; a monoamine with its synthetic precursor being L-DOPA. Levodopa had been isolated in 1910-13 from seedlings of Vicia faba (broad bean). In 1957, Arvid Carlsson and others made important observations, which led to the unraveling of dopamine as a transmitter in the central nervous system (Glenthøj & Fibiger, 2019). Observations during experiments with monoamine oxidase inhibitors showed that the behavioral response must be due to a monoamine. This led to further investigations into noradrenaline synthesis and its precursors, which finally led Carlsson and others to dopamine. Subsequently, L-DOPA was used on patients in several studies in Austria, Canada, and Japan between 1959 and 1962 (Glenthøj and Fibiger, 2019). Finally, L-DOPA became commercially available in the 1970s; a revolutionary discovery and treatment for patients suffering from PD (Ovallath and Sulthana, 2017).

Figure 1: The discovery of the role of substances or families of substances as neurotransmitters and neuromodulators by year. ACTH, Adrenocorticotropic hormone; CRF, Corticotropin-releasing hormone; GABA, γ-aminobutyric acid; TRH, thyrotropin-releasing hormone; CCK, Cholecystokinin; VIP, Vasoactive intestinal peptide; PDML, NPY, *Neuropeptide Y*; GHRH, Growth hormone–releasing hormone; MCH, Melanin-concentrating hormone; ANF - Artial natriuretic factor; FGF, Fibroblast growth factor; NO, Nitric oxide; PACAP Pituitary adenylate cyclase-activating polypeptide; NPFF, Neuropeptide FF (Adaptation from Sandberg & Bostrom, 2008).

Following James Parkinson's observations in 1817, it would take until Arvid Carlsson and the discovery of dopamine before the scientific community started to understand that the root and cause of the tremor observed by the *Asipu* in Babylon, in Ancient Egypt and India, by James Parkinson in England and in hospitals until this day is related to the death of neurons within the SNc. The revolutionary treatment with L-DOPA has since relieved the symptoms for millions of patients. Deep brain stimulation has been added to the possible treatments, but there is still much to understand about PD, a disease that affects about 10 million people worldwide.

## 1.2    ANATOMY OF THE BASAL GANGLIA

One of the first models of the basal ganglia is the Albin-DeLong model (Albin et al., 1989; DeLong, 1990) which incorporated the neurochemistry and the dominating anatomical connectivity available at the time. The model contains the canonical components of the basal ganglia system: the neocortex, the thalamus, the striatum, the globus pallidus externa (GPe), the subthalamic nucleus (STN), the globus pallidus interna (GPi), the substantia nigra pars reticulata (SNr), and the SNc (Figure 2).

The output of the basal ganglia is provided by the SNr and GPi. These nuclei consist of spontaneously active GABAergic neurons that provide continuous tonic inhibition onto several subcortical and brainstem nuclei including the thalamus, pedunculopontine nucleus, reticular formation, and superior colliculus (McElvain et al., 2021). The striatum is the main input nucleus and receives projections from glutamatergic neurons in almost all areas of the cerebral cortex; which are arranged in a topographical manner to different parts of the striatum (Foster et al., 2021). These projections

originate from both the intratelencephalic (IT) and pyramidal tract (PT) neurons. Most of the inputs to the striatum come from layer 5 cortical neurons (Steiner & Tseng, 2016), although recent evidence has provided further details. In a study by Muñoz-Castañeda et al. (2021), the authors demonstrated
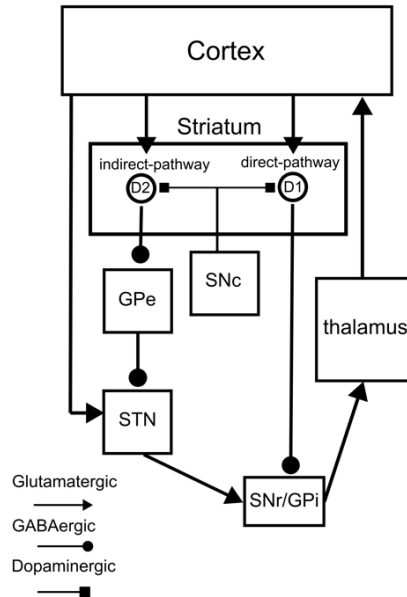


Figure 2: A diagram based on the model of the basal ganglia presented by Albin et al. 1989 and Delong, 1990. The model includes the cortex, thalamus, striatum, GPe, STN, SNr/GPi and SNc. The direct pathway project to SNr/GPi, while the indirect pathway projects to GPe and via STN to SNr/GPi. The SNr/GPi projects via the thalamus to the cortex. The SNc sends dopaminergic projections to the striatum where direct pathway SPNs express D1 receptors and indirect pathway SPNs express D2 receptors.

that the cortical input from the mouse primary motor cortex to the striatum originates from all cortical layers. This study and others also showed that all the nuclei of the basal ganglia receive direct input from cortical areas (Foster et al., 2021; Muñoz-Castañeda et al., 2021). Previously, only the "hyper-direct pathway" had been considered, providing direct cortical input to the STN (Nambu et al., 2000, 2002).

The concept of the "direct" and "indirect" pathways originates in the projections of the primary neuron type within the striatum (95%), the striatal projection neurons (SPN). These GABAergic projection neurons are divided into two types, which give rise to the "direct" pathway to SNr/GPi (dSPNs) and the "indirect" pathway via GPe (iSPNs). The activation of the "direct" SPN inhibits SNr/GPi, hence disinhibiting the downstream areas. The indirect pathway, on the other hand, inhibits GPe, which would remove its tonic inhibition onto SNr/GPi; resulting in increased inhibition of downstream areas (Figure 3). Since the addition of the "hyper-direct" pathway, several other feedback and reverberating circuits have been included in schematics of the basal ganglia (Bevan et al., 2002; Mallet et al., 2016; Nambu et al., 2002) and have been shown to contribute to the modulation of its output. The intrinsic connectivity and cortical and thalamic inputs to the basal ganglia are summarized in Figure 3, a revised schematic model of the basal ganglia.
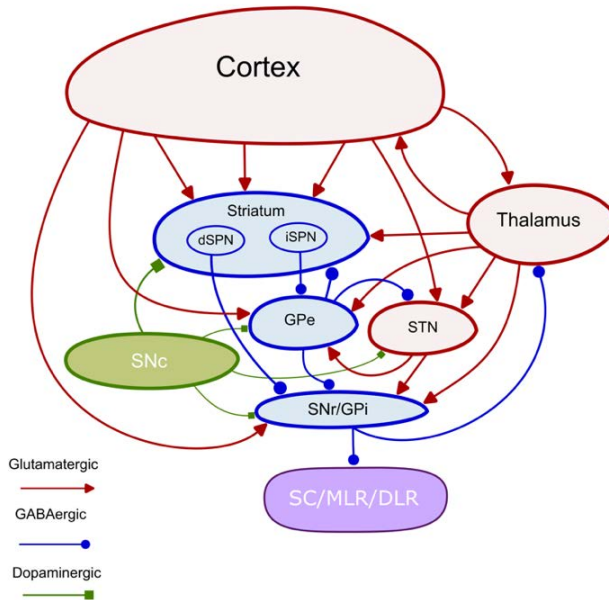
Figure 3: A diagram of the basal ganglia network. The direct pathway (dSPN) projects directly to SNr/GPi while the indirect pathway (iSPN) projects via GPe and STN to SNr/GPi. Within the indirect pathway, the GPe sends GABAergic projections back to the striatum and STN. The STN sends glutamatergic projections to SNR/GPi and GPe. The SNr/GPi have projections back to the cortex via the thalamus and to downstream nuclei like the superior colliculus (SC), mesencephalic locomotor region (MLR), and diencephalic locomotor region (DLR). The cortex and thalamus project to all nuclei and the SNc project mainly to the striatum but sends dopaminergic projections to all nuclei within the basal ganglia.

Another important component of the basal ganglia is the regional specificity. Several laboratories have shown that certain areas of for example the cerebral cortex, thalamus, SNc, and ventral tegmental area (VTA) project to specific parts of the striatum and other basal ganglia nuclei (Foster et al., 2021; Haber, 2016; Hintiryan et al., 2016; Mandelbaum et al., 2019). This is summarized for projections from the sensorimotor cortex by the diagram in Figure 4. It shows the specific organization of the input where a certain part of the cortex maps onto a specific part of the striatum. For instance, the forelimb area of the motor cortex projects to a forelimb area in the dorsolateral striatum, which via the direct pathway targets a specific part of the SNr, and through the indirect pathway, via the GPe, targets the same output area of the SNr (Grillner et al., 2020; Milardi et al., 2019; Smith et al., 2022). These recent findings emphasize the intricate and specific organization of the striatum and the entire basal ganglia.
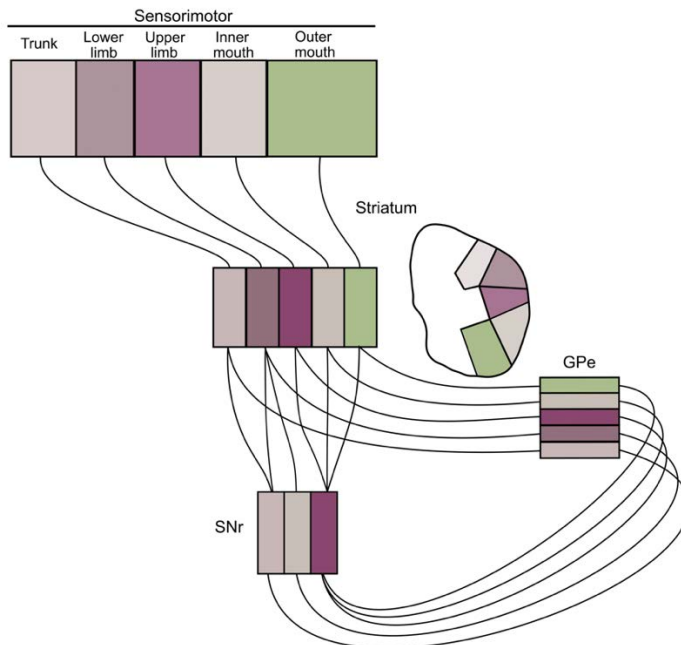
Figure 4: A diagram of the parallel loops throughout the basal ganglia. The sensorimotor cortical areas of the trunk, lower and upper limb, and inner and outer mouth project to the striatum and converge in specific areas (according to the color code). The direct and indirect pathway SPNs maintain these projections to SNr and GPe, respectively, as well as within the GPe projection to SNr. Adaptation from Foster et al. (2021)

## 1.3   DOPAMINE WITHIN THE BASAL GANGLIA

Dopamine is one of the most important neuromodulators within the basal ganglia. The actions of dopamine and other neuromodulators are mediated by G protein-coupled receptors (GPCRs) (Gurevich et al., 2016). GPCRs are characterized by seven membrane-spanning segments and interact with G proteins. The G proteins are heterotrimeric, meaning there are three subunits called alpha, beta, and gamma. These G proteins can interact with other membrane proteins, via second messengers and target specific ion channels (Rosenbaum et al., 2009).

Dopaminergic signaling is mediated by five dopamine receptors ($D_1$-$D_5$). These receptors are grouped into D1-like ($D_1$, $D_3$ and $D_5$) and D2-like ($D_2$, $D_4$) receptors. The D1-like group stimulates $G_s$ and $G_{olf}$ and activates adenylyl cyclase, elevating levels of cyclic adenosine monophosphate (cAMP) and activating protein kinase A (PKA) (Undieh, 2010). The activation of D1 receptors within dSPNs leads to a depolarization of the membrane potential due to the modulation of several ion channels (Lahiri & Bevan, 2020). The D2-like group stimulates $G_{i/o}$. $G_{i/o}$ regulates phospholipase C (PLC), targets ion channels via a membrane-delimited pathway and inhibits adenylyl cyclase (Gerfen & Surmeier, 2011), and provides a net inhibition of iSPNs (through the D2 receptors).

Dopamine is essential for the appropriate functioning of the basal ganglia. The striatum receives the densest innervation from the SNc and particularly the posterior areas of the putamen in humans (corresponding to the dorsolateral striatum (DLS) in rodents; Diedrich et al., 2020) while the GPe, SNr, and STN receive sparser innervation. In Matsuda et al. (2009), the reconstructions of single nigrostriatal dopaminergic neurons showed the extensive and dense arborization within the striatum. The estimated density of dopamine release sites is $0.14/um^3$ (Rice et al., 2011). Both D1- and D2-like dopamine receptors are expressed throughout the striatum and on the terminals of the extrinsic input. The corticostriatal terminals express both D1-like and D2-like receptors, but functional studies have shown that the D2-like effect dominates (Bamford et al., 2018). The dopaminergic terminals also express D2 dopamine receptors, which act as autoreceptors and regulate dopamine release (Ford, 2014). Furthermore, the intrastriatal surround inhibition between SPNs is regulated by dopamine. Burke & Alvarez (2022) showed that dopamine depresses the iSPN lateral inhibition through presynaptic D2 and 5-HT$_{1B}$ receptors.

The extrastriatal dopaminergic modulation in the basal ganglia is also important to consider. Both D1- and D2-like dopamine receptors are expressed pre- and post-synaptically in the GPe, GPi, SNr, and STN (Rommelfanger & Wichmann, 2010). Within the GPe, the application of dopamine agonists has been shown to increase the activity of rat GPe neurons (Napier et al., 1991). GABA release within the GPe originates from the iSPNs and local axonal collaterals (Parent et al., 2000). The GPe neurons are spontaneously active and hence the most probable source of GABA within the GPe. Microdialysis in the rat GPe showed that D2-like receptors caused a decreased GABA release while D1-like receptors caused the opposite (Floran et al., 1990). The modulation of GPe activity could also originate from STN or other extra pallidal sources. There is evidence of presynaptic modulation by dopamine receptors on glutamatergic terminals from the STN and the thalamic centromedian (CM)/parafascicular nuclei (Pf) (Rommelfanger & Wichmann, 2010). On the other hand, the effect of DA within the STN is less straightforward. Studies have indicated both increased and decreased activity of STN neurons following the application of dopamine, D1- and D2-like agonists (Rommelfanger & Wichmann, 2010). Recent evidence has concluded that dopamine increases the activity of STN neurons through a combination of D1/D5 and D2 receptor effects (Baufreton et al., 2005). This effect would consist of both a dopamine-mediated depolarization of neurons (Rice & Cragg, 2004) and a reduction in the magnitude and frequency of evoked GABA$_A$ receptor-mediated currents. In the GPi, the dominating dopaminergic effect seems to be mediated by D1 dopamine receptors, which are found presynaptically on GABAergic terminals, hence dopamine would likely cause GABA release and reduce GPi neuron activity (Rommelfanger & Wichmann, 2010). The dopaminergic modulation of the SNr has been shown to differ from the other basal ganglia nuclei. The source of dopamine within SNr could mainly be dendritic instead of axonal and another question has been whether the release is vesicular. On the other hand, the modulation seems to be mainly via D1 receptors which reduce the SNr firing by facilitating GABA transmission onto SNr neurons (Rommelfanger & Wichmann, 2010). Overall, the extrastriatal sites of dopaminergic modulation affect the response of the basal ganglia via both D1- and D2-like receptors; and investigating these sites of modulation in more detail could be beneficial for understanding the role of the basal ganglia and how the striatal activity modulates these downstream nuclei.

## 1.4   STRIATUM

The striatum is the largest nucleus within the basal ganglia, and it contains approximately x100 more neurons than the output level nuclei, the SNr and GPi (in rats). It receives several converging inputs

from the neocortex, thalamus, other basal ganglia, and brain stem nuclei (Dautan et al., 2014; Doig et al., 2014; Foster et al., 2021; Guo et al., 2015; Haber, 2016).

The striatum has an important role in motor learning, habit formation, and action execution (Grillner et al., 2020). The following is a summary of the major components of the striatal microcircuitry and how these could contribute to further the understanding of the role of the striatum in all aspects of motion.

The main cell type within the striatum is the striatal projection neurons (95 %) (Graveland & Difiglia, 1985). The remaining 5% consists of a diverse population of interneurons, which are mainly GABAergic except for the cholinergic interneuron (Figure 5).
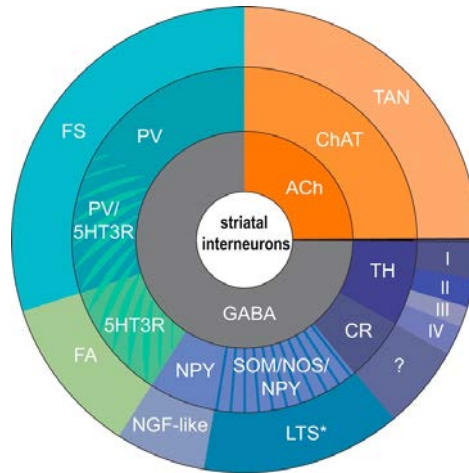


Figure 5: The diversity of interneurons within the striatum (from Burke et al. (2017)). The chart shows different classifications of interneurons within the striatum. The inner ring shows the neurotransmitter released by the striatal interneurons. The second ring shows the molecular marker(s) of each interneuron subtype – ChAT, TH, CR, SOM/NOS/NPY, NPY, 5HT3R, and PV. The outer ring shows the classification based on electrophysiological characteristics – tonically active neurons (TAN), type I-IV of ThINs, low threshold spiking interneurons (LTS), NGF-like, fast adapting (FA) interneurons, fast-spiking interneurons. FS, fast-spiking interneurons; FA, fast-adapting interneurons; NGF, neurogliaform; NPY, neuropeptide Y; SOM, somatostatin; NOS, nitric oxide synthase; CR, calretinin; TH, tyrosine-hydroxylase; ChAT, choline acetyltransferase; TAN, tonically active neurons; PV, parvalbumin.

The dorsal striatum receives input from the cortex and thalamus, which is topographically organized, as exemplified by Foster et al. (2021) (see Figure 4). This results in a subdivision of the dorsal striatum into a dorsomedial (DMS) and dorsolateral (DLS) part (Figure 6). The DMS receives input from associative cortices while the DLS receives sensorimotor input. Generally, DMS is involved in goal-directed learning while the DLS is involved in habitual learning (Yin et al., 2004, 2005, 2006).

Another subdivision of the striatum is made by the histochemically defined regions called striosomes and matrix. Most of the striatum is matrix and the striosomal compartments are intermingled (10-15%) and receive preferential input from limbic areas (Amemori & Graybiel, 2012; Brimblecombe & Cragg, 2017; Graybiel & Ragsdale, 1978). Striosomes have been defined histochemically by expressing high levels of for example µ-opioid receptor (MOR), substance P (SP), while the matrix compartment is enriched in markers like acetylcholine esterase (AChE). The striosomal projections exert direct control of dopamine neurons in the SNc and indirectly via the lateral habenula. The matrix part, via at least the DLS, is engaged in the control of movement.
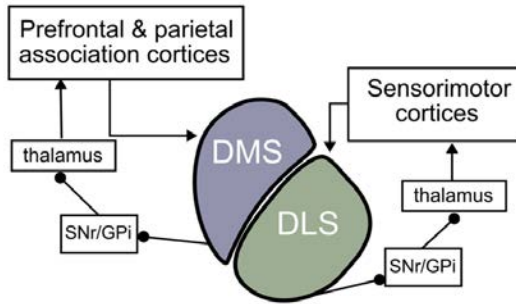
Figure 6: The subdivision of the dorsal striatum into dorsomedial (DMS) and dorsolateral (DLS). DMS receives projections from prefrontal and parietal association cortices, while DLS receives input from sensorimotor cortices (adapted from Liljeholm & O'Doherty, 2012)).

### 1.4.1 Striatal projection neurons

The striatal projection neurons have a characteristic morphology with spines and a medium-sized cell body. Hence, they have several different names including spiny projection neurons and medium spiny neurons (Figure 7) (Somogyi et al., 1981; Wilson & Groves, 1980). Figure 7 shows the dendritic arborization of a reconstructed SPN. The dendrites extend up to 250-500 μm from the soma and spines are found throughout the dendrite, starting 20-50 μm from the soma (Figure 7). (DiFiglia et al., 1976; Wilson & Groves, 1980). The two subpopulations of SPNs share some intrinsic properties but differ in several ways including the intrinsic excitability, the expression of dopamine receptors and the genes for enkephalin and substance P and the downstream targets in the basal ganglia (Gerfen et al., 1990; Gerfen & Scott Young, 1988; Le Moine & Bloch, 1995).

Without synaptic input, SPNs have a hyperpolarized membrane potential which is influenced by the inwardly rectifying $K^+$ currents, $I_{KIR}$ (Calabresi et al., 1987; Wilson, 1992). The KIR current becomes blocked as the membrane potential depolarizes, which endows the SPNs with specific properties.
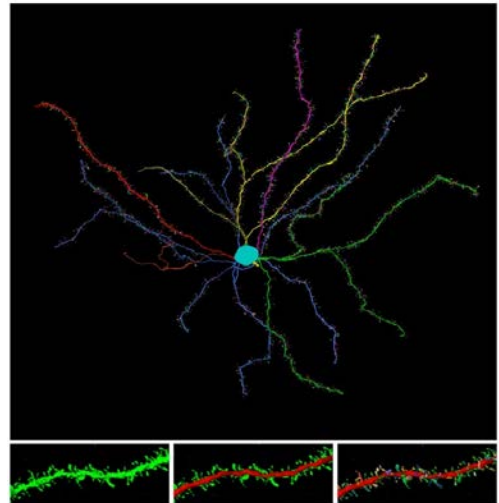


Figure 7: A detailed reconstruction of a direct pathway striatal projection neuron in the mouse striatum. A) The reconstruction shows the dendritic arborization and the density of spines along each dendrite. B) The left panel is a confocal image of a dendritic segment with spines, note the variety of spine shapes. The middle panel is a reconstruction of the dendritic segment with the dendrite in red and each spine reconstructed (other colors). The right panel is an overlay of both images and shows the detailed reconstructions of spine shapes. Courtesy of Prof. Javier DeFelipe and Dr. Lidia Blazquez Llorca.

SPNs have a characteristic delayed spike discharge which is due to the slowly inactivating A-type $K^+$ channel (Nisenbaum et al., 1994) which interacts with inward $Na^+$ and $Ca^{2+}$ currents causing a delayed spike (Wilson, 1995). Furthermore, a single SPN receives convergent input from up to 5000-10000 glutamatergic synapses (Huerta-Ocampo et al., 2014; Kincaid et al., 1998). Clustered activation of

these inputs through glutamate uncaging can induce plateau potentials in the dendrites of SPN (Du et al., 2017; Plotkin et al., 2011). In vivo, the striatum and SPNs are generally silent with short periods of activity (Klaus et al., 2019).

### 1.4.2  Interneurons

#### *Fast spiking interneurons*

The fast-spiking interneurons (FS) represent about 1% of the neurons within the striatum. The dendritic tree of FS extends 200 – 300 μm around the cell body (Steiner & Tseng, 2016) and has medium-sized soma (Figure 8). They express, like the cortical FS, parvalbumin (PV) and the striatal FS share many properties with cortical FS. The density of FS varies within the striatum, with a strong lateral to medial gradient (Berke, 2011). The FS receives fewer inputs compared to SPN, but every input forms several synapses on each FS (Bennett & Bolam, 1994).
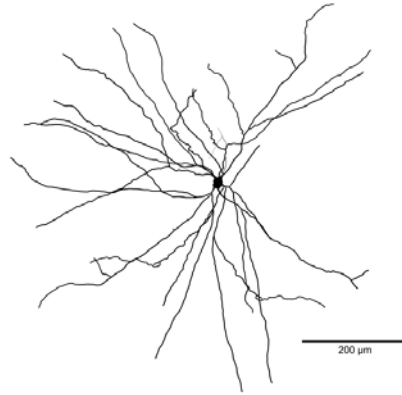
Figure 8: A reconstruction with the dendritic arborizations of a fast-spiking interneuron from Paper I.

FS-FS connections are GABAergic, and they also form gap junctions (Fukuda, 2009; Kita et al., 1990). The FS targets SPNs with high connection probability and projects to the soma and proximal part of the dendritic tree of SPNs. The connection probability to dSPN is higher than to iSPN. Additionally, SPN to SPN GABAergic synapses tend to be on the distal parts of the dendritic tree (Koos et al., 2004; Planert et al., 2010), hence the FS-SPN projection provides a strong inhibition onto SPNs. Moreover, SPNs do not provide reciprocal connections onto FS (Chuhma et al., 2011). Like cortical FS, striatal FS have very brief action potentials (Kawaguchi, 1993) and have a higher average firing rate compared to SPNs ( Plenz & Kitai, 1998).

#### *Cholinergic interneurons*

The cholinergic interneurons (ChINs) represent 1% of the striatal cell population and are spontaneously active at a low rate (Figure 9). They release acetylcholine (ACh) and can activate both nicotinic and muscarinic receptors in the postsynaptic cells (Reynolds et al., 2004). They have a large soma (Kawaguchi, 1992) and extensive axonal arborization (Suzuki et al., 2001) and receive input from both the cortex and thalamus (Ding et al., 2010; Johansson & Silberberg, 2020). The cortical input originates from several discrete regions involved in motor and sensory
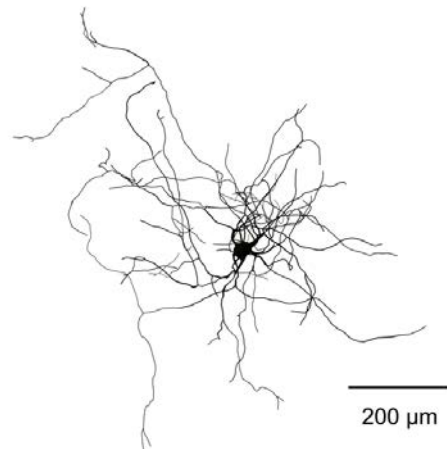
Figure 9: A reconstruction of a cholinergic interneuron from Paper I. The reconstruction shows the extensive ramification of the dendritic tree and the large-size soma.

processing as well as from limbic areas including the cingulate cortex (Guo et al., 2015; Johansson & Silberberg, 2020; Klug et al., 1998).

The spontaneous activity is intrinsically generated and independent of external input (Bennett & Wilson, 1999). The ChINs express several channels including calcium-activated potassium and calcium channel subtypes, which have been shown to contribute to its electrophysiological properties with a broad action potential, spontaneous activity, regular and irregular spiking patterns, and a prominent sag following a hyperpolarizing current injection (Bennett et al., 2000; Maurice et al., 2004; Song et al., 1998; Wilson & Goldberg, 2006). Extracellular recordings in the striatum *in vivo* identified a population of tonically active neurons (TANs), which responded to reward-relevant stimuli with a *pause*, which developed during learning (Aosaki et al., 1994; Kimura et al., 1984). TANs are now synonymous with the population of ChINs found in the striatum (Aosaki et al., 2010). The origin of the pause and its role is debated. There are, however, several mechanisms that are known to contribute to the pause response. Firstly, the pause response is not a uniform phenomenon but has many different features, which suggests some state dependence (Apicella et al., 1997; Joshua et al., 2008). Secondly, the pause response is synchronous throughout the striatum, including the pre and/or post bursts although ChINs are relatively sparsely distributed (Aosaki et al., 1994; Apicella et al., 2011; Ravel et al., 2006). However, the level of synchrony depends on the specific cue and even neighboring TANs/ChINs may not respond synchronously. Hence, the signal which is broadcast throughout the TAN/ChIN population can have varying results (Zhang & Cragg, 2017). Morris et al. (2004) demonstrated that the TAN pause is accompanied by a burst in the dopaminergic neurons, which could contribute to the inhibition via the D2 receptors expressed by ChINs. Furthermore, dopaminergic midbrain input is necessary for the development of a synchronous pause response during learning (Aosaki et al., 1994; Reynolds et al., 2004).

Manipulations of ChIN activity to replicate the pause have provided clues. Inhibition of ChINs via halorhodopsin (eNpHR) (*in vitro*) caused a decrease in the excitability of both dSPNs and iSPNs (Maurice et al., 2015; Zucca et al., 2018). In Zucca et al. (2018), it was further shown that the inhibition increased the duration of down states (anesthetized mice). However, in freely moving mice, inhibition of ChINs did not have any effect on SPN activity (English et al., 2011), except for an inhibition, which was induced following ChIN rebound excitation at the end of eNpHR-induced hyperpolarization. Theoretically, the synchronized changes in ChIN activity with burst and pause responses would provide periods of high and low levels of ACh. During the pause, AChE, the enzyme breaking down ACh, should have had time to clear ACh due to its high expression and fast catabolic activity (Zhang & Cragg, 2017). The fluctuations of the ACh levels could provide a time window for integration and modulation of dopamine release (Aosaki et al., 2010; Cragg, 2006; Goldberg & Reynolds, 2011; Morris et al., 2004).

### *Low threshold spiking interneurons*

Low threshold spiking interneurons (LTS) have a sparse arborization of both the dendrites and the axon, of which the latter reaches up to 1 mm within the striatum. They have a high input resistance, are spontaneously active, and target the distal dendrites of SPNs. The population of LTS can be further subdivided based on the expression of somatostatin (SOM), nitric oxide synthase (NOS), or neuropeptide Y (NPY). The extrinsic input to LTS comes from the cortex and activation of cortical input can cause both spikes and plateau potentials (Assous et al., 2017a; Choi et al., 2019; Ibáñez-Sandoval et al., 2011; Kawaguchi, 1993). The thalamic input to LTS is not significant (Assous et al., 2017b; Tepper et al., 2018) but instead LTS receives disynaptic inhibition from the thalamus mediated

via tyrosine hydroxylase-expressing interneurons (ThINs). Holly et al. (2021) showed that the LTS synapse onto dopaminergic terminals and could, *in vitro*, directly, and locally reduce striatal dopamine via $GABA_B$ signaling and mediate goal-directed learning.
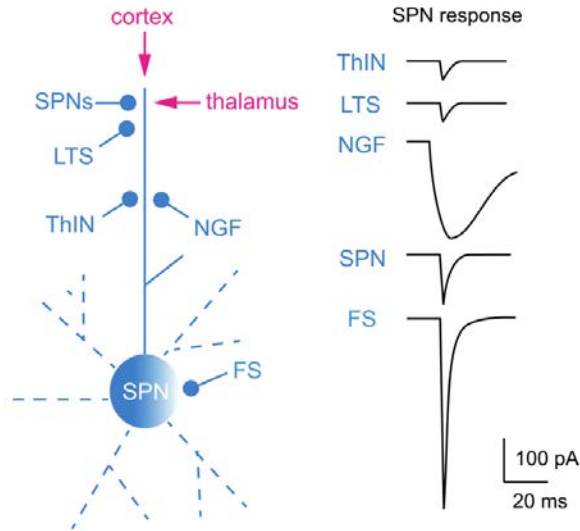


Figure 10: The striatal microcircuitry and the diversity of GABAergic inputs. The left panel shows the distribution of synapses on an SPN from different interneurons and SPNs. The right panel shows the diversity of the time-course and the amplitude of unitary GABAergic IPSC to the SPN from LTS, NGF, SPN, and FS. Adapted from Gittis & Kreitzer, 2012). FS, fast-spiking interneurons; SPN, striatal projection neurons; NGF, neurogliaform; LTS, low-threshold spiking interneurons; ThIN, tyrosine hydroxylase-expressing interneurons.

### Other interneurons

The number of GABAergic interneuron subtypes has expanded markedly as summarized by Tepper et al. (2010, 2018). Due to the low percentage of each type of interneuron in the striatum, studies which extensively characterized them are rare (Tokarska & Silberberg, 2022). Burke et al. (2017) showed that the different interneuron subtypes can be grouped by the neurotransmitter and the expression of different markers (see Figure 5). In this chart, FS, LTS, and ChIN are presented as the three largest groups. The FS group can be subdivided based on the co-expression of 5HT3R and another group called FA (fast adapting) that shares this marker with FS. ThINs are GABAergic and provide disynaptic inhibition onto LTS. Spontaneously active bursty interneurons (SABI) were characterized by Tepper et al. (2018) and exhibit burst firing and show spike frequency adaptation. Figure 10 displays the diversity of the striatal interneuron population (Gittis & Kreitzer, 2012) and the impact on SPNs. Each interneuron, which synapses onto SPNs, has its specific dynamics of the GABAergic IPSCs and short-term plasticity. This further enhances the role of SPNs as integrators of excitatory and inhibitory inputs within the striatum while also providing the sole output.

### 1.4.3 Projections to the striatum

Several tracing studies have demonstrated that the striatum receives input from several brain areas including the cortex, thalamus, midbrain nuclei, pedunculopontine nucleus (PPN), and GPe (Assous et al., 2019; Guo et al., 2015; Hunnicutt et al., 2016). Some of these have been characterized extensively (Johansson & Silberberg, 2020; Mandelbaum et al., 2019), and others have been identified recently and are currently under investigation (Assous et al., 2019; Mallet et al., 2016).

#### *Corticostriatal inputs*

The cortex projects in a topographic manner to the whole striatum. The cortical projections originate from several layers, but the majority come from pyramidal neurons in layer 5 (Johansson & Silberberg, 2020; Muñoz-Castañeda et al., 2021). These pyramidal neurons can be divided into either IT- or PT-type. The IT-type projects bilaterally to the striatum without any projections to downstream nuclei. The PT-type has extensive projections not only to the striatum but also to other nuclei within the basal ganglia and further into the brainstem. The cortical projections target the striatal neurons in a cell-type-specific manner with varying strength (Johansson & Silberberg, 2020).

#### *Thalamostriatal inputs*

The thalamostriatal projections to the striatum originate in mainly two thalamic nuclei – CM and Pf. Mandelbaum et al. (2019) showed that the medial-central-lateral Pf projections targeted different parts of the striatum. This projection was also neuron-type specific as other studies have also shown. The Pf terminals are extensive and cover a large striatal area, while the CM terminals are more clustered (Steiner & Tseng, 2016). The CM nucleus of the thalamus targets SPNs, while the Pf targets both SPNs and interneurons (Lapper & Bolam, 1992; Mandelbaum et al., 2019; Rudkin & Sadikot, 1999).

#### *Pedunculopontine nucleus and laterodorsal tegmental nucleus*

The striatum receives glutamatergic and cholinergic projections from the pedunculopontine nucleus (PPN) and dorsolateral tegmental nucleus (LDT). Several laboratories have characterized these projections *in vitro* and *in vivo*. They have shown that the cholinergic projections are limited to the anterior striatum and are topographically organized. The activation results in the excitation of ChINs while SPNs are inhibited. On the other hand, the glutamatergic projections target the striatal interneurons but not the SPNs (Assous et al., 2019; Dautan et al., 2014, 2020).

### 1.4.4 Pre- and postsynaptic modulation in the striatum

There are a wide variety of G-protein mediated receptors expressed specifically by the different cell types in the striatum, for muscarinic, dopaminergic, $GABA_B$ receptors, and the ionotropic nicotinic receptors (see Table 1). Table 1 also includes the receptors expressed on the cortico- and thalamostriatal terminals and the dopaminergic terminals. The following section will discuss the different transmitters and their effects with a focus on acetylcholine, dopamine, and nitric oxide.

#### 1.4.4.1 Acetylcholine
##### *Acetylcholine release*

The ChINs are the intrinsic source of ACh in the striatum, with PPN/LDT providing an additional source (Dautan et al., 2020; Mallet et al., 2019). ACh is produced by choline and acetyl-CoA via the enzyme, choline acetyltransferase (ChAT). After release, the ACh molecules are degraded by

acetylcholinesterase (AChE) which releases choline, which is taken up by the terminals via NaCl transporters. The estimated number of molecules per synaptic vesicle varies (1 000 – 10 000), while each AChE molecule can degrade 25 000 ACh molecules per second, which provides a limit to the diffusion of ACh within the extracellular space (Colovic et al., 2013).

## *ACh innervation and acetylcholinesterase*

In the striatum, the density of ChAT-positive varicosities is high and estimated to be ~ 1-2 $10^8$ varicosities per mm$^3$ (Lim et al., 2014), which is similar to the dopaminergic innervation. On the other hand, the striatum has a high expression of AChE (except for the striosomes), which implies that the basal level of ACh is kept low although ChINs are spontaneously active and therefore would release ACh continuously.

Table 1: The expression of muscarinic receptors within the striatum.

| | dSPN | iSPN | FS | LTS | ChIN | Corticostriatal terminals | Thalamostriatal terminals | Dopaminergic terminals |
|---|---|---|---|---|---|---|---|---|
| Metabotropic | | | | | | | | |
| M1 | + | + | | + | | | | |
| M2/M4 | + | | | + | +$^S$ | + | + | + |
| D1 | + | | + | + | | | | |
| D2 | | + | | | + | + | + | + |
| GABA$_B$ | +* | +* | | | | + | + | + |
| Ionotropic | | | | | | | | |
| nAChR | | | + | | | + | + | + |

\* mostly presynaptically in the striatum, GPe, and GPi/SNr, respectively. S, extrasynpatically.

## *Muscarinic receptors*

The metabotropic muscarinic receptors exist in five subtypes divided into two groups, although the $M_1$ (group I) and $M_{2/4}$ (group II) subtypes constitute the majority in the striatum. The group I muscarinic receptors ($M_1$, $M_3$, $M_5$) are coupled to $G_{q/11}$ activates phospholipase (PLC) and protein kinase C (PKC), which increases the production of diacylglycerol (DAG) and inositol triphosphate ($IP_3$), leading to several subcellular changes, such as intracellular calcium release. The group II ($M_2$, $M_4$) muscarinic receptors are coupled to $G_{i/o}$. The $G_{i/o}$ inhibits adenylyl cyclase (AC) and closes calcium channels (Cav2) and opens Kir3 (via Gβ and a membrane-delimited pathway). The ChINs express M2 receptors extrasynaptically, which act as auto-receptors (Bernard et al., 1992) and control ACh release (Table 1). The M1 receptor is found on dendritic spines and extrasynaptically on both subtypes of SPNs (Hersch & Levey, 1995; Yan et al., 2001) and increases neuronal excitability by modulating sodium and potassium currents (Akins et al., 1990; Galarraga, Hernández-López, et al., 1999; Shen et al., 2007). Additionally, M1 receptors regulate the L-type calcium channels, which interact with the release of endocannabinoids. Endocannabinoids are involved in long-term depression in the striatum at corticostriatal synapses (Wu et al., 2015). The M4 receptor is mainly found on dSPNs and provides inhibitory modulation (Hernández-Flores et al., 2015).

## *Fast spiking interneurons*

The FS provides feed-forward inhibition onto SPNs and receives strong cortical input. The synaptic connection between ChINs and FS is weak in comparison to other nicotinic interactions within the striatum (Chang & Kita, 1992; English et al., 2011; Koós & Tepper, 2002). FS also express presynaptic

muscarinic receptors which have been shown to attenuate the GABAergic inhibition onto SPNs (Koós & Tepper, 2002).

### Low threshold spiking interneurons

The LTS express both M1 and M4 receptors, whereas the M1 receptor mainly influences spiking activity (Melendez-Zaidi et al., 2019). The effect of M4 receptor activation is prominent following burst activation of ChINs, where it causes inhibition of the LTS spontaneous activity (Paper II). The LTS can also modulate ChINs via GABAergic and nitric oxide (NO) release. The NO release causes a prolonged depolarization of ChINs, which lasts >10 s (Elghaba et al., 2016). This provides a mechanism for regulating NO and ACh levels in the striatum over longer time scales, which was demonstrated in Paper II. Additionally, Blomeley et al. (2015) showed that NO and nicotinic receptors (nAChRs) modulate short-term synaptic facilitation at corticostriatal synapses. Following the application of NO donor, SNAP, paired-pulse facilitation was replaced by paired-pulse depression at iSPN synapses, and this mechanism depended on nAChRs.

### GABAergic interneurons

Several of the other GABAergic interneurons, such as ThINs, are activated by nAChR (Dorst et al., 2020; English et al., 2011; Luo et al., 2013). The activation of these receptors causes a decrease in activity throughout the striatum (Plata et al., 2013). These interneurons target different parts of the dendritic tree of SPNs and the striatal microcircuitry. The recurrent disynaptic network (Dorst et al., 2020; Sullivan et al., 2008) depends on β2-containing nAChRs (as are the majority of nAChRs in the striatum) which are prone to desensitization (Giniatullin et al., 2005). The extent of desensitization will depend on the tonic level of ACh present in the striatum. Although, the presence of AChE would suggest that the level of ACh is kept low; increased levels of ACh could still lead to desensitization, which would modulate the effect of the intrastriatal GABAergic inhibition.

#### 1.4.4.2 Interactions between dopamine and acetylcholine

The interaction between DA and ACh occurs at several sites within the striatum. Firstly, the muscarinic and dopaminergic receptors are expressed on several cell types and terminals. In dSPNs and iSPNs, $M_1$ and $M_4$ receptors (in dSPN) are coexpressed with D1 or D2 receptors; and the receptors are in some cases reported to modulate the same ion channels (Lindroos & Hellgren Kotaleski, 2021). Furthermore, the plasticity mechanisms within the striatum depend on the level of dopamine and ACh. M1 activation is required for corticostriatal long-term potentiation (LTP) in the SPN (Calabresi, et al., 1999; Centonze et al., 1999). Centonze et al. (1999) showed that NO together with M1 activation has a permissive role in corticostriatal plasticity via the regulation of NMDA- and AMPA-receptor currents. Additionally, during a pause, M1 activation decreases, which increases endocannabinoid production (Tozzi et al., 2011; Wang et al., 2006).

Furthermore, the dopaminergic receptors modulate the striatal plasticity via direct modulation of SPNs or indirectly via D2 receptors on ChINs (Augustin et al., 2018; Shen et al., 2007; Surmeier et al., 2014). And simulations of dopaminergic and muscarinic receptors have shown that the levels of ACh and dopamine determines the level of PKA in SPNs (Nair et al., 2015). During basal conditions, D1 receptor activation of PKA production is inhibited by the M4 receptor. Hence, the synchronous pause of ChINs and a burst of dopaminergic neurons can be crucial for the induction of LTP at corticostriatal synapses. A similar mechanism could occur in iSPNs, where the D2 receptor would inhibit PKA production, and a dopamine dip would disinhibit the pathway.

### 1.4.4.3   Nitric oxide

NO is a gaseous transmitter and is produced following the conversion of L-arginine to L-citrulline and can pass through the cell membrane. The conversion is dependent on the presence of neuronal NOS (nNOS) and NADPH. The release of NO is dependent on the expression of the synthase and the influx of calcium via NMDA receptors (Garthwaite, 2008). NO has been associated with different forms of plasticity and causing either LTP or long-term depression (LTD). Within the striatum, LTS express nitric oxide synthase (Beatty et al., 2012). High-frequency stimulation of frontal cortical areas causes the release of NO within the striatum, a process that is NMDA-dependent (Ondracek et al., 2008; Sammut et al., 2006, 2007). NO is involved in synaptic plasticity within the striatum where LTS induces a NO-dependent LTD at glutamatergic synapses (Calabresi et al., 1999; Rafalovich et al., 2015).

### 1.4.4.4   Other neuromodulators

Neuromodulation changes how neurons interact, which allows for anatomically defined networks to reconfigure. The effects of neuromodulation are dynamic and can alter every aspect of neuronal and synaptic function hence providing neural circuits with enormous flexibility (Avery & Krichmar, 2017; Nadim & Bucher, 2014). The striatum is no exception. Dopamine, ACh, and NO are just three of the neuromodulators from either extrinsic or intrinsic sources. Serotonin is released within the striatum from projections from the raphe nucleus. The serotonergic modulation within the striatum affects SPNs, several of the interneurons, and glutamatergic and GABAergic synapses (Benarroch, 2009). Histamine is another neuromodulator that is released in the striatum from projections from the tuberomammillary nucleus (Bolam & Ellender, 2016). Additionally, recent evidence has shown that adenosine affects the level of PKA within the SPNs (Ma et al., 2022). The dSPNs express substance P and iSPNs express enkephalin, which are evolutionarily conserved throughout the vertebrate phylum (Grillner & Robertson, 2016). The significance of this is still not apparent. To consider these effects individually and simultaneously will be important, especially to be able to investigate their impact on striatal activity.

### 1.4.5   The role of the striatum in the control of movement

The basal ganglia have an important role in movement control and action selection. The striatum via the direct and indirect pathways can modulate the activity within the SNr and GPi to disinhibit downstream motor centers. The idea that the direct and indirect pathways are prokinetic and anti-kinetic originated from the box-and-arrow diagram of Albin-DeLong (see Figure 2). Although, technical improvements have brought new evidence, which has revealed a more complicated interaction with consequences for how the striatum behaves and what role it has during movement.

Firstly, the prokinetic and antikinetic idea would predict that iSPN would be inactive during movement. Recent studies show that both dSPNs and iSPNs are active during behavior (Cui et al., 2013; Jin et al., 2014; Tecuapetla et al., 2016; Yttri & Dudman, 2016). Yttri and Dudman (2016) showed that manipulation of either the direct or indirect pathway would affect the speed of the subsequent trial. Secondly, the idea that iSPNs would suppress competing movements has been challenged. Both dSPNs and iSPNs seem to be action-specific and correlate with task components hence not merely due to suppression of other movements (Klaus et al., 2017; Markowitz et al., 2018; Parker et al., 2018). Klaus et al. (2017) showed that the decoding of SPN ensemble activity was related to the similarity between

the behaviors. Another important component to consider is the anatomy and topographically defined subdivisions of the striatum. It is important to consider if the study focused on the DLS or DMS. As the DLS receives sensorimotor input and projects in a topographic manner (Foster et al., 2021) (Foster et al., 2021) to GPe and SNr, while the DMS receives its input mostly from the prefrontal and associative cortices and is associated with goal-directed behavior.

Dopamine is generally associated with reward and reinforcement learning, but dopamine neurons are also activated by salient stimuli particularly those in the SNc. As a movement is initiated it is generally preceded by a dopamine burst (da Silva et al., 2018) which will enhance the activity of dSPNs with D1 receptors and inhibit the iSPNs. Often dSPNs (D1) and iSPNs (D2) are coactivated initially but dSPNs tend to remain active, while the iSPNs fade out.

In conclusion, the examples above demonstrate that the role of the striatum in movement control is more complicated than the arrow-and-box diagrams. But these have been useful models and have provided hypotheses to challenge and create new experiments and research questions. Hence, they have contributed to several notable conclusions about the role of the striatum. The populations/ensembles of both dSPN and iSPN are active during behavior. These are coordinated both in spatial and temporal terms and this is important for action initiation. As outlined in the previous sections, the intrastriatal inhibition arises from a collection of interneurons and the axon collaterals of SPNs (Dobbs et al., 2016; Klaus & Plenz, 2016; Tecuapetla et al., 2016). The SPNs process both glutamatergic and GABAergic input from a convergent set of intrastriatal and extrastriatal sources. In conjunction with the numerous neuromodulators, the SPNs integrate these inputs and provide modulation of downstream nuclei. Hence, on both the single neuron and the population level, the SPN must respond to specific combinations of inputs to cause the appropriate action outcome.

## 1.5    BUILDING NETWORKS OF MULTI-COMPARTMENTAL MODELS

The previous sections have focused on the knowledge and questions within the field of basal ganglia research, and especially the striatum. To tackle the multiple-level nature of these questions, a complementary method to neurobiological experimentation is to make simulations of the operation of these circuits based on detailed experimentation. In the forthcoming sections, the background and considerations involved in building networks of multi-compartmental models are discussed. These include modeling voltage-gated ion channels, modeling synapses, the reconstruction of neuronal morphologies, optimization of multi-compartmental models, dendritic processing, and finally the challenges of large-scale network simulations.

### 1.5.1    Modeling voltage-gated ion channels

The seminal work for understanding the role of ion channels in membrane excitability was the discovery of the role of voltage-gated sodium and potassium conductances in the generation and propagation of the action potential in the squid axon (Hodgkin & Huxley, 1952). Hodgkin and Huxley and others demonstrated that the sodium and potassium conductances could be activated and inactivated by the membrane potential. The idea of a "Na channel" and a "K channel" was still at the time not an accepted phenomenon. They also modeled the sodium and potassium currents, in a way that had a major and lasting impact on the field (Hille, 2001). In several critical experiments using tetrodotoxin (TTX) and tetraethylammonium (TEA), it was shown that the sodium and potassium currents were separate entities (Hille, 2001). The idea of a pore, which allows the passage of Na or K ions was finally proven by the single channel recordings of Neher & Sakmann (1976) which was made possible by their development

of the patch clamp technique. The development of the patch clamp technique and the single channel recordings further showed the behavior of single ion channels. Since then, several different types of voltage-gated ion channels have been identified. These contribute to the rich repertoire of electrical behavior observed in neurons (Toledo-Rodriguez et al., 2005) with voltage-gated ion channels which are selectively permeable to $Na^+$, $K^+$, $Ca^{2+}$, and $Cl^-$. The following section will focus on voltage-gated sodium, calcium, and potassium channels.

## 1.5.2  Voltage-gated sodium channels

The group of voltage-gated sodium channels is comparatively small. The channel consists of one α and one or two β subunits. The α subunit forms the pore and the β subunit is auxiliary. The pore-forming α subunit consists of seven transmembrane (TM) domains. The 4 TM domain is voltage-sensing due to a positive charge (amino acids). There are currently nine varieties of the α subunits of the $Na_v$ channel. The groups can further be divided into TTX-resistant and TTX-sensitive (Hille, 2001). Hodgkin and Huxley (1952) characterized the fast sodium currents by observing how the membrane potential affects sodium conductance ($g_{Na}(V)$). They hypothesized that the regulation was due to a collection of gating particles within the membrane (Hodgkin and Huxley, 1952). The sodium conductance was described by two gating mechanisms:

$$\frac{dm}{dt} = \alpha_m(V)(1-m) - \beta_m(V)m$$

$$\frac{dh}{dt} = \alpha_h(V)(1-h) - \beta_h(V)h$$

The non-linear behavior of the sodium current was hence described by:

$$g_{Na} = \overline{g}_{Na}m^3 h(V - V_{Na})$$

## 1.5.3  Voltage-gated calcium channels

Calcium channels were among the first to evolve and can be subdivided into three broad groups: L (class 1), N, P/Q, R (class 2), and T (class 3) channels (Catterall, 2011). The first two groups (1, 2) are mostly high voltage-activated, like within the action potential. The L-type received the name due to the long-lasting inward currents, compared to the fast decaying (T-type). The third group can be activated by low-voltage changes (Zamponi et al., 2015). The $Ca^{2+}$ entry can trigger secondary activation of calcium-activated potassium channels (such as BK and SK channels) that contribute to the afterhyperpolarization following the action potential (Guéguinou et al., 2014). At the synaptic junction, the $Ca^{2+}$ entry triggers the release of transmitters from the synaptic vesicles (Dolphin & Lee, 2020).

## 1.5.4  Voltage-gated potassium channels

The voltage-gated potassium channel group has diversified the most, with 12 subfamilies (Kv1-12). The $K_v$ channel consists of four α-subunits which form the pore with additional auxiliary β-subunits which

can further specify its function and location within the neuron (Kim & Nimigean, 2016). The α-subunit contains six transmembrane segments (S1-S6), and S1-S4 constitutes the voltage sensor (Yellen, 2002). The importance of voltage-gated potassium channels was demonstrated by Hodgkin & Huxley's experiments with the squid axon. They used a similar formalism to describe the delayed rectifying potassium current, but observed important differences in the gating mechanism:

$$g_K = \overline{g}_K n^4 (V - V_K)$$

Later, the gating variables were shown to be equivalent to activating and inactivating gates within the structure of the voltage-gated sodium and potassium ion channels. The characterization of the action potential in the squid axon is summarized by the following equations:

$$C_m \frac{dV}{dt} = -\overline{g}_L(V - V_L) - \overline{g}_K n^4(V - V_K) - \overline{g}_{Na} m^3 h(V - V_{Na})$$

$$\frac{dm}{dt} = \alpha_m(V)(1 - m) - \beta_m(V)m$$

$$\frac{dh}{dt} = \alpha_h(V)(1 - h) - \beta_h(V)\text{h}$$

$$\frac{dn}{dt} = \alpha_n(V)(1 - n) - \beta_n(V)\text{n}$$

The different ion channels are distributed in a nonuniform distribution along the axo-somato-dendritic membrane of neurons (Lai & Jan, 2006). In the presynaptic terminals, a collection of Nav, Cav, and Kv are expressed with the Cav channels being directly involved in the release of synaptic vesicles (Figure 11). With the axon, the axon initial segments (AIS) and the nodes of Ranvier contain Nav and KCNQ channels among others, which are fundamental for the initiation of action potentials and its propagation along the axon. The dendritic tree contains a collection of Nav, Kv, and Cav channels (and others). The Kv2 channels are found in proximal dendrites while Kv3 channels are expressed throughout the whole dendritic tree (Figure 11).
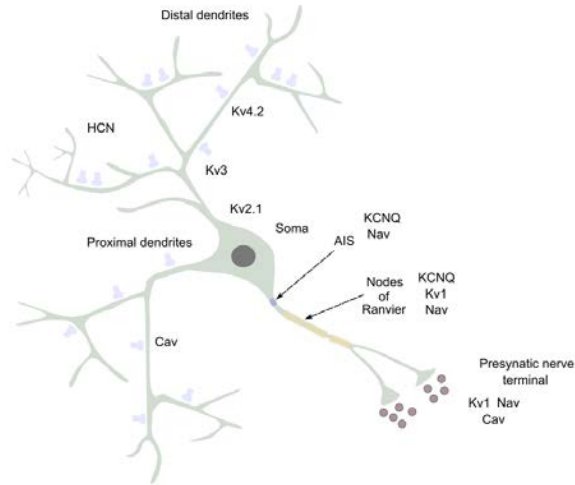
Figure 11: The general localization of voltage-gated ion channels within the axon, soma, and dendritic segments. This diagram shows the specific localization of a selection of sodium, potassium, and calcium voltage-gated ion channels. The Kv1, Nav, and Cav are present in the presynaptic nerve terminal. The axon initial segment (AIS) and the nodes of Ranvier contain Kv1, Nav, and KCNQ among other channels. The distribution of HCN cation channels has a gradient expression that increases from soma to distal dendrite. The dendritic tree contains a variety of potassium channels including Kv2.1, Kv3, and Kv4.2. The Kv2.1 channel is expressed on the soma and proximal dendrites. The Kv3 channel is expressed through the whole dendritic tree. The Kv4.2 channel is more expressed on distal dendrites. The Cav channels are found throughout the whole dendritic tree. HCN, hyperpolarization-activated cyclic nucleotide-gated. Adapted from Lai & Jan (2006) and Claudi, (2020).

## 1.5.5 Ionic currents and voltage-gated ion channels

Each neuron is characterized by the type of ion channels that are expressed in the different parts of its soma-dendritic-axonal membrane. The combinations of these currents in conjunction with the passive properties of neurons determine their electrophysiological behavior. Analyzing neuronal behavior using patch clamp and other techniques has identified the currents which are participating in certain behaviors. The importance of the sodium current was identified by Hodgkin and Huxley (1952) for the generation of action potentials and the importance of the potassium current for repolarization. The roles of the different potassium currents have expanded as more features have been analyzed. The potassium currents involved in the action potential have further been functionally divided into delayed-rectifier $K^+$ currents, delayed $K^+$ currents, and A-type $K^+$ currents. These currents are attributed to several subtypes of ion channels. The delayed $K^+$ and A-type $K^+$ currents are involved in the delay to spike. The persistent inward current is involved in repetitive firing. In bursts, there are N- and P/Q-type $Ca^{2+}$ currents, $Ca^{2+}$-activated $K^+$ currents (BK, SK), and $Na^+$-activated $K^+$ currents. The sag response within certain neurons, including ChINs, is attributed to hyperpolarization-activated $Na^+/K^+$ currents (HCN; Toledo-Rodriguez et al. (2005)).
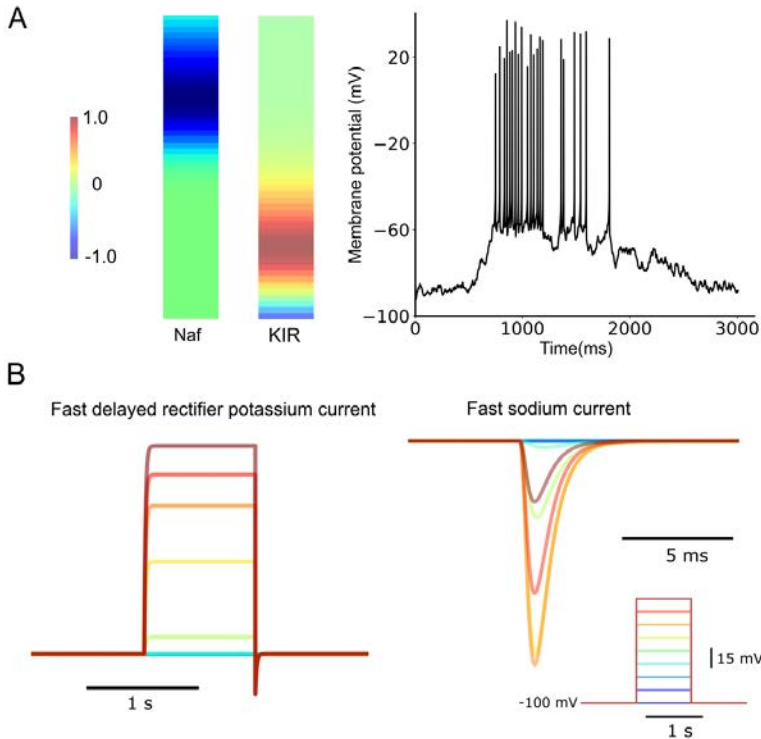
Figure 12: Building multi-compartmental models. A) A simulation of a direct pathway striatal projection neuron. The simulation shows the dSPN with both subthreshold and suprathreshold activity. The left-hand panel shows normalized currents of fast sodium current and the inward rectifying KIR current which are included in the model. The conductances are dependent on the membrane potential; the KIR current is generally activated at subthreshold membrane potentials, while the sodium current is the basis for the action potential. In general, voltage-gated ion channels are open within different membrane potential intervals and with a variety of dynamics (fast, slow, rectifying, etc). All these features are considered in the development of multi-compartmental models. (Normalized current, the inward and outward currents) B) The response of fast delayed rectifier potassium current and fast sodium current following steps in voltage clamp (-100 to 40 mV). These currents have very different dynamics, the sodium current is fast (<2 ms) while the potassium current is open throughout the voltage step.

The fact that certain ion channels generate certain types of electrophysiological features depends on several components. Certain ion channels are open at very hyperpolarized membrane potentials, such as the KIR (Figure 12). Other ion channels are positioned at, for example, the nodes of Ranvier or along the dendrite; and are responsible for the membrane dynamics in these sections of the neuron. Individually, the dynamics of each ion channel can also differ (Figure 12). Some have fast dynamics and inactivate quickly, like the fast sodium current which determines its effect on membrane dynamics. These and other features are important to consider when building multi-compartmental models of neurons.

## 1.5.6   Modeling synapses

Synaptic transmission is a highly dynamic process. Synaptic efficacy is activity-dependent, which is demonstrated in both short-term and long-term plasticity. Within the striatum, the main source of fast transmission (via ionotropic receptors) is attributed to glutamate (NMDA and AMPA receptors) and GABA (GABA$_A$ receptors). The models of synaptic currents and receptors range from instantaneous rise and decay, via an alpha function or the difference of two exponentials to a more detailed description

of NMDA conductance and its $Mg^{2+}$ block. The Tsodyks-Markram (TM) model was presented in 1997 for modeling depressing synapses between cortical pyramidal neurons (Tsodyks & Markram, 1997). Extensions of the TM models allowed for modeling various behaviors of facilitating and depressing short-term plasticity of both glutamatergic and GABAergic models. Additionally, the glutamatergic TM model includes a separation of AMPA and NMDA currents and the important $Mg^{2+}$ dependence of NMDA (Carannante et al., 2022). Incorporating the short-term plasticity within synaptic models can have important effects on network performance, especially in combination with detailed multi-compartmental models (Izhikevich et al., 2003).

### 1.5.7    Dendritic processing

The input to SPNs is distributed from the proximal position on the soma and dendrites to the distal regions of the dendritic tree. The synaptic integration along the dendrite is affected both by passive and active properties (Euler & Denk, 2001; Yuste & Tank, 1996). At one extreme, dendrites can be viewed as passive cylinders. Although, previous sections have demonstrated that this is not the case. There are important considerations, however, as many active properties are influenced by passive properties (Rall et al., 1967). The passive properties are crucial for understanding the properties of the dendritic tree. One effect is that synaptic potentials are attenuated along the dendrite. Although, this can be modified by the voltage-gated ion channels found throughout the dendritic tree (Figure 11). Furthermore, if inputs colocalize, the increased conductance following the activation of one input would sum smaller than two individual responses due to the increased conductance of the membrane. An example of this is shunting inhibition (Paulus & Rothwell, 2016). The excitatory input can be shunted by inhibition due to the increased conductance of the membrane which reduces the input resistance.

An interesting feature of dendrites is dendritic spikes and other dendritic non-linearities. With technological advancement, researchers have been able to record from dendrites and investigate the induction of NMDA spikes and plateau potentials in distal dendrites (Antic et al., 2010). The voltage-dependent NMDA receptor can induce non-linear plateau potentials within the dendrites, which can be further modulated by passive and active properties. The NMDA receptors are composed of several different subunits and the $Mg^{2+}$ blockage is voltage-dependent. Following the activation of a group of glutamatergic synapses, NMDA spike/plateau potentials were induced in cortical neurons (Antic et al., 2010), which has been repeated for several neuron types (Augustinaite et al., 2014; Du et al., 2017). Future advancements in optical and electrophysiological techniques could uncover further computational mechanisms, which would highlight the importance of dendritic processing and computational methods for simulating the complex dendritic trees of neurons.

### 1.5.8    Multi-compartmental models and large-scale networks

Multi-compartmental neuronal models incorporate the passive and active properties of the cell membranes in different parts of the complex somatodendritic membrane. This allows for investigations into the interaction between neuronal excitability and morphology and the integration of synaptic inputs. The basic unit within multi-compartmental models is based on an RC circuit (De Shutter, 2009). The compartment acts like a capacitor due to the separation of conducting ionic solutions by the cell membrane, which is charged following the flow of ions across the membrane. As shown in the previous section, a common formalism for modeling ion channels is Hodgkin-Huxley. The equations presented in Hodgkin & Huxley (1952) have been expanded to include several currents and ion channel subtypes. The dynamics of the ion channel and the voltage dependence of the opening, closing, and other features of the individual ion channel type can be investigated using a range of current and voltage clamp

protocols; and included in the final model. Figure 13 shows an example of the RC circuit within each compartment of a multi-compartmental model (Appukuttan et al., 2017; Sterratt et al., 2011) with sodium, potassium, and a leak current, with the axial resistance between each compartment.
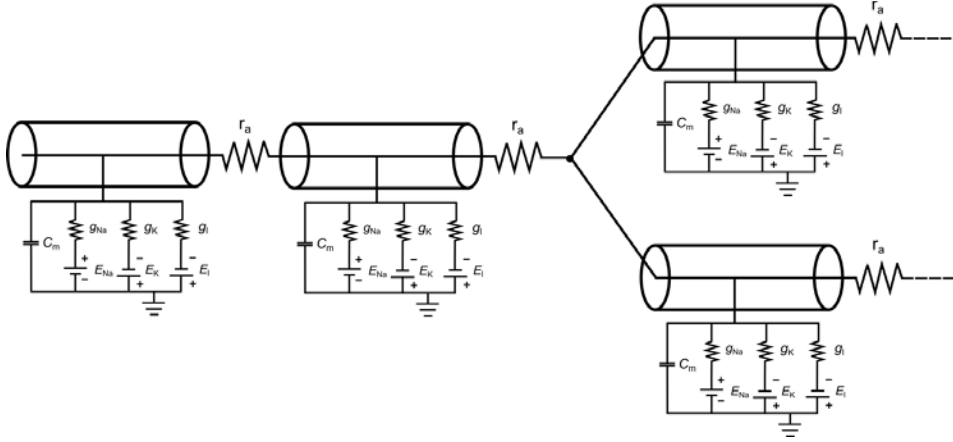


Figure 13: A description of the principles behind multi-compartmental neuronal models with Hodgkin-Huxley ion channel models. The morphology is divided into compartments (iso-potential). Each compartment is described as an equivalent electrical circuit. In this example, the circuit contains a capacitor (the lipid bilayer) and the resistors (with voltage-dependent conductance) representing the sodium, potassium, and leak currents. The compartments branch (like a dendritic morphology) and the current flow between compartments is regulated by the axial resistance ($r_a$). In a full multi-compartmental model, each compartment can contain several types of sodium, potassium, calcium, or other currents which are represented using the Hodgkin-Huxley formalism.

Within a simulation, the interaction between individual RC circuits is determined by the axial resistance, and the total current across a section is determined by the surface area of the individual soma or dendritic section including the contribution from adjacent sections. The rate of change of the potential can be calculated by the following equation, which includes several ion channel subtypes ($k$) and leak current (Bower & Beeman, 2003), but the signing convention may differ between simulators, like GENESIS:

$$C_m \frac{dV_m}{dt} = \frac{(E_m - V_m)}{R_m} + \sum_k [(E_k - V_m)G_k] + \frac{(V'_m - V_m)}{R'_a} + \frac{(V''_m - V_m)}{R_a} + I_{inject}$$

$C_m$, membrane capacitance; $R_a$, axial resistance; $(V'_m - V_m)$, the difference in potential between two compartments; $G_k$, channel conductance; $E_k$, reversal potential; $R_m$, membrane resistance; $I_{inject}$, additional injection current

NEURON is a widely used simulation environment for modeling single neurons and networks of neurons (available at https://github.com/neuronsimulator/nrn) of multi-compartmental models. In 2009, Python interaction with the NEURON simulator was enabled (Hines et al., 2009). This enabled the development of Python-based software packages for large-scale simulations, which have been extensively utilized by the computational community.

This is especially useful for handling and incorporating the data needed to describe and validate the neuron models, the network connectivity, and the analysis following the simulations. Large-scale simulations of multi-compartmental models benefit from standardization, structure, and systematic incorporation of models and data. The network requires data on the voltage-gated ion channels to the

description of network interaction and connectivity, which puts considerable demands on the amount of data required to build these networks.

As outlined by De Shutter and others (2009) but modified for the striatum, the minimal requirements to build a large-scale striatal network include:

- The reconstructed neuronal morphology of the neuron types
    - dSPN, iSPN, FS, LTS, and ChIN
    - Including soma, axon, and dendrites
    - Complete axonal and dendritic tree, if possible
- The characterization of voltage-gated ion channels within each neuron type
    - The localization within each neuron type
    - The kinetics of each current or voltage-gated ion channel
    - The reversal potentials (for specific experiments)
- The passive and active properties – extracted from electrophysiological recordings
    - Literature reviews on the electrophysiological behavior of each neuron type
    - Optimization of each model
    - Validation of the electrophysiological behavior
- Calcium dynamics within the neurons
- The synaptic input and the network connectivity
    - The receptor type and the dynamics of the synaptic inputs (including $Mg^{+2}$ block for NMDA receptors)
    - The density of synaptic input along the soma and dendrites
    - The reversal potentials
    - Distance-dependent connectivity
    - Experimental data on the response for each neuron type and external input
    - Including short-term dynamics, the number of synapses, and the strength

In conclusion, the striatal microcircuit is complex with several neuron types and extrinsic inputs, which could be incorporated into a large-scale network model. This model could provide new insight into how these components interact and lead to further understanding of the role of the striatal microcircuit and its interactions with other basal ganglia nuclei. Hence, this is the basis for the developments and investigations performed in this thesis.

# 2 RESEARCH AIMS

The general aim of this thesis is to create a detailed reconstruction of the striatal microcircuit and investigate the role of the striatal microcircuit in shaping striatal activity.

The specific aims are:

- To create a detailed microcircuit of the striatum with multi-compartmental models of dSPN, iSPN, FS, LTS, and ChIN (Paper I).

- To investigate the reciprocal interaction between LTS and ChIN within the striatal microcircuit (Paper II).

- To include neuromodulation within the model to investigate the role of dopamine and other neuromodulators (Paper III).

- To investigate the integration by SPNs and their effect on the striatal microcircuit (Paper IV)

# 3 MATERIALS AND METHODS

Our aim was to develop a model network of the dorsal striatum, which as closely as possible corresponds to its biological counterpart, and investigate the impact of the striatal microcircuit on the integration of inputs in the striatal projection neurons. This involved:

1) Developing multi-compartmental models of each type of neuron, based on the available electrophysiological data, including ion channels expressed, somatodendritic morphology, and axonal arborizations.

2) Distributing the different types of neurons with appropriate density in a volume that can encompass thousands of neurons, including their dendritic arbors and axonal ramifications.

3) Developing the software *Snudda* for building the microcircuit, with appropriate synaptic connectivity and synaptic properties for each type of connection (ionotropic synapses).

4) Develop simulations of G protein-coupled receptor-mediated neuromodulation within large-scale microcircuits, for example, simulations of dopamine receptors of the D1 and D2 type within the striatum.

5) Simulating large-scale networks of the striatal microcircuit and investigating the impact of intrastriatal inhibition, dendritic processing, and neuromodulation on the activity of the striatal projection neurons.

## 3.1 MULTI-COMPARTMENTAL MODELS

The simulations included multi-compartmental models of dSPNs, iSPNs, FS, ChINs, and LTS, in each case based on detailed data on the electrophysiological properties and the somatodendritic morphology (papers I-IV). Most of the experimental data used within the simulations was from the extensive collaboration with the Silberberg group, with important additions from extensive literature reviews and the usage of online databases for the morphologies and the ion channel expressions within each cell type (Ascoli et al., 2007; Muñoz-Manchado et al., 2016). The electrophysiological and morphological diversity within each cell type were used to create larger populations of models. The continuous development of the software and the database of striatal neuronal models are maintained on Github (software and data versioning). These steps are described in the following sections.

### 3.1.1 Electrophysiology

The mouse lines D1-Cre, D2-Cre, SOM-Cre, PV-Cre, and ChAT-Cre (crossed with homozygous tdTomato reporter mouse line) were used to extract *in vitro* electrophysiological features of dSPNs, iSPNs, LTS, FS, and ChINs, respectively. The patch clamp recordings utilized a collection of protocols with varying timing and strength of current injection to characterize the electrophysiological behavior of each cell type. Neurons identified in the dorsal striatum were recorded and a subset of these were intracellularly filled with Neurobiotin. The recordings were corrected for the liquid junction potential.

### 3.1.2 Morphology

The reconstruction of the neuronal morphology involved straining, reconstruction, corrections, and validations. In collaboration with the Silberberg group, neurons were intracellularly filled with Neurobiotin during the electrophysiological recordings. The filled neurons were visualized either using the diaminobenzidine (DAB) method (ChINs) or Cy5-streptavidin (LTS). The neurons stained with DAB were reconstructed manually using Neurolucida (MBF Bioscience) with Zeiss Axio Imager.A1. The Cy5-streptavidin-stained neurons were imaged in a confocal microscope (ZEISS LSM 800) and reconstructed with a semi-automated process using Neutube (Feng et al., 2015). The reconstructions of dSPNs, iSPNs, and FS were included from online repositories (Ascoli et al., 2007) and validated based on known morphometric parameters (Paper I).

The neuronal morphologies used within the multi-compartmental models were reconstructed from slice preparation of the mouse brain. The slice preparation provides an amazing opportunity to record individual neurons, and pairs of neurons and modify their environment to uncover the structure of the microcircuit, but it also has some drawbacks (De Shutter, 2000, 2009). The slice preparation consists of an approximately 250 μm thick slice. The top and bottom layers will contain many damaged or dead cells, which results in an effective slice thickness of 100-150 μm of healthy neurons. Typically, neurons have dendritic and axonal arbors, which extend more than 50 μm away from the soma, hence the slice poses a problem, and some dendrites may most likely be cut or damaged. Therefore, the depth of the cells within the slice will determine how much of the morphology will remain intact. These and other natural constraints, like slice shrinkage, will leave artifacts in the reconstruction. The corrections for these artifacts require careful analysis and validation and will produce a more accurate representation of the neuronal morphology. The corrections and validations utilized in Paper I and the subsequent papers were collected within the software, *Treem* (https://github.com/a1eko/treem). This Python

package incorporated the corrections of the slice artifacts, including shrinkage, cut dendrites and axons, and the standardization of sampling steps.

### 3.1.3 Ion channels

Each cell type expresses a specific combination of ion channels, which may also differ between the different compartments within the neuronal morphology. The ion channels expressed in the different striatal neurons have been investigated in several papers through both pharmacological experiments and RNA sequencing (Muñoz-Manchado et al., 2016, see Paper I). The ion channels models used within the multi-compartmental models were extracted from previous publications (Du et al., 2017; Lindroos et al., 2018; Maurice et al., 2004) and the parameters were optimized for each cell type.

### 3.1.4 Optimization

The multi-compartmental models were optimized using a combination of hand-tuning and the utilization of the optimization software for model parameters, BluePyOpt (Van Geit et al., 2016). The hand-tuning provided a general exploration and incorporated the knowledge of ion channel dynamics and the electrophysiological features of the cell type. The optimization was divided into the following steps. The electrophysiological features were divided into the subthreshold and suprathreshold ranges. The features were extracted using Electrophysiology Feature Extract Library (eFEL) (Blue Brain Project, 2015). The passive membrane parameters were optimized followed by the parameters of the ion channel models within each neuron type. BluePyOpt (Van Geit et al., 2016) is a feature-based optimizer and utilizes DEAP (Distributed Evolutionary Algorithms in Python) which contains a collection of algorithms (here, the default Indicator-Based Evolutionary Algorithm (*IBEA*) was used) (Fortin et al., 2012). The optimization produced a population of models which were validated against the electrophysiological features and included in the database of multi-compartmental models.

## 3.2 BUILDING NETWORKS – SNUDDA

*Snudda* is a tool for creating and simulating large-scale networks of multi-compartmental models (Paper I) written in Python with the simulator NEURON (Hines et al., 2009). The steps for building large-scale networks within *Snudda* are – initialization, placement, detection, pruning, and simulation.

Here is a summary of the process of generating large-scale networks using *Snudda*. The initialization (*snudda.init*) creates *network-config.json,* which specifies the parameters of the network model. The placement step involves assigning coordinates for each neuron model within the microcircuit, according to the specific density of each neuron subtype. The neurons are rotated according to the specification in the config file. Following placement, the connectivity within the microcircuit is constructed by touch detection of axons and dendrites. The basis of putative synapses between two neurons is that the axon (neuron 1) and dendrite (neuron 2) occupy the same voxel ($3x3x3 \ \mu m^3$). The putative synapses within the microcircuit are pruned in accordance with experimental data. The pruning algorithm consists o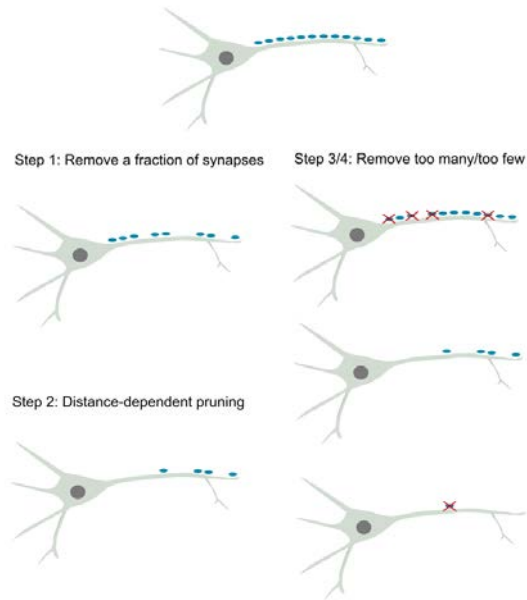f the steps: 1) a fraction of synapses is removed; 2) distance-dependent filter; 3) removing excessive synapses between highly connected neurons; 4) removing synapses between sparsely connected neurons; 5) removing all synapses between fractions of neuron pairs (for more detail see Paper I) (Figure 14). This algorithm is similar to the algorithm presented by Markram et al. (2015).

The extrastriatal and intrastriatal synaptic inputs were modeled using Tsodyks-Markram models of glutamate (NMDA and AMPA) and GABA$_A$ receptors (*tmglut.mod* and *tmgabaa.mod*). The

experimental data to fit the synaptic models were retrieved via collaboration with the Silberberg group and literature reviews. The strengths of the synaptic inputs were validated through a collection of virtual experiments (Straub et al., 2016; Szydlowski et al., 2013). The cortical and thalamic input can be activated via a config file, *input.json*, which specifies the frequency, duration, correlation, and other properties of neural spike trains.

The network generation and simulation using *Snudda* can be performed on a laptop, desktop computer, and supercomputer facilities (depending on the size of the network). The generation of networks and the simulations in Paper I-IV were performed on supercomputer facilities at the PDC Center for High Performance Computing at KTH Royal Institute of Technology and the Swiss National Supercomputing Centre.



Figure 14: The steps involved in touch detection: 1) a fraction of synapses is removed; 2) distance-dependent filter; 3) removing excessive synapses between highly connected neurons; 4) removing synapses between sparsely connected neurons.

### 3.2.1    Snudda – the general description

*Snudda* is available for download at https://github.com/Hjorthmedh/Snudda and is under continuous development by the authors of the following publications and others (Paper I-IV; Hjorth et al., 2021; Lindroos & Hellgren Kotaleski, 2021). The first version of *Snudda* was published as a part of Paper I. The subsequent projects using *Snudda* required further development of the code base and the inclusion of new features, refinement of previous features, and general code optimizations (Hjorth et al., 2021). The development utilized the distributed version control system Git (https://git-scm.com/) and the cloud-based git repository (https://github.com/). The multi-compartmental models are stored in a separate repository and each model is described by a unique key for the reconstruction and the parameter set.

### 3.2.2    Code development and simulations within each paper

In Paper I, the *Snudda* software was written to create networks through placement, touch detection, and pruning and simulate the networks with varying external stimuli and dopaminergic modulation. The following sections will define the additional developments of *Snudda* in Paper II-IV.

In Paper I, *Snudda* implemented dopaminergic neuromodulation of dSPN, iSPN, FS, ChIN, and LTS. Neuromodulation was simulated through the variation of the conductance of a list of ion channels within each neuron type during the simulation. This is the current mode of simulating neuromodulation within

*Snudda*, with the addition of neuromodulation of synaptic input (see https://github.com/Hjorthmedh/Snudda for details). The degree of modulation of each ion channel was extracted from literature reviews and the percentage (increase/decrease) of conductance was implemented in the model. In Paper III, the development of parameter sets for neuromodulation was generalized into *Neuromodcell*. This software combined the process developed in Paper I and expanded the formalism to multiple neuromodulators; including the ability to define any time-dependent modulation.

The multi-compartmental models in Paper II were developed using the process defined in Paper I. Paper II explored the interaction between ChIN and LTS, the muscarinic M4 receptor modulation of LTS, and the NO modulation of ChIN. The NO modulation produces a slow depolarization of ChIN. The modulation was implemented as a slow current injection with the specific time constants extracted from Elghaba et al. (2016). The modulation was activated by a *frequency-checker* which modeled the frequency dependence of the nitric oxide modulation. The muscarinic M4 receptor modulation was simulated through a subcellular cascade (Blackwell et al., 2019). The cascade was activated by the simulated release of acetylcholine from the ChIN model. For more details see Paper II.

Paper IV required further development of the connectivity, the formalism for external input, and the organization of recordings performed during simulations. The information about each model within the network is contained within *network-synapses.hdf5*. The ablation simulations within Paper IV required modifications of the connectivity. The class *SnuddaAblateNetwork* enables the modification of *network-synapses.hdf5* and the removal of connections between specific neuron types. Each model can be accessed by the *neuronID* and populations of neurons can be collected into population units (0, 1, 2 etc.) based on the *populationUnit* array. The formalism for the external input was developed to include input to specific population units (collection of neurons). The implementation of the current clamp and voltage clamp of neurons during a simulation was refined and utilized in Paper IV. The creation of clusters of glutamatergic input on distal dendrites was included in the formalism of external input. The cluster can be defined by the distance from the soma, the size, and the spread along the dendrite. The requirement of dendritic recordings for Paper IV prompted a re-organization of the output. The *SnuddaSaveNetworkRecordings* class was created, and the output was classified and saved using the *SynapseData* or *CompartmentData* class. The organization was necessary to control the recordings of somatic, dendritic compartments, and receptor models, and the types of recordings included membrane potential, ion channel currents, and synaptic currents.

# 4 RESULTS

## 4.1 Creating the striatal microcircuit *in silico* (Paper I)

In Paper I, the platform for investigating the striatal microcircuit *in silico* was built. Figure 15 shows the organization of the basal ganglia (Figure 15A) and the composition of the striatal microcircuit. The main cell types within the striatum (95%) are the striatal projection neurons (Figure 15B1). The remaining 5% are GABAergic and cholinergic interneurons (Figure 15B2). The connection probabilities between the cell types are distance-dependent (Figure 15C). Within 100 μm, the connection probability between FS to dSPN and FS to iSPN is 89% and 67%, respectively. The connection probabilities within SPN are the highest between iSPN-iSPN and the lowest between dSPN-dSPN both within 50 and 100 μm (Figure 15C). The connection probabilities presented in Figure 15C were used within the *Snudda – pruning step* (see Materials and Methods) to constrain the connectivity within the striatal microcircuit.
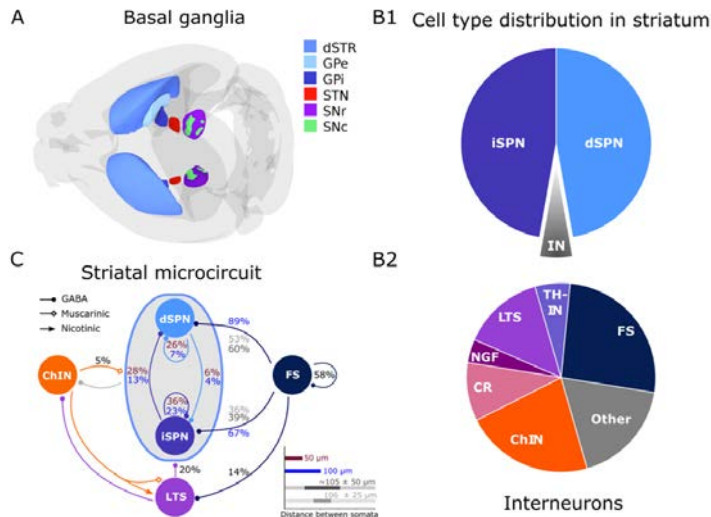


Figure 15: Organization of the striatal microcircuit and the neuronal subtypes. (A) Dorsal view of the mouse brain showing the basal ganglia subnuclei. The dorsal striatum (dSTR), globus pallidus external and internal segment (GPe and GPi, respectively), subthalamic nucleus (STN), substantia nigra pars reticulata and pars compacta (SNr and SNc, respectively) are shown in relative sizes. The color coding is as indicated. (B1) The principal cells of the striatum are the striatal projection neurons (SPNs). They account for about 95% of all striatal neurons and form two approximately equal pools of cells that differ by their projection targets and belong to the direct and indirect pathways, dSPNs and iSPNs, respectively. (B2) The interneurons include cholinergic and GABAergic interneurons (INs) Burke et al. 2017. By unbiased counts available for the mouse of the total number of neostriatal neurons, the parvalbumin-expressing fast-spiking (FS) cells make up 1.3%, NPY/SOM+ low-threshold spiking (LTS) interneurons 0.8%, calretinin-positive cells (CR) around 0.5% in rodents, tyrosine hydroxylase-positive interneurons (THINs) 0.3%, NPY/SOM - neurogliaform (NGF) cells 0.2% and cholinergic interneurons (ChINs) 1.1%. (C) Schematic connectivity within dSTR involving dSPNs, iSPNs, FS, LTS, and ChINs. Connection probabilities within and between neuronal subtypes are shown by respective arrows; numbers in dark red correspond to connection probabilities for a somatic pair within 50 μm, the numbers in blue correspond within 100 μm, the dark grey and light grey numbers correspond to 105 μm ± 50 μm and 106 μm ± 50 μm. (From Paper I with updated C panel). (Adapted from Paper I with additional connectivity data)

### 4.1.1 Striatal projection neurons

The cell types included within the Paper I version of the striatal microcircuit were dSPN, iSPN, FS, ChIN, and LTS. Figure 16 shows the multi-compartmental model of dSPN with morphological reconstruction and electrophysiological behavior. The reconstruction in Figure 16A demonstrates the extensive arborization of both dendritic and axonal arbors (blue and gray) with the terminal branch of the dendritic tree contributing to 80% of the total dendritic length. Figure 16 B and C show the experimental data in red and the model simulation in black. The protocols were used to investigate the electrophysiological behavior of the dSPN and extract the features for optimization (see Materials and Methods). The model reproduces both subthreshold and suprathreshold behavior (Figure 16B). The process was repeated for four models in Paper I and the sub- and suprathreshold responses are shown in Figure 16C. The ability to induce plateau potentials within the distal dendrites of SPN is an important property. The model was validated against experimental data from Du et al. (2017), where plateau potentials were induced in distal dendrites of SPN following glutamate uncaging. Figure 16D shows the response of the model (in black) to clustered input onto distal dendrites. The model reproduces the NMDA-dependent plateau potential observed in Du et al. (2017) (in red) in terms of both the amplitude and the duration. Day et al. (2008) estimated the $Ca^{2+}$ entry following a backpropagating action potential in SPNs. Figure 16E shows the experimental data (in red) with the results of the *in silico* experiment using the dSPN model. The generation of an action potential within the dSPN model caused a calcium entry that decreased with distance from the soma, like the observations in Day et al. (2008) (in red). The same process was performed to create the iSPN models in Paper I (see Supplementary Paper I).
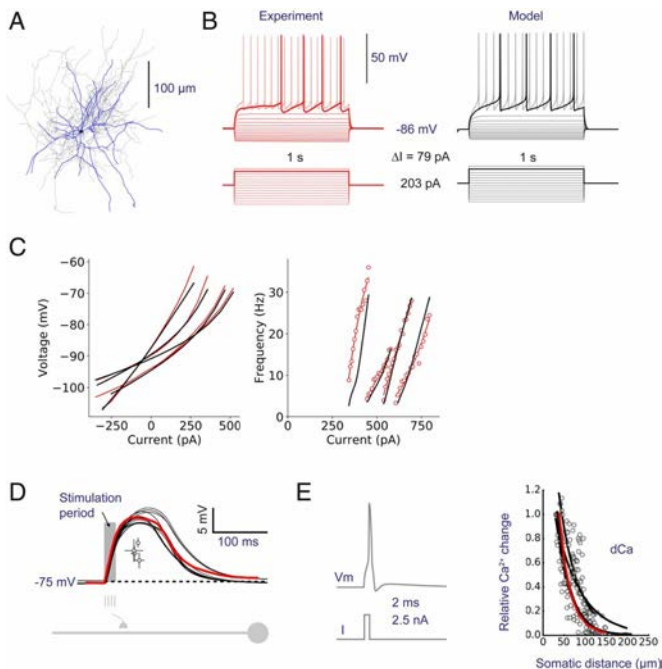


Figure 16: The direct pathway striatal projection neuron (dSPN) expressing dopamine D1 receptors. (A) Neurolucida reconstruction of a single dSPN with dendrites (blue) and axon collaterals (gray). A black dot marks the soma. (B) Sub- and suprathreshold responses to current injections for a model neuron (black) and the corresponding experimental data (red). An example model fit experimental data, with the current protocol used; holding current 203 pA to keep the baseline membrane potential around −86 mV. (C) Population behavior for models and experiment: voltage–current and frequency–current relations are

shown for four dSPNs optimized to corresponding data. (D) Somatic potential response to spatiotemporal clustered synaptic input, demonstrating the model's ability to trigger NMDA-dependent plateau potentials. The dots in the middle give the mean midpoint (half duration, half amplitude) of the plateaus triggered at a somatic distance of 90 to 120 μm. Experimental data (red) digitized Du et al. 2017 (E) Normalized change in calcium concentration in response to a backpropagating action potential (triggered with a short duration 2 ms high amplitude 2.5 nA current injection). Experimental data are extracted from Day et al 2008. Model data are in black, and experimental data are in red. (From Paper I)

### 4.1.2  Interneurons

The striatal interneurons are mainly GABAergic. In Paper I, the GABAergic interneurons in the *in silico* striatum were FS and LTS. The FS targets the soma and proximal dendrites of SPN with a high connection probability (Figure 15C). The LTS has a high input resistance and targets the distal dendrites of SPNs. Figure 17 shows the multi-compartmental model of the cholinergic interneuron. The Neurolucida reconstruction of the ChIN (Figure 17A) shows the large soma (in black) and the dendritic arborization (in blue) which extends over a large area. The response of the model (in black) compared to the experimental data (in red) (Figure 17B), demonstrates the prominent sag response in both the experimental data and the model. The model produces a rebound response to a hyperpolarizing current injection in Figure 17C as well as a pause response following a short depolarizing current injection in Figure 17E. Finally, the multi-compartmental models of the ChIN, FS, and LTS were integrated into the database of models produced in Paper I and utilized in the creation of the *in silico* striatal microcircuit.
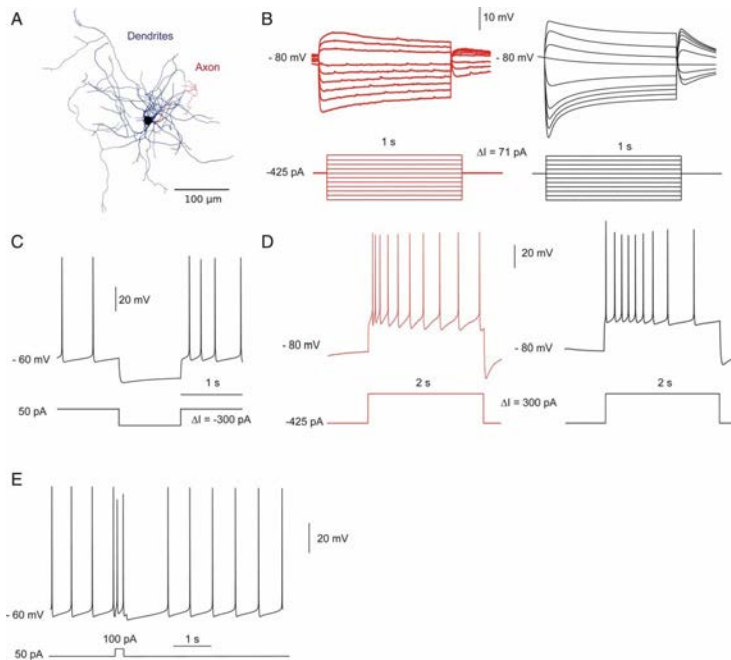


Figure 17: Cholinergic interneuron (ChIN) model. (A) Neurolucida reconstruction of a ChIN with dendrites (blue), axon collaterals (red), and soma (black). (Scale bar, 100 μm.) (B) Electrophysiological responses of the ChIN from the experiment (red) and model (black). (C) Hyperpolarizing current injection to illustrate the rebound behavior in the model. (D) Responses to suprathreshold current injection in the model (black) and the experiment (red). (E) Injected depolarizing current of 100 pA for 300 ms during activity, to illustrate the pause response in the ChIN model. (From Paper I).

### 4.1.3 Connecting the striatal microcircuit

The process of creating the *in silico* striatal microcircuit is summarized in Figure 18 (see Materials and Methods). The neuronal reconstructions of each neuron type are important during the construction as the dendritic and axonal arbors are utilized for touch detection. Hence, the quality of the reconstructions will impact the ability to reproduce the connectivity data (see Materials and Methods). The reconstructions are placed inside a cube (or other mesh) and Figure 18A shows an example of a hyper voxel within the DLS with 2174 neurons (distributed with appropriate density, approximately 80500/mm³ for the striatum) (Figure 18B). The axonal and dendritic arborizations from the 2174 somas are illustrated in Figure 18C. The touch detection algorithm produces putative synapses between axons and dendrites within each voxel (see Materials and Methods). The pruning step modifies the number of synapses according to experimental data with the goal of reproducing the striatal microcircuit connectivity (like Figure 15C). Figure 18D shows the result of the pruning step with an example pair of dSPN and iSPN with synapses in red.
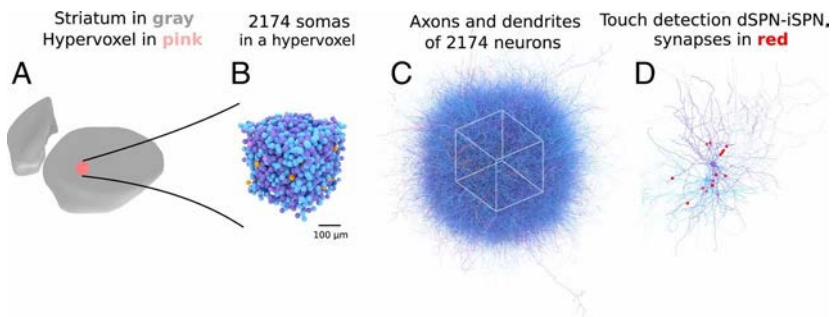


Figure 18: Synapse placement using touch detection algorithm. A) Striatal three-dimensional (3D) mesh in gray, the touch detection is parallelized, and each process handles a subset of the space, here shown as a cube (hyper voxel). B) The somas of all neurons within the hyper voxel, ~2,174 neurons. C) Axonal and dendritic arborization of the 2,174 neurons. D) Touch detection of two neurons using 3 μm voxel resolution. Synapses are shown in red. (From Paper I).

The connectivity within the *in silico* striatal microcircuit was further analyzed in terms of the distance-dependent connectivity, the number of synapses per pair, and several other factors. The analysis was repeated for each neuron type and Figure 19 shows the connectivity of dSPN (as the postsynaptic neuron). Figure 19A (i-v) shows the distance dependence of each connection type (dSPN-dSPN, iSPN-dSPN, FS-dSPN, LTS-dSPN, and ChIN-LTS). The number of synapses in each pair varied between presynaptic neurons. (Figure 19Bi-v) The iSPN-dSPN and dSPN-dSPN had the lowest number of synapses in each pair. This is consistent with experimental data as paired recordings have shown that the SPN-SPN connections are weak and sparse (Planert et al., 2010). On the other hand, the number of presynaptic neurons was the most numerous for dSPN and iSPN, which is due to the ratio between interneurons and SPN within the microcircuit (5% vs 95%). The connection probabilities were further validated by several virtual experiments presented in Figure 19Di-iv. The experimental conditions were simulated and the response in the dSPN model was compared with the experimental data. These virtual experiments further constrained the connectivity like the number of synapses between LTS and dSPN. The presynaptic neurons terminate differently on the dendritic tree of dSPNs. Figure 19Dv shows the cumulative distribution of synapses on the dendrite of the dSPN model, as a function of the distance from the soma. As expected, the FS model terminated on the soma and proximal dendrites while the LTS and SPN input target more distal dendrites (Figure 19D).
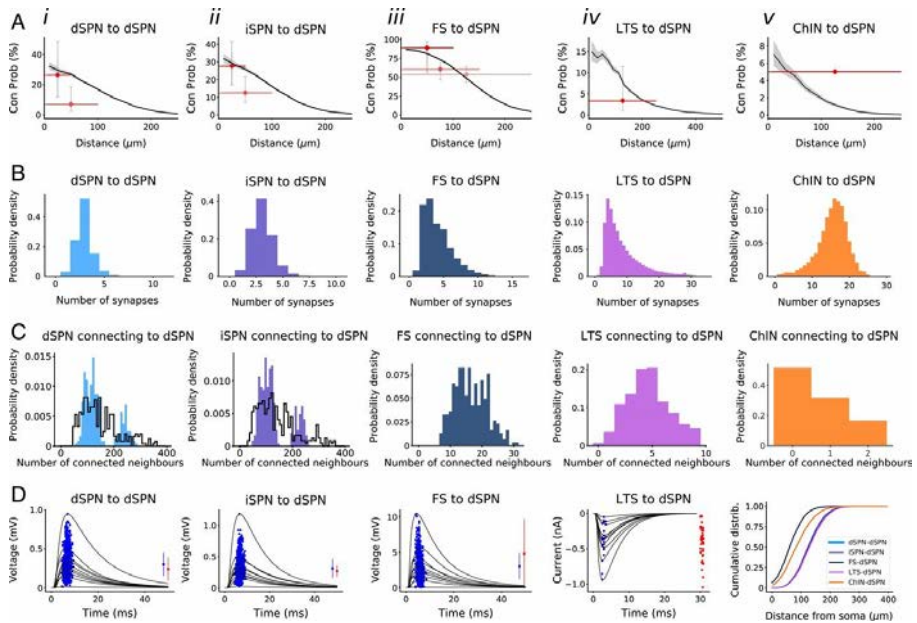
Figure 19: Statistics of connections projecting to dSPN in the striatal microcircuitry. Connections are shown for (i) dSPN–dSPN, (ii) iSPN–dSPN, (iii) FS–dSPN, (iv) LTS–dSPN, and (v) ChIN–dSPN. (A) Pairwise connection probability for the different neuron types projecting to dSPN. The black curve corresponds to the simulated network and the gray region shows the Wilson score (see Paper I) for the model. The red line shows experimental data with error bars showing the Wilson score, and the line length indicates the spread of lateral distance between connected neuron pairs. Experimental measurements were made for neuron pairs within a 50-μm distance (A, i–iii) in Taverna et al. 2008, 100-μm distance (A, i–iii) in Planert et al. 2010, 250-μm distance (A, iii and iv) in Gittis et al. 2010, and 250-μm distance (A, v) (B) Distribution of number of synapses between individual connected neuron pairs. The pairs are indicated above each graph in i–v. (C) Distribution of several connected neurons for each type of presynaptic neuron. The connectivity between presynaptic to postsynaptic neurons is indicated above each graph in i–v. Here we show statistics for neurons in the center of the volume to avoid edge effects. Note that the bimodal distribution seen here is a consequence of only using a limited number of reconstructions for dSPN and iSPN. Preliminary modeling shows that adding a larger number of reconstructions creates a unimodal distribution; however, currently, we only have optimized models for the morphology of four dSPNs. Future versions will include more reconstructions. (C, i and ii) The black line shows the distribution obtained for a larger set of reconstructions (n=100,000) using a jitter to promote morphological variability (see also SI Appendix, Fig. S4 in Paper I). (D, i–iii) Response in a dSPN when a presynaptic (i) dSPN, (ii) iSPN, and (iii) FS is activated. Blue dots mark peaks of postsynaptic potentials. (Insets) Mean and SD for model peaks (blue) and experimental data (red) from Planert et al. 2010. (i and ii) With a chloride reversal potential of −40 mV and (iii) from Straub et al. 2016 with a chloride reversal of 0 mV. (iv) Response in dSPN when LTS neurons are activated. Model peaks are marked with a blue dot, and experimental peaks Straub et al. 2016 marked with red dots (Inset). (v) Cumulative distribution of synapses on the dendrites as a function of the distance from the soma. Connection statistics for other neuron pairs are shown in SI Appendix. (From Paper I).

### 4.1.4 Cortical and thalamic input to the striatal microcircuit

The simulations of external input focused on the cortical and thalamic projections to the striatum. This was characterized extensively in Johansson & Silberberg (2020), which was the basis for the creation of the models with short-term synaptic plasticity from the contra- and ipsilateral motor cortex (M1), somatosensory area (S1) and thalamus to SPNs. Figure 20 shows the responses in SPN models to stimulations of cortical input from M1, S1, and thalamic input with experimental data in red and the model in black. The models of NMDA and AMPA receptors have been further

developed in Carannante et al. (2022) to improve the description of the NMDA and AMPA currents within the Tsodyks-Markram model. The process was repeated for each neuron type within the microcircuit and for the GABAergic connections, which used the *tmgabaa.mod* instead of the *tmglut.mod* (see Paper I).
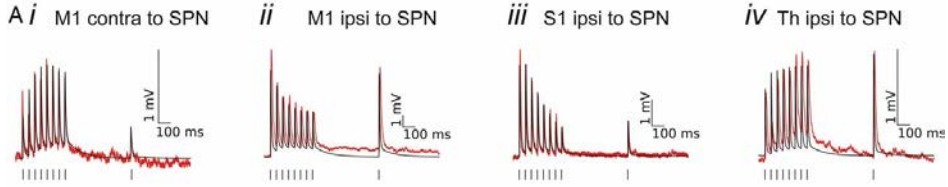


Figure 20: Fitting SPN synaptic dynamics. The Tsodyks–Markram model was fitted using a single compartment. (A) Example response traces of optogenetic activation of cortical and thalamic input (Johansson & Silberberg, 2020). The black trace is the model; the red trace is the experimental data. The protocol includes eight pulses at 20 Hz followed by a recovery pulse. (From Paper I)

### 4.1.5   Simulating the striatal microcircuit

The overarching goal of Paper I was to create an integrated simulation tool for the striatum, which includes dSPNs, iSPNs, FS, LTS, and ChINs and the intrastriatal connectivity and the input from the cortex, thalamus, and SNc as described above. This resulted in the software *Snudda*, which is a platform for creating and connecting networks of multi-compartmental models (see Methods, and Appendix Paper I) and simulating virtual experiments of the striatal microcircuit. Figure 21 illustrates a virtual experiment with the activity pattern of a network of 10 000 striatal neurons with input from the cortex and thalamus with dopaminergic modulation. The cortical command was activated for 500 ms, which increased the activity of dSPN and iSPN. Following the cortical command, dopaminergic modulation was initiated and lasted for 300 ms. The modulation caused decreased activity of iSPN due to the D2 dopamine receptors while the dSPN activity was increased (D1 dopamine receptors).
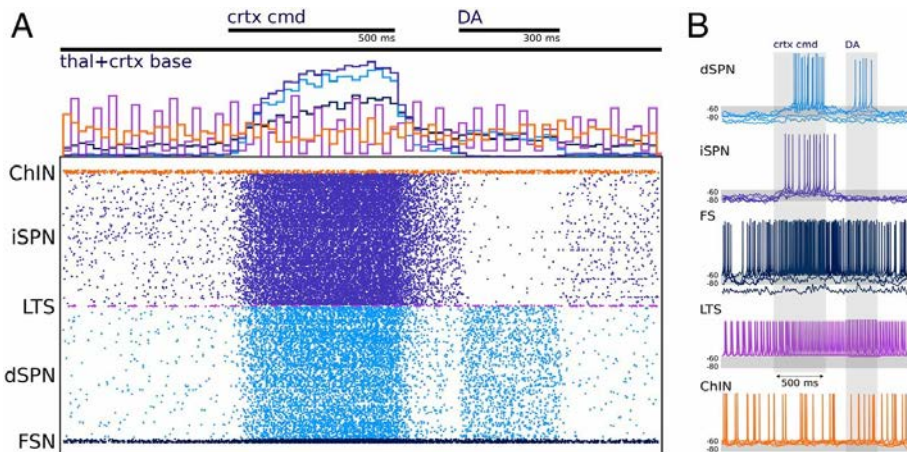


Figure 21: Network simulation of 10,000 neurons. (A) The activity of the network is shown in the form of a raster plot (Bottom) and spike histogram (Top). (B) Example traces of each cell type in the network are shown. The network is driven with cortical and thalamic input and modulated by dopamine, as indicated at the Top of the figure and the shaded areas (in A and B, respectively). The three inputs represent 1) baseline activation of cortical and thalamic input (thal+crtx baseline), 2) a cortical command signal (crtx cmd), during which the cortical activation is increased (given to all cells except the ChINs), and 3) a

dopaminergic modulation signal that acts on conductances in accordance with Fig. 6,SI Appendix, Tables S7–S10 in Paper I, and Lindroos et al. 2018. (From Paper I).

In summary, Paper I resulted in the *Snudda* platform and the database of detailed multi-compartment models which represented 98% of the striatal neurons. The next step was to apply the capabilities of *Snudda* to research the aims defined in previous sections. As described in *Materials and Methods*, the simulations performed in the subsequent studies required further development of *Snudda* and the related models. This demonstrates the importance of continuous integration and letting the research questions guide software development.

## 4.2   Investigating the role of nitric oxide and muscarinic modulation between ChIN and LTS (Paper II)

The aim of Paper II was to investigate the interaction within a striatal subcircuit of ChIN and LTS, which consists of two spontaneously active interneurons within the striatum. ChINs are strongly activated by thalamic input, while LTS are disynaptically inhibited via the thalamic input to ThINs. In addition to GABA, LTS also releases somatostatin (SOM), neuropeptide Y (NPY), and NO. Previous studies have shown that prolonged activation of LTS causes a slow depolarization of ChINs which lasts for >10s (Elghaba et al., 2016). On the other hand, direct activation of ChINs produces a muscarinic M4 receptor-dependent inhibitory response (Melendez-Zaidi et al., 2019) in LTS. Paper II incorporates models of the nitric oxide and muscarinic M4 receptor responses in a model of LTS and ChIN interaction. Paper II demonstrates the impact that the timing and relative strengths of external input could have on the levels of neuromodulators within the striatum, with potential impact on several processes including synaptic plasticity and the release of dopamine (Calabresi et al., 1999; Centonze et al., 2001; Hartung et al., 2011; Rafalovich et al., 2015).

### 4.2.1   Nitric oxide model

To simulate the nitric oxide response of ChIN, a phenomenological model of NO response was developed in Paper II (Figure 22A). The NO model consisted of a *frequency checker* of LTS spiking, which induced a long depolarizing current that consisted of two time constants. Figure 22B shows the response of the ChIN model to the activation of the NO model. The increase in the activity of the ChIN model was quantified and compared to experimental data extracted from Elghaba et al. (2016) (Figure 22C). The NO model reproduced the responses observed in Elghaba et al. (2016) which lasted for >10 s.
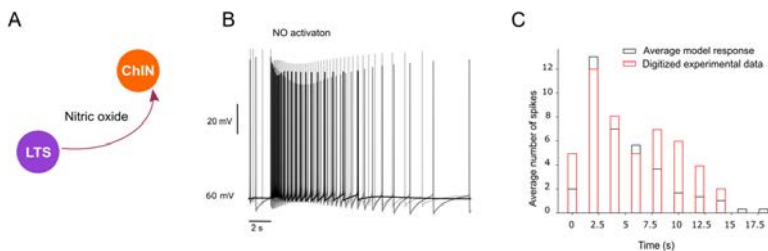


Figure 22: (A) Modelling the NO effect of LTS on the ChIN. (B) Superposition of traces of three different multi-compartment models of ChIN (based on different morphologies) with an activation of the NO input, which

caused a prolonged depolarization. (C) The average response of the three models with NO activation compared to experimental data extracted from Figure 8 of Elghaba et al. (2016) (From Paper II).

### 4.2.2 Muscarinic model

The muscarinic M4 receptor (M4R) model was based on a previous model developed by Blackwell et al. (2019). The spiking activity of the ChIN model produced an ACh accumulation within the M4R model which was coupled to the KIR channel within the LTS model (Figure 23B). Figure 23C shows the activation of the ChIN model in light blue, which causes an accumulation of ACh and an increase in the KIR current within the LTS model. The response of the LTS model (in black) was compared to experimental data from Melendez-Zaidi et al. (2019) (in red). The model reproduces the response observed in Melendez-Zaidi et al. (2019) with a pause that lasts for approximately 1 s (Figure 23D).
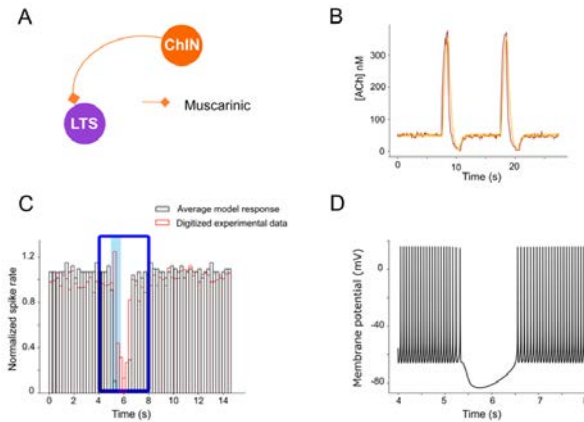


Figure 23: (A) Modelling the muscarinic (M4R) effect of cholinergic interneuron (ChIN) on the low-threshold spiking interneuron (LTS). (B) The ACh release is based on Blackwell et al. (2019) (see Materials and Methods). The ACh release model (orange) is stimulated repeatedly to replicate the average spontaneous activity of ChINs with intermittent bursts of 20 Hz (every 10 s). It replicates the input (red) generated for the model by Blackwell et al. (2019). (C) An experiment from Figure 5b of Melendez-Zaidi et al. (2019) is simulated. Optogenetic stimulation of ChINs results in a pause in LTS. The muscarinic M4R model was stimulated in 10 multi-compartmental models of LTS after five seconds of spontaneous activity (light blue box). The normalized spike rate of the models (black) reproduced the pause seen in the experiment (red). (D) The response of a LTS multi-compartmental model during the period indicated by the blue window in (C). (From Paper II).

### 4.2.3 Corticostriatal and thalamostriatal inputs to the ChIN – LTS network

Following the completion of the NO and M4R models, the interaction between the LTS and ChIN models was investigated by activating cortical and thalamic inputs individually and in combination. The strengths of the cortical and thalamic input to LTS and ChIN vary within the striatum (Johansson and Silberberg, 2020). Hence, a cortical activation would cause excitation of both LTS and ChIN (to varying degrees), while a thalamic activation would activate the ChIN directly. Firstly, a simulation of a thalamic activation of ChINs caused an accumulation of ACh that activates the M4 receptors within the LTS and a period of inhibition of the LTS (Figure 24A, A1), as described in Melendez-Zaidi et al. (2019). On the other hand, when the LTS model is activated the release of NO causes a depolarization of the ChIN (Figure 24A, B). But due to the M4R model in the LTS model, the prolonged activation of the ChIN causes a long inhibition of the LTS model (Figure 24B1). Hence, demonstrating the potential reciprocal control performed by these interneurons. The final panel in Figure 24 shows the effect of the combined activation of cortical and thalamic input in the network. The prolonged cortical activation induced NO response within the ChIN model, which caused a long inhibition (like Figure 24B1). The inhibition of

42

the LTS model could be further controlled by thalamic activation of the ChIN model, via the M4R model.
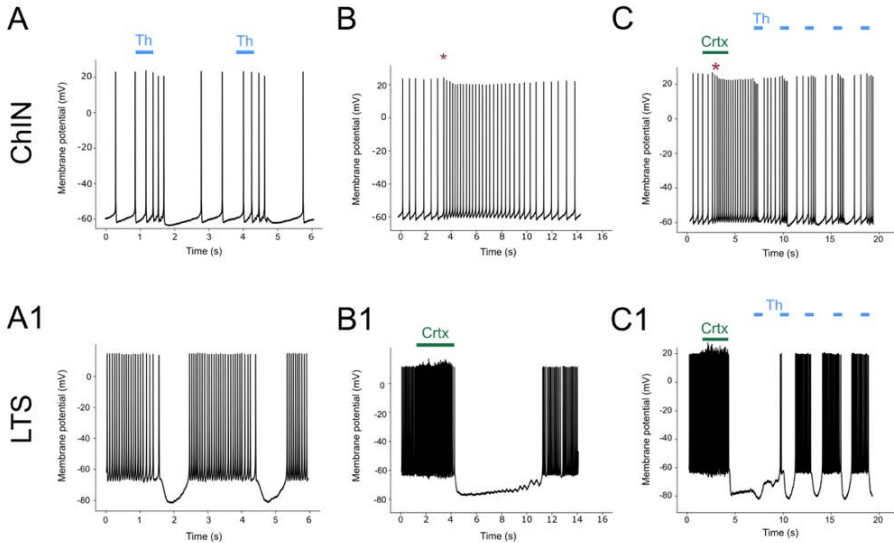


Figure 24: The simulation of thalamic bursts and cortical activity within the cholinergic interneuron (ChIN) and low-threshold spiking interneuron (LTS) interaction. (A) The response of the ChIN model to thalamic bursts (700 ms at 20 Hz every 3 s, light blue line) with cortical and thalamic background activity. (A1) The response of the LTS model to the same stimulation as in (A) with a pronounced decrease in spiking during bursts in the ChIN model. (B1) The response of the LTS model to cortical activation (20 Hz for 3 s, green line) which induces a depolarization of the ChIN model (B) due to the activation of the nitric oxide model (brown asterisk, indicates the LTS frequency checker activation, see Materials and Methods). This leads to prolonged muscarinic inhibition of the LTS model. (C) The activation of cortical and thalamic inputs in the cholinergic and low-threshold spiking interneuron network. The thalamic input (20 Hz for 700 ms, every 3 s, light blue line) was activated with a cortical input (3 s with an average rate of 20 Hz), before the thalamic bursts. (C) The response of the ChIN model to this activation scheme with pauses of varying length due to thalamic activation as well as NO-mediated depolarization (brown asterisk indicates LTS frequency checker activation, see Materials and Methods in Paper II). (C1) The LTS model responds with an initial increase in spiking rate due to cortical activation. This is followed by a prolonged muscarinic inhibition which is converted into a burst pattern here due to recurring thalamic activation of the ChIN model (A)(A1). (From Paper II).

Paper II resulted in the development of NO and M4R models for ChINs and LTS interaction and the effect of slow neuromodulatory action within the striatum. The NO model incorporated a *frequency checker* which caused the ChIN model to only respond to bursts of LTS activity. This is consistent with the report that high-frequency stimulation (HFS) of cortical areas can produce an increase in NO levels in the striatum (Ondracek et al., 2008; Sammut et al., 2007). Activation of D1-like receptors has also been shown to increase levels of NO (and GABA) within the striatum (Harsing & Zigmond, 1997). The interaction between neuromodulators is an interesting topic for large-scale simulations, due to the multiple effects on network activity including synaptic plasticity (Nadim & Bucher, 2014). This prompted the expansion and generalization of the dopaminergic modulation presented in Paper I, which resulted in the software *Neuromodcell* and additional simulation classes within *Snudda* developed in Paper III and applied on the striatal microcircuit in Paper IV.

## 4.3 Introducing large-scale neuromodulation within the striatal microcircuit *in silico* (Paper III)

The aim of Paper III was to generalize the formalism and simulation methods for neuromodulation developed in Lindroos et al. (2018) and Paper I beyond dopamine. Hence, the *in silico* striatal microcircuit could, following the developments in Paper III, simulate a range of neuromodulators, either individually or simultaneously. The formalism is influenced by Lindroos et al. (2018) and Paper I but combined the creation of the models into the software *Neuromodcell*, expanded the number and shapes of simulated transients, and the possibility for several neuromodulators. Figure 25 shows the components of *Neuromodcell* which include modulation, protocol, transient, and selection. The *modulation* defines the changes elicited in the ion channel or receptor models by the specific neuromodulator (Figure 25). The protocol (current or voltage clamp) and the selection describe the experiment which the software will simulate to select the appropriate sets of modulation parameters. Finally, the transient within an experimental setup would generally be a bath application of an agonist or antagonist, but other transients are possible (Figure 25). Hence, *Neuromodcell* can simulate a bath application of a neuromodulator which would induce the changes defined under *modulation*. Following the selection by *Neuromodcell*, the populations of *modulation* sets were incorporated for each model within the database presented in Paper I.
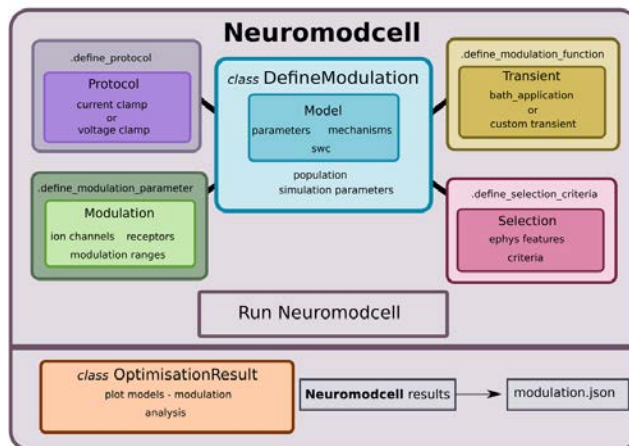


Figure 25: *Neuromodcell* structure with classes and methods. *Neuromodcell* specifies the model and optimization parameters using the *DefineModulation* class. The associated methods define the protocols, parameters, modulation, and selection criteria for the optimization. Following the simulation, the *OptimisationResult* class assists in loading and analyzing the results and saving the final modulation (modulation.json). (From Paper III).

### 4.3.1 Creating models of dopaminergic modulation

Figure 26 shows an example of a dSPN model with dopaminergic (D1) modulation and the validation of the response. The modulations by dopamine D1 receptor on dSPN were collected following an extensive literature review in Lindroos et al. (2018) and Paper I, with additional modulation included in Paper III. In Figure 26A, the black trace represents the model without any modulation. The modulation was simulated within the same model and the *modulation* sets which passed validation are plotted in Figure 26A. The selection criterion for the modulation is plotted in Figure 26B, which shows the modulated models in black and the control model in green. The dopaminergic modulation increases the

excitability of dSPN via D1 receptors. The procedure was repeated for dSPN, iSPN, FS, LTS, and ChIN for both dopamine and acetylcholine, with specific virtual experiments for neuron type and neuromodulator.
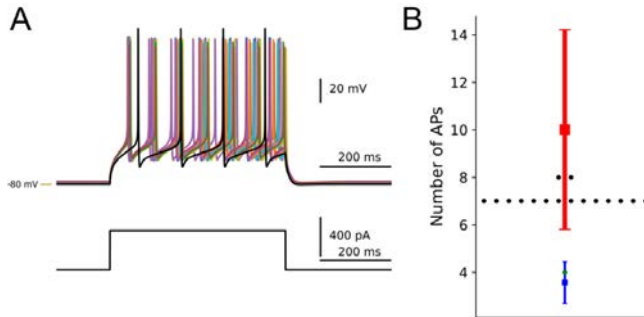


Figure 26: Optimization of dopaminergic modulation of dSPN. By using the *Neuromodcell* package, parameter sets that reproduced the dopaminergic modulation are applied to the multi-compartmental model of dSPNs. (A) Simulation of current clamp recordings of dSPN. Control simulation without dopamine modulation in black and dopamine-modulated simulations which passed the selection criteria (non-black traces). (B) The change in the number of action potentials is compared to control (in green) and the parameter sets which are passed in black. The mean and standard deviation of the control behavior from Planert et al. (2013) is in blue, and the DA-modulated mean and standard deviation are in red. –80 mV marked by the yellow line. (From Paper III).

### 4.3.2 Transients and site-specific modulation

In Paper I, the dopaminergic modulation was simulated throughout the striatal microcircuit. The transient is equivalent to a homogeneous change throughout the network although different neurons such as dSPNs and iSPNs express different receptor subtypes (D1 and D2) and will respond in different ways. However, recent evidence has indicated that the relationship between the activity of dopaminergic neurons and the release might not be in a 1:1 relation; and local regulation of dopamine can occur in the striatum both via presynaptic facilitation and inhibition (Cragg, 2006; Exley & Cragg, 2008; Hartung et al., 2011; Holly et al., 2021; Rice & Cragg, 2004). Hence, the possibility of local regulation of dopamine would challenge the homogeneous assumption of dopaminergic modulation.

The simulation of a neuromodulator transient within a microcircuit consists of a vector which throughout the simulation changes the *level* of a modulation parameter. This vector is defined before the start of the simulation and, due to the technical limitations of NEURON, cannot be changed during the simulation. Therefore, in addition to the homogeneous transient simulation, another method of neuromodulation was developed, which relies on a site-specific process. A phenomenological implementation of dopamine receptors integrates the spiking activity of a simulated dopaminergic neuron. The dopamine receptor model would regulate the degree of modulation of the ion channel within a specific segment of the model. Therefore, neighboring segments could have different levels of neuromodulator activity (which could also be achieved by the transient method). But additionally, dopamine release can be affected by changes in the receptor or the activity of the dopaminergic neuron model. Hence, allowing for the investigation into the local regulation of dopamine release and its effect on striatal activity.

Figure 27 shows the dopaminergic modulation using the transient method within the striatum and its effect on dSPN, iSPN, and FS. The network consists of 10 000 neurons (Figure 27A) and Figure 27C shows the response of individual dSPN, iSPN, and FS to a transient of dopaminergic modulation which

lasts for approximately 1 s. During the dopaminergic modulation, cortical activation was simulated within the network and the response of dSPN, iSPN, and FS was compared to control (without dopaminergic modulation). Figure 27B shows the increased activity in dSPN and FS while iSPN is slightly inhibited by dopamine. The individual traces show the depolarization in the dSPN and FS models as the modulation level increases (Figure 27C), while the number of action potentials decreases in the iSPN model.
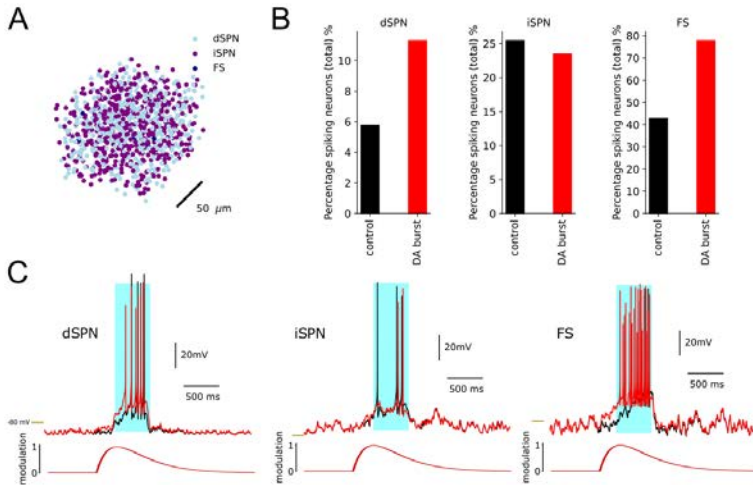


Figure 27: Simulation of dSPN with and without dopamine within a network of 10 000 neurons with 4950 dSPNs and iSPNs and 100 FS. (A) A network of 10,000 neurons. Here we plot the soma positions. A dopamine transient was initiated at 0.5 and a cortical stimulation at 1 s. (B) The response of dSPN with the dopamine modulation is in red and the control is in black. The dopamine modulation causes a depolarization in the dSPN which increases the percentage of spiking dSPNs. The iSPN responded with a decrease in the percentage of spiking neurons, while FS increased. (C) Examples of dSPN, iSPN, and FS models and the response with dopamine modulation (red) and control (black), with cortical stimulation in light blue. –80 mV marked by the yellow line. (From Paper III).

### 4.3.3 Simulating multiple neuromodulators – dopamine and acetylcholine

Within the striatum, or any part of the brain, there is a combination of neuromodulators interacting at any point in time. The experimental techniques are becoming more and more sophisticated including the ability to monitor the levels of neuromodulators *in vitro* and *in vivo* with sensors such as Dlight (Jing et al., 2020; Leopold et al., 2019; Patriarchi et al., 2018). The large-scale network simulations can aid in understanding how these neuromodulators interact and modulate the circuit alone and simultaneously, with a combined single neuron and network-level perspective. Hence, Figure 28 demonstrates how the developments in *Snudda* can be applied to large-scale neuromodulation with dopamine and acetylcholine. Several papers have demonstrated the variety of transients of dopamine and acetylcholine during behavior (Howe et al., 2019). Figure 28A shows a burst and pause transient of acetylcholine and a burst of dopamine. The muscarinic modulation of dSPN is dependent on muscarinic M1 and M4 receptors while iSPN expresses only muscarinic M1 receptors. The combined modulation of dopamine and acetylcholine changed the response of the network with the basal acetylcholine causing an increased excitability of both dSPN and iSPN. The muscarinic M1 receptor effect reduced the inhibition by the dopamine D2 receptor in iSPNs (Figure 28C).

46

In Paper III, the methods for simulating large-scale neuromodulation were developed further to include a pipeline for creating models for any neuromodulator within both multi-compartmental models and receptor models. Recent publications have shown further presynaptic and postsynaptic modulation within the striatum by serotonin, dopamine, and adenosine (Burke & Alvarez, 2022; Krok et al., 2022; Ma et al.). With the current formalism, these studies and others could be incorporated into the striatal microcircuit *in silico* to uncover the implications of these neuromodulators on striatal activity. The results of Paper III were applied in Paper IV to investigate the impact of dopaminergic modulation on the interaction between populations of dSPN and iSPN.
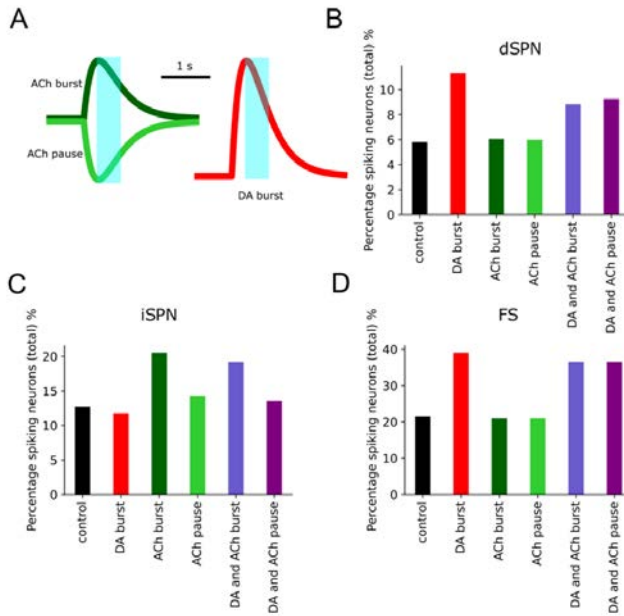


Figure 28: Simulation of five neuromodulation scenarios involving dopamine and acetylcholine in a network of 10,000 neurons, 4950 dSPNs and iSPNs, and 100 FS. The network received a cortical simulation at 1 s, for 500 ms. (A) Examples of the acetylcholine (ACh) burst and pause transients and the dopamine burst transient. In light blue, the timing of the cortical activation is in relation to the transients. The percentage of spiking neurons is measured during the cortical simulation. (B) The response of dSPNs in the five neuromodulation scenarios, where dopamine (DA; red) produced the largest effect. The ACh burst and pause (light and dark green) and combinations of DA burst and ACh burst and pause (light and dark purple, respectively). (C) The response of iSPNs in the five neuromodulation scenarios and (D) the response of FS. (From Paper III).

## 4.4  The role of intrastriatal inhibition within the striatal microcircuit (Paper IV)

The aim of paper IV was to investigate the role of intrastriatal inhibition and its effect on the activity of dSPN and iSPN. *Snudda* was used to create networks of up to 40 000 neurons, which correspond to the size of the forelimb module in the mouse dorsal striatum (Figure 29A). As described in Figure 5, the input onto SPN is distributed differently depending on the presynaptic source. The corticostriatal and thalamostriatal input target the distal dendrites of SPNs whereas the FS targets the soma and proximal dendrites. Several of the interneurons and SPNs collaterals also target the distal dendrites (Figure 29B; Paper I and Figure 10). The distance-dependent connection probability results in a spatially limited

impact from a focal activation of SPNs (Figure 29C). Figure 29Di shows the striatal microcircuit with the axonal and dendritic arborizations. A pair of iSPN and dSPN with four synapses (Figure 29Dii-iii) and the targeting of SPN collaterals to more distal dendrites.
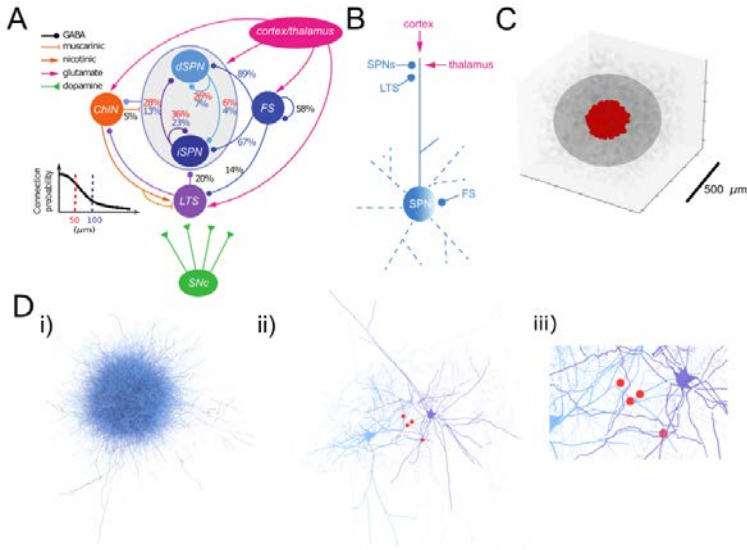


Figure 29: Connectivity of the striatal microcircuit, the distribution of inputs to SPNs, and axonal and dendritic arborization of SPNs. (A) The striatal model contains dSPNs, iSPNs, FS, LTS, and ChINs. The striatal microcircuit receives input from the cortex and thalamus and dopaminergic modulation from the substantia nigra pars compacta (SNc). The connection probability between pairs of neurons in red and blue, shows the probability within an inter-pair distances of 50 and 100 μm, respectively. (B) The GABAergic inputs to SPNs are organized with FS synapses located on proximal dendrites and the soma, while the cortical and thalamic input as well as the GABAergic input from SPNs and interneurons such as the LTS target distal dendrites. (C) The axons of a population of SPNs (red) project extensively into the surrounding striatal microcircuit within a limited area as indicated by the sphere (light gray). (D) i) Axons and dendrites of a population of neurons within the striatum, ii) Two SPNs connected by four synapses (red circles), and iii) High magnification of the synapses between the pair in ii (see Methods). (From Paper IV).

## 4.4.1    The extent of the intrastriatal inhibition

The effect on the distal dendrites of surrounding SPNs was investigated by focal activation of a small population of SPNs. Figure 30A shows the stimulation of the population (in blue) and the effects on the surrounding (postsynaptic neurons). The stimulation caused a depolarization (Figure 30B) as the resting membrane potential of SPN was below the reversal of GABA. The effect was varied with the maximal depolarization of 11 mV (Figure 30C). The mean depolarization per postsynaptic neuron was dependent on the distance from the focal activation (Figure 30D). This is consistent with the distance-dependent connection probability as postsynaptic neurons further away from the center would receive fewer synapses.
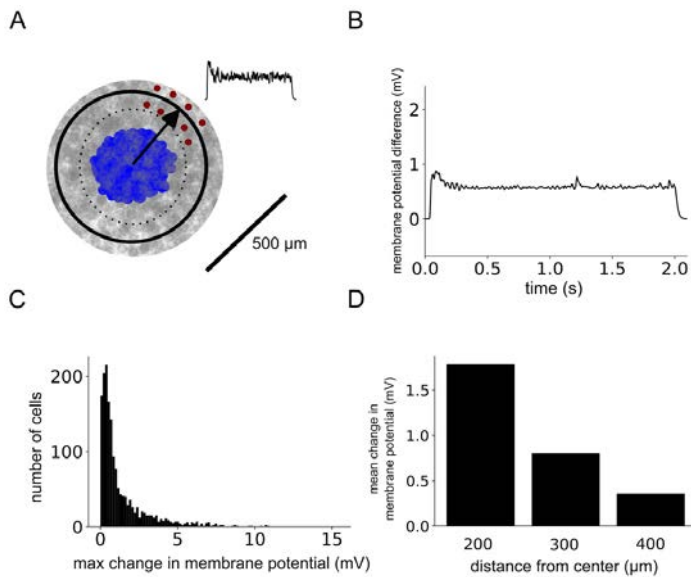
Figure 30: The surround inhibition of SPNs around a population of 350 active SPNs. (A) The SPN synapses are positioned on the distal dendrites of other SPNs. A population of activated 350 SPNs (in blue) produces a depolarizing effect on surrounding postsynaptic SPNs at different distances from the cell cluster. (B) The average dendritic membrane potential during the focal stimulation of postsynaptic SPNs. The activation of these neurons produces depolarization of the distal dendrites of the SPN, as the resting membrane potential on distal dendrites is below the GABA reversal. (C) The maximum peak of the depolarization during the focal stimulation. The largest depolarization caused by the activation is 11 mV, while the majority of depolarizations are below 5 mV. (D) The average change in dendritic membrane potential with increasing distance from the population unit center (between 150-250, 250-350, and >400 μm). (From Paper IV).

### 4.4.2 Dendritic integration, shunting inhibition, and plateau potentials

Shunting inhibition is an important feature of dendritic processing, and it can regulate the impact of the excitatory glutamatergic input. The population (in blue) from Figure 30A was stimulated for 2 s with simulated corticostriatal input. The simulation was repeated with inhibition and with only inhibition (no corticostriatal input). Figures 31A and 31C show the response within the dendrites of the SPN (current and voltage clamp mode, respectively). The excitatory corticostriatal input in isolation (black trace) depolarized the SPNs on average. The area-under-the-curve (AUC) of the response in Figure 31A was quantified with and without inhibition (Figure 31B, D). The inhibition reduced the response by 60% both in current and voltage clamp mode. Hence, the inhibition from surrounding SPNs can effectively shunt the cortical input and reduce the amplitude of the excitatory input onto SPNs.
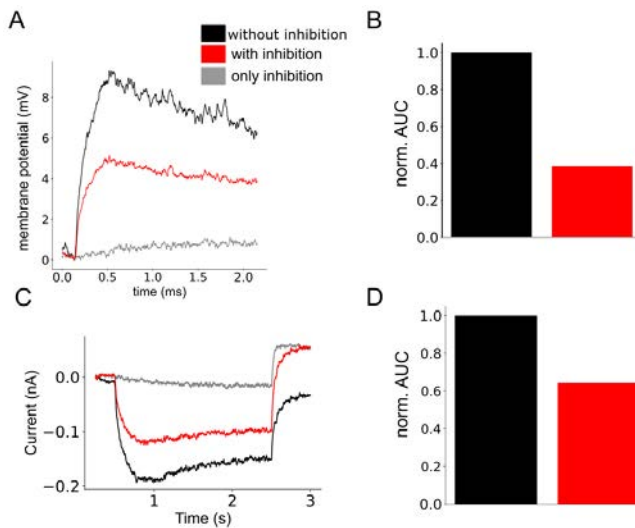
Figure 31: Shunting of corticostriatal EPSPs within a population of 350 SPNs (A) A simulation with corticostriatal activation of the population unit, without inhibition, with inhibition and only inhibition from the surrounding population (in black, red, and gray, respectively). The average membrane p (B) The area under the curve (AUC) is reduced following the activation of presynaptic SPNs and shows the effect of shunting inhibition on dendritic membrane potential. (C) The simulation in (A) with a voltage clamp on each neuron within the population of SPNs shows the effect of inhibition on the size of the current. (D) The quantification using AUC of the current response with and without inhibition (black and red, respectively). (From Paper IV).

Another important feature of SPNs is the generation of plateau potentials in response to the activation of clustered input on distal dendrites (Du et al., 2017). A network of 40 000 neurons (Figure 32A) was generated to investigate the effect of intrastriatal inhibition on the plateau potentials. Within the network, 1000 SPNs were selected at random and plateau potentials were induced in the distal dendrites by clustering 20 synapses (Figure 32A). The plateau potentials were simulated with and without the activation of the surrounding SPNs. This would simulate the effect of the inhibition which is generated following the activation of surrounding SPNs (Figure 32B, C). Firstly, the response in the dendrites of the selected SPNs (Figure 32A) showed shunting of the plateau potentials (Figure 32D, on average 20%). However, within a specific section of the dendrite, the inhibition can exert a dual effect on the plateau potentials. The resting membrane potential in the dendrites of the SPNs can vary and be both above and below the reversal potential of GABA ( -65 mV). This will influence the impact of the SPN input and result in both depolarizing and inhibiting responses. When the membrane potential is more negative than the reversal of GABA, the activation would initially be depolarizing and could thereby facilitate the induction of plateau potentials. This resulted in a dual response in the plateau potentials recorded in 1000 SPNs. One population was inhibited by the SPN activation while another population was enhanced by the inhibition (Figure 32E), and the same was observed in the NMDA current (Figure 32F). The simulations in Figures 31 and 32 demonstrate the variety of responses to intrastriatal inhibition.
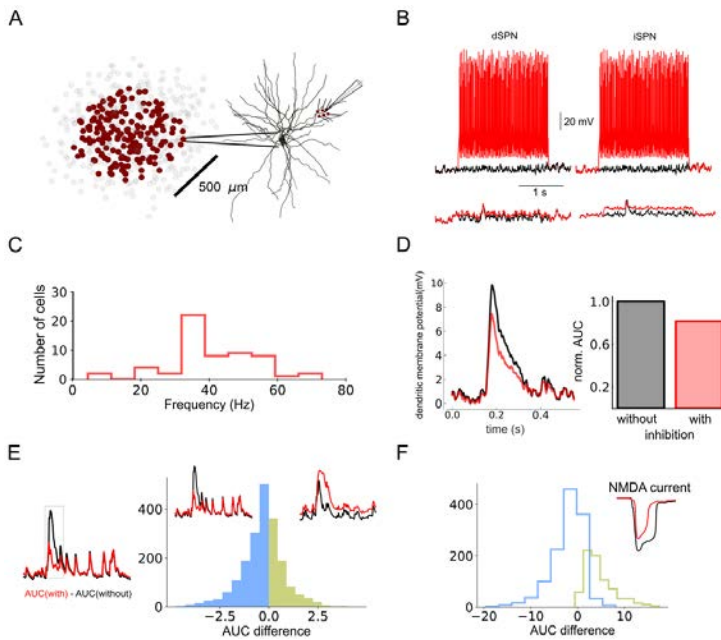
Figure 32: Plateau potential in SPNs. (A) A simulation of 20 000 neurons where a selected population (1000 neurons, in dark red) received a corticostriatal clustered input on distal dendrites. (B) A second population of SPNs could be activated with an additional current injection to the surrounding neurons (red). The dSPN and iSPN with plateaus show a small depolarization in the somatic compartment (in black) with a depolarization in red following the inhibition. (C) The distribution of firing frequencies of the presynaptic SPNs. (D) The mean dendritic depolarization was compared with and without inhibition. This showed that the inhibition causes an overall shunting of the dendritic potentials in all dendrites of these SPNs (without and with inhibition, in black and red, respectively). (E) A histogram of the Area Under the Curve (AUC$_{diff}$) with and without inhibition. An example of a dendritic plateau potential, which was reduced in amplitude is shown in the left panel, and in the right panel a facilitation of a plateau potential (in light blue and green, respectively). (F) The NMDA current within the clustered synapses with and without inhibition. A histogram of the AUC$_{diff}$ was calculated for the negative and positive populations in light blue and green, respectively. In the right panel, an example of the NMDA current is reduced by inhibition. (From Paper IV).

### 4.4.3   The competition between populations – the contribution of dopamine

During movement, populations of SPNs have been recorded and correlated with different body movements and behavioral parameters and manipulation of SPNs has been shown to affect task performances (Klaus et al., 2019). Within the network, population units were created (see *Materials and Methods*) and activated to investigate to what extent populations of neurons within the striatum can interact and suppress each other. Figure 33A shows a schematic of the simulations performed, where a single population unit was stimulated (in red) followed by a simulation with both units (in blue and red). The population unit, P1, was activated with different strengths while the second population unit (P2) had a higher activity (40 Hz). The simulation was repeated with 3, 5, and 10 Hz activity of P1 and the suppression was measured by the percentage of active neurons in P1. Figure 33 demonstrates the reduction in P1 following P2 activation, which is dependent on the strength of the P1 population. Hence, populations of neurons within the striatum can suppress each other which depends on the relative strength of activation.
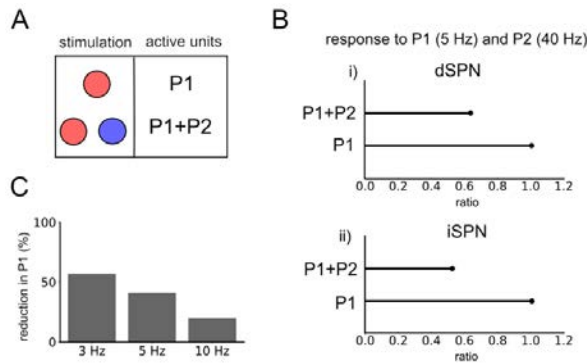
Figure 33: Competing population units – the effect on the activity of a population unit when another unit is activated. (A) The population unit P1 (red) is activated alone and together with another unit P2 (blue). (B) The number of spiking neurons within a population of SPNs before and after the activation of a competing population unit, active at 40Hz. I) dSPN and ii) iSPN. (C) The percentage of inhibited neurons in P1 (3, 5, and 10Hz) following the activation of a competing unit (P2), with increasingly weaker activation of the population unit. (From Paper IV).

In paper III, the simulation of dopaminergic modulation was generalized within *Snudda* and here the improvement was used to investigate the role of dopamine within the competition between populations of neurons. Figure 34A shows a simulation with the dopamine drive (red) and the cortical drive (in blue), which lasted for 500 ms. The simulations were performed as described in Figure 33A, where a population (P1) was stimulated with and without the activation of a second population unit (P2). The dSPNs in P1 are markedly excited by dopamine (Figure 34B). As in Figure 34, the activation of P2 reduced the activity of SPNs within P1 (in black and blue). The dopamine and the P1+P2 simulations were repeated in four trials, which resulted in only P1, P1+DA, P1+P2, and P1+P2+DA. With a concurrent P1+dopamine, the response of dSPN was increased while the response of iSPN was reduced (due to the D1 and D2 receptor expression) (Figure 34C). The competition between P1 and P2 reduced the activity of dSPN and iSPN (P1), while the competition was changed in the P1+P2+DA simulation. Dopamine caused an excitation of the dSPNs (P1) which competed against the inhibition produced by P2, while the inhibition was further enhanced in P2 for iSPN.
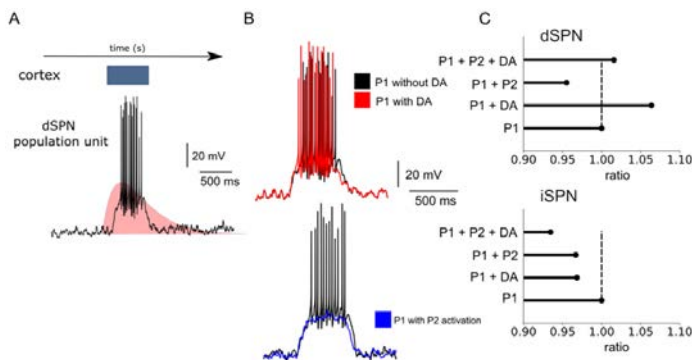


Figure 34: Dopaminergic modulation of competing population units. (A) The simulation consisted of cortical and thalamic background activation throughout the simulation and a cortical command given to each population unit. In a set of simulations, a dopaminergic transient (red) was activated within the circuit. (B) In the top panel, an example of the response of a dSPN to a cortical command with and without dopamine (in black and red,

respectively). In the bottom panel, the response of a dSPN within the P1 with and without the activation of the secondary population unit (P2, in blue). (C) A summary of the four simulations with the primary population unit (P1, with and without dopamine) and following the activation in the secondary population unit (P2, with and without dopamine) within dSPNs and iSPNs. (From Paper IV).

### 4.4.4 The effect of ablations within the large-scale striatal network

Having the striatal network active, we investigated the effect at the network level of removing connectivity of certain neurons, by simply removing synapses between neuron types (ablation). The whole network was activated using current injection for 2.0 or 0.5s. The network was then ablated with SPN, FS, and a complete ablation (left and right graph in Figure 35A). The SPN ablations showed that the SPN surround inhibition affects network activity for both dSPN and iSPN (Figure 35B1, B2). The SPNs are the major cell type in the striatum hence the ablation of SPN connections would cause a large impact, although pairs of SPN are sparsely connected (Figures 15 and 19). The activity of dSPN and iSPN were measured and Figures 35B/C2 demonstrate that both SPN and FS ablation affected the network, although the SPN ablation dominated. The FS ablation produced an interesting effect in both dSPN and iSPN, where the initial response was strong (Figure 35B3, C3). This demonstrates the short-term plasticity within FS-SPN synapses (Figure 35B3), which results in a larger effect of FS ablation during the shorter stimulation (Figure 35C3). Although the SPN ablation had the largest effect on network activity; during normal behavior, the whole population of SPNs is not active. Hence, feedforward inhibition provided by FS could dominate especially for spike-timing and initiation.
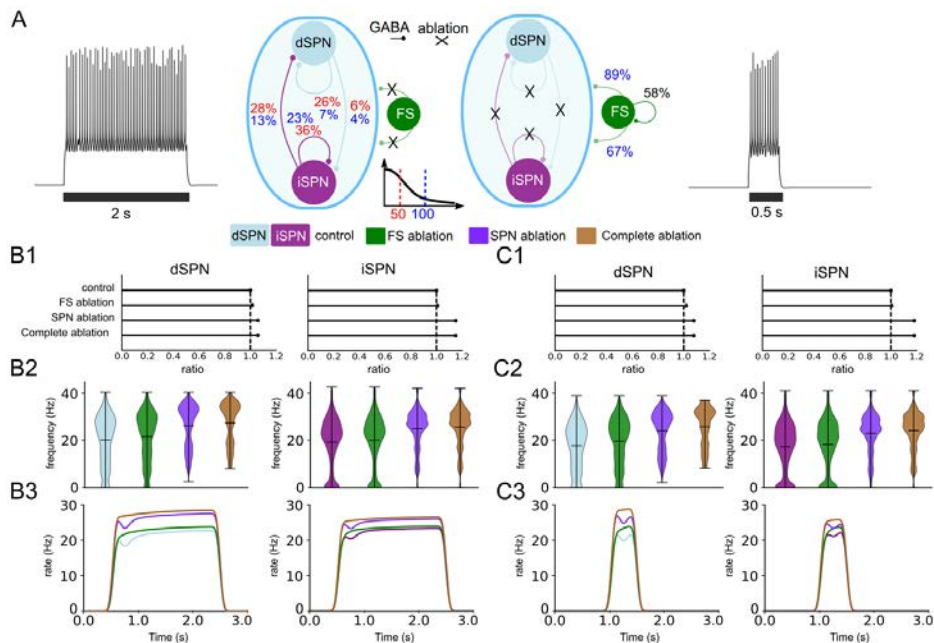


Figure 35: Ablation of intrastriatal connections (A) The activation of a network of 20 000 striatal neurons during 2 and 0.5 seconds with the SPN-SPN and FS-SPN ablations. (B1) The ratio of spiking neurons within the population compared to control in each ablation group for the simulation period of 2 seconds. The dotted line shows the response of the control network (completely connected). (B2) The average firing frequency of dSPN and iSPN within each ablation group (control, FS ablation, SPN ablation, and complete ablation). (B3) The instantaneous rate of dSPN and iSPN during the activation in each ablation group. (C1) The ratio of spiking neurons within the population compared to control in each ablation group for the simulation period of 0.5 seconds. The dotted line shows the response of the control network (completely connected). (C2) The average firing

frequency of dSPN and iSPN within each ablation group (control, FS ablation, SPN ablation, and complete ablation). (C3) The instantaneous rate of dSPN and iSPN during the activation in each ablation group. (From Paper IV).

In summary, paper IV utilized the striatal microcircuit *in silico* in *Snudda* to investigate the impact of intrastriatal inhibition on populations of SPNs. The study required the refinement of the ablation feature and the construction of external input within *Snudda*. Following the inclusion of these features, the research question was investigated by modifying the external input, the activity of the striatal SPNs through current injection, and dopaminergic modulation. The simulations demonstrated the impact of intrastriatal inhibition. The collaterals within the striatum can shunt incoming corticostriatal input onto SPNs during long stimulations. The generation of plateau potentials was also modified by intrastriatal inhibition, which resulted in both enhancement and suppression (depending on the GABA reversal). The activation of populations of neurons can cause suppression, which is dependent on both the strength, the size, and the position of population units (see Paper IV for details). The competition between neurons was modified by dopaminergic modulation according to the expression of D1 or D2 dopamine receptors (dSPN and iSPN, respectively). The impact of the intrastriatal inhibition will depend on the source and in part on the short-term plasticity of the GABAergic synapses (see Figure 10). The SPN collaterals within the striatum are sparse and target distal dendrites, but further investigation is needed into the dependence on the GABA reversal and the contribution from other distally-targeting interneurons.

# 5 DISCUSSION & PERSPECTIVE

The striatum is the main input nucleus of the basal ganglia. The role of the striatum and the striatal microcircuit has been investigated in several studies, both *in vitro* and *in vivo* during behavior (Klaus et al., 2018; see Introduction). These studies have demonstrated important features of the striatum which could contribute to understanding its role in the basal ganglia and the control of movement. Some of these features are the two main types of neurons, the striatal projection neurons, the diversity of interneurons that target SPN with varying degrees, synaptic dynamics, and somatic-dendritic position, and the numerous external sources of input to the striatum including cortex, thalamus, and PPN. Lastly, the dorsal striatum is modulated extensively by the dopaminergic projections from SNc, which have been shown to affect both movement vigor and action initiation (Klaus et al., 2019). This combination of neural subtypes, connectivity, glutamatergic and GABAergic synaptic transmission, and dopaminergic modulation results in a complex network of interactions that could modify the state and response of dSPNs and iSPNs (as the sole output of the striatum). The aim of this thesis was to create a tool and methodology to incorporate data from both single neuron and network levels, and investigate the striatal network *in silico* by simulating and modifying the microcircuit to unravel the role of the intrinsic properties of the neuron types and the impact of network connectivity.

**Paper I** presented *Snudda*, a Python Package, for creating, simulating, and analyzing detailed large-scale networks of multi-compartmental models. Multi-compartmental models of dSPN, iSPN, FS, LTS, and ChIN were based on electrophysiological recordings and reconstructions of the neuronal morphology. The models were optimized using *BluePyOpt* and the validated models were incorporated into a database of models, which is utilized by *Snudda* to construct the *in silico* striatal microcircuit. The connectivity within the microcircuit is constrained by experimental data through a process called touch detection. The external input and intrastriatal inhibition were modeled with Tsodyks-Markram models and the model parameters were optimized and fitted to match experimental data. In Paper I, the striatal microcircuit was simulated with cortical and thalamic input and dopaminergic modulation. This demonstrated that the network can be modified and simulated with different inputs and under different scenarios, which is the method applied in the subsequent projects.

The striatal microcircuit presented in Paper I represented 98% of the neuron types within the striatum. But, as shown in Figures 5 and 10, there is a diverse population of interneurons within the striatum. These interneurons have different impacts on SPNs, especially the ones targeting distal dendrites like NGF-NPY interneurons (Ibáñez-Sandoval et al., 2011). Additionally, the ThIN provides a disynaptic inhibition of LTS via its activation from the thalamus. ThINs are also involved in the disynaptic inhibition of ChINs, which is a source of common inhibition within the ChIN population (Dorst et al., 2020; Sullivan et al., 2008). Furthermore, in Paper I, the density of neurons within the network was assumed to be homogeneous. Studies (Steiner & Tseng, 2016) have demonstrated that FS, LTS, and ChIN are distributed differently throughout the whole striatum. Another factor is the subdivision of the striatal volume into matrix and striosomes. These compartments demonstrate different properties and have different external inputs (Eblen & Graybiel, 1995; McGregor et al., 2019), which could affect the interaction within the striatum.

In Paper I, the multi-compartmental models of SPN were simulated without dendritic spines. In previous publications, similar models included spines, but due to the computational costs, the spines were excluded at this stage. Although, the conclusions of Paper IV highlight the importance of dendritic

processing and the effect of clustered input. A recent study has shown that there is a reorganization of dendritic spines following learning (Hwang et al., 2022). The introduction of dendritic spines would be important to investigate the interaction between glutamatergic and GABAergic input along the distal dendrites of SPNs. Furthermore, in Paper I, long-term synaptic plasticity was not implemented within the glutamatergic and GABAergic receptor models. Synaptic plasticity is critical for learning and is known to be modified by dopamine and other neuromodulators (Citri & Malenka, 2008). Previously, receptor-induced signaling cascades have been modeled within dSPNs (Lindroos et al., 2018) and the interaction between dopamine and acetylcholine at dSPN spines (Nair et al., 2015). Hence, these models could be incorporated into the striatal microcircuit *in silico*, although they would affect the computational efficiency and would require extensive code optimizations and careful implementation.

Lastly, the external input from the cortex and thalamus was distributed according to experimental estimates. Although, the axonal projections from the cortex and thalamus arborize differently depending on the neuron type or source. The IT projections from the cortex target bilaterally and arborize extensively while the PT neurons project ipsilateral and make sparse focused arborizations in the striatum (Kress et al., 2013; Reig & Silberberg, 2014). The extent of the axonal arborizations would affect the number of activated neurons and the position of these neurons. The striatal microcircuit could incorporate reconstructions of IT and PT neurons to simulate and predict their effect on the striatal microcircuit.

**Paper II** investigated a network of ChIN and LTS and the impact of NO and ACh. The project required the implementation of a frequency-dependent NO model to model the slow depolarization of ChINs, following NO release from LTS (Elghaba et al., 2016). The M4R model was taken from Blackwell et al. (2019) and was connected to the KIR current in the LTS model. In the present model, NO release was simulated through cortical activation of the LTS model.

The neuromodulators released within the striatum have been shown to affect microcircuit activity and synaptic plasticity at corticostriatal synapses onto SPNs (Abudukeyoumu et al., 2019; Colangelo et al., 2019; Garthwaite, 2008; Haam & Yakel, 2017). The phenomenological model of NO in Paper II prevents the investigation into the role of synaptic plasticity. The nitric oxide model would have to be implemented similarly to the M4R model (Blackwell et al., 2019). The interaction between ACh and NO has been reported in several studies. Blomeley et al. (2015) demonstrated that nitrergic and cholinergic transmission can control glutamatergic transmission onto SPNs. Muscarinic modulation of SPN consists of both M1 and M4 receptors for dSPN and only M1 receptor modulation for iSPNs (Galarraga, Herna, et al., 1999). The prolonged depolarization of ChINs, following NO release, would modulate both dSPN and iSPN. Additionally, the pause in ChIN activity following thalamic activation can hyperpolarize (due to the reduced M1R activation) as shown by Zucca et al. (2018). Moreover, the nicotinic modulation of dopaminergic terminals can affect dopamine release within the striatum (Threlfell & Cragg, 2011). Calabresi et al. (1999) and others have demonstrated the necessity of NO for LTD at corticostriatal synapses onto SPNs. As mentioned above, the signaling pathways involved in LTD and LTP require a different type of model and additional modification of the striatal microcircuit *in silico*. These simulations would introduce challenges in both the implementation and the analysis of synaptic plasticity in detailed large-scale simulations.

In **Paper III**, the large-scale neuromodulation introduced in Paper I and Lindroos et al. (2018) was developed further. The new software *Neuromodcell* combined the steps of previous publications and prepared for the inclusion of any neuromodulator into the striatal microcircuit *in silico*. The

neuromodulation focused on the specific modulation of receptors and ion channels. This method of simulating large-scale neuromodulation can incorporate the advancements in biosensor technology, such as Dlight and other sensors (Leopold et al., 2019). The present model included dopamine and acetylcholine transients, but serotonin and other neuromodulators could be included by supplying *Neuromodcell* with the appropriate modulations and experimental protocols.

Several neuromodulators are released within the striatum including DA, ACh, 5-HT, histamine, endocannabinoids, and norepinephrine (Benarroch, 2009; Bolam & Ellender, 2016). The receptors are expressed on both pre- and post-synaptic sites within the striatum. Certain neuromodulators such as DA, ACh, and serotonin are important for understanding Parkinson's disease and other basal ganglia disorders like L-DOPA-induced dyskinesia. Serotonin is released from projections that originate in the raphe nucleus (Benarroch, 2009). The effects of serotonin are diverse with both pre- and post-synaptic excitation and depression. Serotonin induces LTD at corticostriatal synapses (Mathur & Lovinger, 2012). LTS are inhibited by 5-HT, while FS are excited (Blomeley & Bracci, 2009; Cains et al., 2012). Serotonin has opposite effects on ChIN in the ventral and dorsal striatum (Virk et al., 2016). Fischer & Ullsperger (2017) reviewed both animal and human studies concerning the interplay between 5-HT and DA. They conclude that the interaction is extensive and complex, and that certain reward behaviors require the interplay of 5-HT and DA. In general, the studies demonstrate the complex dependence between different neuromodulatory systems; but also highlight the necessity of studying these neuromodulators together.

In **Paper IV**, the effect of the GABAergic surround inhibition within the striatum was investigated. The majority of the corticostriatal and thalamostriatal projections target the distal parts of the dendritic trees of SPNs, whereas FS targets the soma and proximal dendrites (Figure 29). The GABAergic inputs onto the distal dendrites of SPNs come from SPNs, LTS, and other interneurons. The roles of these GABAergic inputs are technically difficult to investigate experimentally, but possible to explore *in silico*. We could show that the SPN-induced inhibition could exert a marked effect by shunting the excitatory input from the cortex/thalamus at the level of the distal dendrites. Additionally, the plateau potentials in distal dendrites could be suppressed by surround inhibition, but also facilitated if the initiation of the inhibitory input started below the reversal potential of GABA. The timing of the inhibition was not fine-tuned to the excitatory input, which could change the effect of inhibition on the plateau potentials. Studies have shown that timed inhibition is sufficient to shorten plateau potentials and additionally affect calcium transients in dendrites (Dorman et al., 2018; Du et al., 2017).

By simulating competing populations of SPNs, we could show that the surround inhibition can suppress the weaker of the two population units, and these effects were further amplified by dopaminergic modulation and the effects exerted on dSPNs and iSPNs. Furthermore, the SPN-induced surround inhibition is limited by the length of the axonal ramifications which extends around 250 μm. Within the whole striatum, the surround inhibition from a focal activation of SPNs could have profound effects within a striatal module such as the forelimb area (Figure 4), but it cannot exert an overarching control of patterns of behavior involving different parts of the body such as fore- and hind-limbs or jaws, since these striatal modules are too far away.

*Snudda* has been developed continuously since the publication of Paper I; based on the research questions of the subsequent projects. In the current thesis, the focus was the neuromodulation within the striatum (DA, NO, and ACh, specifically) and the intrastriatal inhibition. There are several other paths to investigate, both within and outside the striatal microcircuit. *Snudda* is not limited to simulating the

striatal microcircuit *in silico.* The long-term goal is to integrate all the nuclei of the basal ganglia, which has partially been achieved for the fore-limb channel (Figure 4). The GPe sends GABAergic projections to the striatum, but together with SNr/GPi and STN, create a complex inter-connected network with important implications in normal function and PD. The inclusion of these nuclei with detailed multi-compartmental models will give a single neuron and network perspective, like the striatum *in silico* has achieved, and will also include the basal ganglia output level.

In conclusion, the work presented in this thesis has provided an initial development and investigation into the important interactions within the striatal microcircuit. It has highlighted the importance of both single-neuron and network-level understanding, the characterization of external and intrinsic connectivity, and the complex interaction between neuromodulators. The results presented here can supply a basis for introducing new components of the striatal microcircuit; to investigate their effect on the dendritic processing within SPN and the modulation by multiple neuromodulators at both single neuron and network-level activity.

# 6 ACKNOWLEDGMENTS

my best support and friend, although we have chosen quite different paths in life, we have so much to share and support each other in. Let's see what the next adventure will bring!

*Bryt upp, bryt upp! Den nya dagen gryr. Oändligt är vårt stora äventyr.*

# 7 REFERENCES

Abudukeyoumu, N., Hernandez-Flores, T., Garcia-Munoz, M., & Arbuthnott, G. W. (2019). Cholinergic modulation of striatal microcircuits. *European Journal of Neuroscience*, *49*(5), 604–622. https://doi.org/10.1111/ejn.13949

Akins, P. T., Surmeier, D. J., & Kitai, S. T. (1990). Muscarinic modulation of a transient K+ conductance in rat neostriatal neurons. *Nature*, *344*(6263), 240–242. https://doi.org/10.1038/344240a0

Albin, R. L., Young, A. B., & Penney, J. B. (1989). *The functional anatomy of basal ganglia disorders*.

Amemori, K., & Graybiel, A. M. (2012). Localized microstimulation of primate pregenual cingulate cortex induces negative decision-making. *Nature Neuroscience*, *15*(5), 776–785. https://doi.org/10.1038/nn.3088

Antic, S. D., Zhou, W. L., Moore, A. R., Short, S. M., & Ikonomu, K. D. (2010). The decade of the dendritic NMDA spike. In *Journal of Neuroscience Research* (Vol. 88, Issue 14, pp. 2991–3001). https://doi.org/10.1002/jnr.22444

Aosaki, T., Miura, M., Suzuki, T., Nishimura, K., & Masuda, M. (2010). Acetylcholine-dopamine balance hypothesis in the striatum: An update. In *Geriatrics and Gerontology International*. https://doi.org/10.1111/j.1447-0594.2010.00588.x

Aosaki, T., Tsubokawa, H., Ishida, A., Watanabe, K., Graybiel, A. M., & Kimura, M. (1994). Responses of tonically active neurons in the primate's striatum undergo systematic changes during behavioral sensorimotor conditioning. *Journal of Neuroscience*, *14*(6), 3969–3984. https://doi.org/10.1523/jneurosci.14-06-03969.1994

Apicella, P., Legallet, E., & Trouche, E. (1997). Responses of tonically discharging neurons in the monkey striatum to primary rewards delivered during different behavioral states. *Experimental Brain Research*, *116*(3), 456–466. https://doi.org/10.1007/PL00005773

Apicella, P., Ravel, S., Deffains, M., & Legallet, E. (2011). The role of striatal tonically active neurons in reward prediction error signaling during instrumental task performance. *Journal of Neuroscience*, *31*(4), 1507–1515. https://doi.org/10.1523/JNEUROSCI.4880-10.2011

Appukuttan, S., Brain, K. L., & Manchanda, R. (2017). Modeling extracellular fields for a three-dimensional network of cells using NEURON. *Journal of Neuroscience Methods*, *290*, 27–38. https://doi.org/10.1016/j.jneumeth.2017.07.005

Ascoli, G. A., Donohue, D. E., & Halavi, M. (2007). NeuroMorpho.Org: A central resource for neuronal morphologies. In *Journal of Neuroscience* (Vol. 27, Issue 35, pp. 9247–9251). https://doi.org/10.1523/JNEUROSCI.2055-07.2007

Assous, M., Dautan, D., Tepper, J. M., & Mena-Segovia, J. (2019). Pedunculopontine glutamatergic neurons provide a novel source of feedforward inhibition in the striatum by selectively targeting interneurons. *Journal of Neuroscience*, *39*(24), 4727–4737. https://doi.org/10.1523/JNEUROSCI.2913-18.2019

Assous, M., Kaminer, J., Shah, F., Garg, A., Koós, T., & Tepper, J. M. (2017a). Differential processing of thalamic information via distinct striatal interneuron circuits. *Nature Communications*, *8*(May). https://doi.org/10.1038/ncomms15860

Assous, M., Kaminer, J., Shah, F., Garg, A., Koós, T., & Tepper, J. M. (2017b). Differential processing of thalamic information via distinct striatal interneuron circuits. *Nature Communications*, *8*(May). https://doi.org/10.1038/ncomms15860

Augustin, S. M., Chancey, J. H., & Lovinger, D. M. (2018). Dual Dopaminergic Regulation of Corticostriatal Plasticity by Cholinergic Interneurons and Indirect Pathway Medium Spiny Neurons. *Cell Reports*, *24*(11), 2883–2893. https://doi.org/10.1016/j.celrep.2018.08.042

Augustinaite, S., Kuhn, B., Helm, P. J., & Heggelund, P. (2014). NMDA spike/plateau potentials in dendrites of thalamocortical neurons. *Journal of Neuroscience*, *34*(33), 10892–10905. https://doi.org/10.1523/JNEUROSCI.1205-13.2014

Avery, M. C., & Krichmar, J. L. (2017). Neuromodulatory systems and their interactions: A review of models, theories, and experiments. *Frontiers in Neural Circuits*, *11*(December), 1–18. https://doi.org/10.3389/fncir.2017.00108

Ball, N., Teo, W. P., Chandra, S., & Chapman, J. (2019). Parkinson's disease and the environment. In *Frontiers in Neurology* (Vol. 10). Frontiers Media S.A. https://doi.org/10.3389/fneur.2019.00218

Bamford, N. S., Wightman, R. M., & Sulzer, D. (2018). Dopamine's Effects on Corticostriatal Synapses during Reward-Based Behaviors. In *Neuron* (Vol. 97, Issue 3, pp. 494–510). Cell Press. https://doi.org/10.1016/j.neuron.2018.01.006

Baufreton, J., Zhu, Z. -T., Garret, M., Bioulac, B., Johnson, S. W., & Taupignon, A. I. (2005). Dopamine receptors set the pattern of activity generated in subthalamic neurons. *The FASEB Journal*, *19*(13), 1771–1777. https://doi.org/10.1096/fj.04-3401hyp

Beatty, J. A., Sullivan, M. A., Morikawa, H., & Wilson, C. J. (2012). Complex autonomous firing patterns of striatal low-threshold spike interneurons. *J Neurophysiol*, *108*, 771–781. https://doi.org/10.1152/jn.00283.2012.-During

Benarroch, E. E. (2009). Serotonergic modulation of basal ganglia circuits Complexity and therapeutic opportunities. *Neurology*, *73*(11), 880–886.

Bennett, B. D., & Bolam, J. P. (1994). Localisation of parvalbumin-immunoreactive structures in primate caudate-putamen. *Journal of Comparative Neurology*, *347*(3), 340–356. https://doi.org/10.1002/cne.903470303

Bennett, B. D., Callaway, J. C., & Wilson, C. J. (2000). Intrinsic Membrane Properties Underlying Spontaneous Tonic Firing in Neostriatal Cholinergic Interneurons. *Journal of Neuroscience*, *20*(22), 8493–8503. https://doi.org/10.1523/JNEUROSCI.20-22-08493.2000

Bennett, B. D., & Wilson, C. J. (1999). Spontaneous activity of neostriatal cholinergic interneurons in vitro. *Journal of Neuroscience*, *19*(13), 5586–5596. https://doi.org/10.1523/jneurosci.19-13-05586.1999

Bentivoglio, M., Cotrufo, T., Ferrari, S., Tesoriero, C., Mariotto, S., Bertini, G., Berzero, A., & Mazzarello, P. (2019). The original histological slides of camillo golgi and his discoveries on neuronal structure. *Frontiers in Neuroanatomy*, *13*. https://doi.org/10.3389/fnana.2019.00003

Berke, J. D. (2011). Functional properties of striatal fast-spiking interneurons. *Frontiers in Systems Neuroscience*, *JUNE 2011*. https://doi.org/10.3389/fnsys.2011.00045

Bernard, V., Normand, E., & Bloch, B. (1992). Phenotypical characterization of the rat striatal neurons expressing muscarinic receptor genes. *Journal of Neuroscience*, *12*(9), 3591–3600. https://doi.org/10.1523/jneurosci.12-09-03591.1992

Bevan, M. D., Magill, P. J., Terman, D., Bolam, J. P., & Wilson, C. J. (2002). Move to the rhythm: oscillations in the subthalamic nucleus–external globus pallidus network. *Trends in Neurosciences*, *25*(10), 525–531. https://doi.org/https://doi.org/10.1016/S0166-2236(02)02235-X

Blackwell, K. T., Salinas, A. G., Tewatia, P., English, B., Hellgren Kotaleski, J., & Lovinger, D. M. (2019). Molecular mechanisms underlying striatal synaptic plasticity: relevance to chronic alcohol consumption and seeking. *European Journal of Neuroscience*, *49*(6), 768–783. https://doi.org/10.1111/ejn.13919

Blomeley, C. P., & Bracci, E. (2009). Serotonin excites fast-spiking interneurons in the striatum. *European Journal of Neuroscience*, *29*(8), 1604–1614. https://doi.org/10.1111/j.1460-9568.2009.06725.x

Blomeley, C. P., Cains, S., & Bracci, E. (2015). Dual Nitrergic/Cholinergic Control of Short-Term Plasticity of Corticostriatal Inputs to Striatal Projection Neurons. *Frontiers in Cellular Neuroscience*, *9*(November). https://doi.org/10.3389/fncel.2015.00453

Bogousslavsky, J., & Tatu, L. (2017). The history of basal ganglia anatomy. *Revue Neurologique*, *173*(10), 605. https://doi.org/https://doi.org/10.1016/j.neurol.2017.10.007

Bolam, J. P., & Ellender, T. J. (2016). Histamine and the striatum. *Neuropharmacology*, *106*, 74–84. https://doi.org/10.1016/j.neuropharm.2015.08.013

Bower, J., & Beeman, D. (2003). *The Book of Genesis: Vol. Free Internet Ed.*

Brimblecombe, K. R., & Cragg, S. J. (2017). The Striosome and Matrix Compartments of the Striatum: A Path through the Labyrinth from Neurochemistry toward Function. In *ACS Chemical Neuroscience* (Vol. 8, Issue 2, pp. 235–242). American Chemical Society. https://doi.org/10.1021/acschemneuro.6b00333

Burke, D. A., & Alvarez, V. A. (2022). Serotonin receptors contribute to dopamine depression of lateral inhibition in the nucleus accumbens. *Cell Reports*, *39*(6). https://doi.org/10.1016/j.celrep.2022.110795

Burke, D. A., Rotstein, H. G., & Alvarez, V. A. (2017). Striatal Local Circuitry: A New Framework for Lateral Inhibition. *Neuron*, *96*(2), 267–284. https://doi.org/10.1016/j.neuron.2017.09.019

Burn, D. (2013). *Oxford Textbook of Movement Disorders, Oxford Textbooks in Clinical Neurology: Vol. online edition*. Oxford Academic.

Cains, S., Blomeley, C. P., & Bracci, E. (2012). Serotonin inhibits low-threshold spike interneurons in the striatum. *Journal of Physiology*, *590*(10), 2241–2252. https://doi.org/10.1113/jphysiol.2011.219469

Calabresi, P., Centonze, D., Gubellini, P., & Bernardi, G. (1999). Activation of M1-like muscarinic receptors is required for the induction of corticostriatal LTP. *Neuropharmacology*, *38*(2), 323–326. https://doi.org/10.1016/S0028-3908(98)00199-3

Calabresi, P., Gubellini, P., Centonze, D., Sancesario, G., Morello, M., Giorgi, M., Pisani, A., & Bernardi, G. (1999). *A Critical Role of the Nitric Oxide/cGMP Pathway in Corticostriatal Long-Term Depression*.

Calabresi, P., Misgeld, U., & Dodt, H. U. (1987). Intrinsic membrane properties of neostriatal neurons can account for their low level of spontaneous activity. *Neuroscience*, *20*(1), 293–303. https://doi.org/https://doi.org/10.1016/0306-4522(87)90021-2

Catterall, W. A. (2011). Voltage-gated calcium channels. *Cold Spring Harbor Perspectives in Biology*, *3*(8), 1–23. https://doi.org/10.1101/cshperspect.a003947

Centonze, D., Bracci, E., Pisani, A., Gubellini, P., Bernardi, G., & Calabresi, P. (2002). Activation of dopamine D1-like receptors excites LTS interneurons of the striatum. *European Journal of Neuroscience*, *15*(12), 2049–2052. https://doi.org/10.1046/j.1460-9568.2002.02052.x

Centonze, D., Gubellini, P., Bernardi, G., & Calabresi, P. (1999). Permissive role of interneurons in corticostriatal synaptic plasticity. *Brain Research Reviews*, *31*(1), 1–5. https://doi.org/10.1016/S0165-0173(99)00018-1

Centonze, D., Pisani, A., Bonsi, P., Giacomini, P., Bernardi, G., & Calabresi, P. (2001). Stimulation of nitric oxide-cGMP pathway excites striatal cholinergic interneurons via protein kinase G activation. *Journal of Neuroscience*, *21*(4), 1393–1400. https://doi.org/10.1523/jneurosci.21-04-01393.2001

Chang, H. T., & Kita, H. (1992). Interneurons in the rat striatum: relationships between parvalbumin neurons and cholinergic neurons. *Brain Research*, *574*(1–2), 307–311. https://doi.org/10.1016/0006-8993(92)90830-3

Choi, K., Holly, E. N., Davatolhagh, M. F., Beier, K. T., & Fuccillo, M. V. (2019). Integrated anatomical and physiological mapping of striatal afferent projections. *European Journal of Neuroscience*, *49*(5), 623–636. https://doi.org/10.1111/ejn.13829

Chuhma, N., Tanaka, K. F., Hen, R., & Rayport, S. (2011). Functional connectome of the striatal medium spiny neuron. *Journal of Neuroscience*, *31*(4), 1183–1192. https://doi.org/10.1523/JNEUROSCI.3833-10.2011

Citri, A., & Malenka, R. C. (2008). Synaptic Plasticity: Multiple Forms, Functions, and Mechanisms. *Neuropsychopharmacology Reviews*, *33*, 18–41. https://doi.org/10.1038/sj.npp.1301559

Colangelo, C., Shichkova, P., Keller, D., Markram, H., & Ramaswamy, S. (2019). Cellular, synaptic and network effects of acetylcholine in the neocortex. In *Frontiers in Neural Circuits* (Vol. 13). Frontiers Media S.A. https://doi.org/10.3389/fncir.2019.00024

Colovic, M. B., Krstic, D. Z., Lazarevic-Pasti, T. D., Bondzic, A. M., & Vasic, V. M. (2013). Acetylcholinesterase Inhibitors: Pharmacology and Toxicology. *Current Neuropharmacology*, *11*(3), 315–335. https://doi.org/10.2174/1570159x11311030006

Cragg, S. J. (2006). Meaningful silences: How dopamine listens to the ACh pause. *Trends in Neurosciences*, *29*(3), 125–131. https://doi.org/10.1016/j.tins.2006.01.003

Cui, G., Jun, S. B., Jin, X., Pham, M. D., Vogel, S. S., Lovinger, D. M., & Costa, R. M. (2013). Concurrent activation of striatal direct and indirect pathways during action initiation. *Nature*, *494*(7436), 238–242. https://doi.org/10.1038/nature11846

da Silva, J. A., Tecuapetla, F., Paixão, V., & Costa, R. M. (2018). Dopamine neuron activity before action initiation gates and invigorates future movements. *Nature*, *554*(7691), 244–248. https://doi.org/10.1038/nature25457

Dautan, D., Huerta-Ocampo, I., Gut, N. K., Valencia, M., Kondabolu, K., Kim, Y., Gerdjikov, T. V., & Mena-Segovia, J. (2020). Cholinergic midbrain afferents modulate striatal circuits and shape encoding of action strategies. *Nature Communications*, *11*(1), 1–19. https://doi.org/10.1038/s41467-020-15514-3

Dautan, D., Huerta-Ocampo, I., Witten, I. B., Deisseroth, K., Paul Bolam, J., Gerdjikov, T., & Mena-Segovia, J. (2014). A major external source of cholinergic innervation of the striatum and nucleus accumbens originates in the Brainstem. *Journal of Neuroscience*, *34*(13), 4509–4518. https://doi.org/10.1523/JNEUROSCI.5071-13.2014

De Shutter. (2000). *Computational Neuroscience: Realistic Modeling for Experimentalists : Vol. CRC Press.*

De Shutter. (2009). *Computational Modeling Methods for Neuroscientists*. The MIT Press.

DeLong, M. R. (1990). Primate models of movement disorders of basal ganglia origin. *Trends in Neurosciences*, *13*(7), 281–285. https://doi.org/10.1016/0166-2236(90)90110-V

DiFiglia, M., Pasik, P., & Pasik, T. (1976). A Golgi study of neuronal types in the neostriatum of monkeys. *Brain Research*, *114*(2), 245–256. https://doi.org/https://doi.org/10.1016/0006-8993(76)90669-7

Ding, J., Guzman, J., Peterson, J., Goldberg, J., & Surmeier, D. (2010). Thalamic Gating of Corticostriatal Signaling by Cholinergic Interneurons. *Neuron*, *67*, 294–307. https://doi.org/10.1016/j.neuron.2010.06.017

Dobbs, L. K. K., Kaplan, A. R. R., Lemos, J. C. C., Matsui, A., Rubinstein, M., & Alvarez, V. A. A. (2016). Dopamine Regulation of Lateral Inhibition between Striatal Neurons Gates the Stimulant Actions of Cocaine. *Neuron*, *90*(5), 1100–1113. https://doi.org/10.1016/j.neuron.2016.04.031

Doig, N. M., Magill, P. J., Apicella, P., Bolam, J. P., & Sharott, A. (2014). Cortical and thalamic excitation mediate the multiphasic responses of striatal cholinergic interneurons to motivationally salient stimuli. *Journal of Neuroscience*, *34*(8), 3101–3117. https://doi.org/10.1523/JNEUROSCI.4627-13.2014

Dolphin, A. C., & Lee, A. (2020). Presynaptic calcium channels: specialized control of synaptic neurotransmitter release. In *Nature Reviews Neuroscience* (Vol. 21, Issue 4, pp. 213–229). Nature Research. https://doi.org/10.1038/s41583-020-0278-2

Dorman, D. B., Jędrzejewska-Szmek, J., & Blackwell, K. T. (2018). Inhibition enhances spatially-specific calcium encoding of synaptic input patterns in a biologically constrained model. *ELife*, *7*, 1–28. https://doi.org/10.7554/eLife.38588

Dorst, M. C., Tokarska, A., Zhou, M., Lee, K., Stagkourakis, S., Broberger, C., Masmanidis, S., & Silberberg, G. (2020). Polysynaptic inhibition between striatal cholinergic interneurons shapes their network activity patterns in a dopamine-dependent manner. *Nature Communications*, *11*(1), 5113. https://doi.org/10.1038/s41467-020-18882-y

Du, K., Wu, Y. W., Lindroos, R., Liu, Y., Rózsa, B., Katona, G., Ding, J. B., & Kotaleski, J. H. (2017). Cell-type–specific inhibition of the dendritic plateau potential in striatal spiny projection neurons. *Proceedings of the National Academy of Sciences of the United States of America*, *114*(36), E7612–E7621. https://doi.org/10.1073/pnas.1704893114

Eblen, F., & Graybiel, A. M. (1995). Highly restricted origin of prefrontal cortical inputs to striosomes in the macaque monkey. *Journal of Neuroscience*, *15*(9), 5999–6013. https://doi.org/10.1523/jneurosci.15-09-05999.1995

Elghaba, R., Vautrelle, N., & Bracci, E. (2016). Mutual control of cholinergic and low-threshold spike interneurons in the striatum. *Frontiers in Cellular Neuroscience*, *10*(APR), 1–15. https://doi.org/10.3389/fncel.2016.00111

English, D. F., Ibanez-Sandoval, O., Stark, E., Tecuapetla, F., Buzsáki, G., Deisseroth, K., Tepper, J. M., & Koos, T. (2011). GABAergic circuits mediate the reinforcement-related signals of striatal cholinergic interneurons. *Nature Neuroscience*, *15*(1). https://doi.org/10.1038/nn.2984

Euler, T., & Denk, W. (2001). Dendritic processing. *Current Opinion in Neurobiology*, *11*(4), 415–422. https://doi.org/https://doi.org/10.1016/S0959-4388(00)00228-2

Exley, R., & Cragg, S. (2008). Presynaptic nicotinic receptors: a dynamic and diverse cholinergic filter of striatal dopamine neurotransmission. *British Journal of Pharmacology*, *153*, 283–297. https://doi.org/10.1038/sj.bjp.0707510

F J Hwang, R H. Roth, Y W Wu, Y Sun, D K. Kwon, Y Liu, & J B. Ding. (2022). Motor learning selectively strengthens cortical and striatal synapses of motor engram neurons. *Neuron*, *110*(17), 2790-2801.e5. https://doi.org/10.1016/j.neuron.2022.06.006

Feng, L., Zhao, T., & Kim, J. (2015). neuTube 1.0: A New Design for Efficient Neuron Reconstruction Software Based on the SWC Format. *ENeuro*, *2*(1). https://doi.org/10.1523/ENEURO.0049-14.2014

Finger, S. (1994). Origins of neuroscience: A history of explorations into brain function. In *Origins of neuroscience: A history of explorations into brain function.* Oxford University Press.

Fischer, A. G., & Ullsperger, M. (2017). An update on the role of serotonin and its interplay with dopamine for reward. In *Frontiers in Human Neuroscience* (Vol. 11). Frontiers Media S. A. https://doi.org/10.3389/fnhum.2017.00484

Floran, B., Aceves, J., Sierra, A., & Martinez-Fong, D. (1990). *Activation of D 1 dopamine receptors stimulates the release of GABA in the basal ganglia of the rat*.

Ford, C. P. (2014). The role of D2-autoreceptors in regulating dopamine neuron activity and transmission. In *Neuroscience* (Vol. 282, pp. 13–22). Elsevier Ltd. https://doi.org/10.1016/j.neuroscience.2014.01.025

Fortin, F.-A., Marc-André Gardner, U., Parizeau, M., & Gagné, C. (2012). DEAP: Evolutionary Algorithms Made Easy François-Michel De Rainville. In *Journal of Machine Learning Research* (Vol. 13). http://deap.gel.ulaval.ca,

Foster, N. N., Barry, J., Korobkova, L., Garcia, L., Gao, L., Becerra, M., Sherafat, Y., Peng, B., Li, X., Choi, J. H., Gou, L., Zingg, B., Azam, S., Lo, D., Khanjani, N., Zhang, B., Stanis, J., Bowman, I., Cotter, K., … Dong, H. W. (2021). The mouse cortico–basal ganglia–thalamic network. *Nature*, *598*(7879), 188–194. https://doi.org/10.1038/s41586-021-03993-3

Fukuda, T. (2009). Network architecture of gap junction-coupled neuronal linkage in the striatum. *Journal of Neuroscience*, *29*(4), 1235–1243. https://doi.org/10.1523/JNEUROSCI.4418-08.2009

Galarraga, E., Herna, S., Reyes, A., Miranda, I., Bermudez-rattoni, F., & Vilchis, C. (1999). *Cholinergic Modulation of Neostriatal Output : A Functional Antagonism between Different Types of Muscarinic Receptors*. *19*(9), 3629–3638.

Galarraga, E., Hernández-López, S., Reyes, A., Miranda, I., Bermudez-Rattoni, F., Vilchis, C., & Bargas, J. (1999). Cholinergic modulation of neostriatal output: A functional antagonism between different types of muscarinic receptors. *Journal of Neuroscience*, *19*(9), 3629–3638. https://doi.org/10.1523/jneurosci.19-09-03629.1999

Garthwaite, J. (2008). Concepts of neural nitric oxide-mediated transmission. *European Journal of Neuroscience*, *27*(11), 2783–2802. https://doi.org/10.1111/j.1460-9568.2008.06285.x

Gerfen, C. R., Engber, T. M., Mahan, L. C., Susel, Z., Chase, T. N., Monsma, F. J., & Sibley, D. R. (1990). D1 and D2 Dopamine Receptor-regulated Gene Expression of Striatonigral and Striatopallidal Neurons. *Science*, *250*(4986), 1429–1432. https://doi.org/10.1126/science.2147780

Gerfen, C. R., & Scott Young, W. (1988). Distribution of striatonigral and striatopallidal peptidergic neurons in both patch and matrix compartments: an in situ hybridization histochemistry and fluorescent retrograde tracing study. *Brain Research*, *460*(1), 161–167. https://doi.org/https://doi.org/10.1016/0006-8993(88)91217-6

Gerfen, C. R., & Surmeier, D. J. (2011). Modulation of striatal projection systems by dopamine. *Annual Review of Neuroscience*, *34*, 441–466. https://doi.org/10.1146/annurev-neuro-061010-113641

Giniatullin, R., Nistri, A., & Yakel, J. L. (2005). Desensitization of nicotinic ACh receptors: Shaping cholinergic signaling. In *Trends in Neurosciences*. https://doi.org/10.1016/j.tins.2005.04.009

Gittis, A. H., & Kreitzer, A. C. (2012). Striatal microcircuitry and movement disorders. In *Trends in Neurosciences* (Vol. 35, Issue 9, pp. 557–564). https://doi.org/10.1016/j.tins.2012.06.008

Glenthøj, B., & Fibiger, H. C. (2019). In Memoriam: Arvid Carlsson—Pioneering Researcher and Nobel Laureate. *Neuropsychopharmacology*, *44*(2), 457–458. https://doi.org/10.1038/s41386-018-0244-0

Goldberg, J. A., & Reynolds, J. N. J. (2011). Spontaneous firing and evoked pauses in the tonically active cholinergic interneurons of the striatum. *Neuroscience*, *198*, 27–43. https://doi.org/10.1016/j.neuroscience.2011.08.067

Graveland, G. A., & Difiglia, M. (1985). The frequency and distribution of medium-sized neurons with indented nuclei in the primate and rodent neostriatum. *Brain Research*, *327*(1–2), 307–311. https://doi.org/10.1016/0006-8993(85)91524-0

Graybiel, A. M., & Ragsdale, C. W. (1978). Histochemically distinct compartments in the striatum of human, monkeys, and cat demonstrated by acetylthiocholinesterase staining. *Proceedings of the National Academy of Sciences*, *75*(11), 5723–5726. https://doi.org/10.1073/pnas.75.11.5723

Grillner, S., & Robertson, B. (2016). The Basal Ganglia Over 500 Million Years. *Current Biology*, *26*(20), R1088–R1100. https://doi.org/10.1016/j.cub.2016.06.041

Grillner, S., Robertson, B., & Kotaleski, J. H. (2020). Basal ganglia—a motion perspective. *Comprehensive Physiology*, *10*(4), 1241–1275. https://doi.org/10.1002/cphy.c190045

Guéguinou, M., Chantome, A., Fromont, G., Bougnoux, P., Vandier, C., & Potier-Cartereau, M. (2014). KCa and Ca2+ channels: The complex thought. In *Biochimica et Biophysica Acta - Molecular Cell Research* (Vol. 1843, Issue 10, pp. 2322–2333). Elsevier. https://doi.org/10.1016/j.bbamcr.2014.02.019

Guo, Q., Wang, D., He, X., Feng, Q., Lin, R., Xu, F., Fu, L., & Luo, M. (2015). Whole-Brain Mapping of Inputs to Projection Neurons and Cholinergic Interneurons in the Dorsal Striatum. *PLOS ONE*, *10*(4), 1–15. https://doi.org/10.1371/journal.pone.0123381

Gurevich, E. V., Gainetdinov, R. R., & Gurevich, V. V. (2016). G protein-coupled receptor kinases as regulators of dopamine receptor functions. *Pharmacological Research*, *111*, 1–16. https://doi.org/10.1016/j.phrs.2016.05.010

Gustafson, N., Gireesh-Dharmaraj, E., Czubayko, U., Blackwell, K. T., & Plenz, D. (2006). A comparative voltage and current-clamp analysis of feedback and feedforward synaptic transmission in the striatal microcircuit in vitro. *Journal of Neurophysiology*, *95*(2), 737–752. https://doi.org/10.1152/jn.00802.2005

Haam, J., & Yakel, J. L. (2017). Cholinergic modulation of the hippocampal region and memory function. *Journal of Neurochemistry*, *142*, 111–121. https://doi.org/10.1111/jnc.14052

Haber, S. N. (2016). Corticostriatal Circuitry. In N. D. Pfaff Donald W. and Volkow (Ed.), *Neuroscience in the 21st Century: From Basic to Clinical* (pp. 1721–1741). Springer New York. https://doi.org/10.1007/978-1-4939-3474-4_135

Harry Whitaker, C. U. M. Smith, & Stanley Finger. (2007). *Brain, Mind and Medicine: Essays in Eighteenth-Century Neuroscience*. Springer.

Harsing, L. G., & Zigmond, M. J. (1997). Influence of dopamine on GABA release in striatum: Evidence for D1-D2 interactions and non-synaptic influences. *Neuroscience*, *77*(2), 419–429. https://doi.org/10.1016/S0306-4522(96)00475-7

Hartung, H., Threlfell, S., & Cragg, S. J. (2011). Nitric oxide donors enhance the frequency dependence of dopamine release in nucleus accumbens. *Neuropsychopharmacology*, *36*(9), 1811–1822. https://doi.org/10.1038/npp.2011.62

Hernández-Flores, T., Hernández-González, O., Pérez-Ramírez, M. B., Lara-González, E., Arias-García, M. A., Duhne, M., Pérez-Burgos, A., Prieto, G. A., Figueroa, A., Galarraga, E., & Bargas, J. (2015). Modulation of direct pathway striatal projection neurons by muscarinic M4-type receptors. *Neuropharmacology*, *89*, 232–244. https://doi.org/10.1016/j.neuropharm.2014.09.028

Hersch, S. M., & Levey, A. I. (1995). Diverse pre- and post-synaptic expression of m1-m4 muscarinic receptor proteins in neurons and afferents in the rat neostriatum. *Life Sciences*, *56*(11–12), 931–938. https://doi.org/10.1016/0024-3205(95)00030-A

Hille, B. (2001). Ion Channels of Excitable Membranes. In *Ion Channels of Excitable Membranes* (Vol. 18).

Hines, M. L., Davison, A. P., & Muller, E. (2009). NEURON and Python. *Frontiers in Neuroinformatics*, *3*(JAN). https://doi.org/10.3389/neuro.11.001.2009

Hintiryan, H., Foster, N. N., Bowman, I., Bay, M., Song, M. Y., Gou, L., Yamashita, S., Bienkowski, M. S., Zingg, B., Zhu, M., Yang, X. W., Shih, J. C., Toga, A. W., & Dong, H.-W. (2016). The mouse cortico-striatal projectome. *Nature Neuroscience*, *19*(8), 1100–1114. https://doi.org/10.1038/nn.4332

Hodgkin, A. L., & Huxley, A. F. (1952). A QUANTITATIVE DESCRIPTION OF MEMBRANE CURRENT AND ITS APPLICATION TO CONDUCTION AND EXCITATION IN NERVE. In *J. Physiol*.

Holly, E. N., Davatolhagh, M. F., España, R. A., & Fuccillo, M. V. (2021). Striatal low-threshold spiking interneurons locally gate dopamine. *Current Biology*, *31*(18), 4139-4147.e6. https://doi.org/10.1016/j.cub.2021.06.081

Howe, M., Ridouh, I., Mascaro, A. L. A., Larios, A., Azcorra, M., & Dombeck, D. A. (2019). Coordination of rapid cholinergic and dopaminergic signaling in striatum during spontaneous movement. *ELife*, *8*, 1–24. https://doi.org/10.7554/eLife.44903

Huerta-Ocampo, I., Mena-Segovia, J., & Bolam, J. P. (2014). Convergence of cortical and thalamic input to direct and indirect pathway medium spiny neurons in the striatum. *Brain Structure & Function*, *219*(5), 1787–1800. https://doi.org/10.1007/s00429-013-0601-z

Hunnicutt, B. J., Jongbloets, B. C., Birdsong, W. T., & Gertz, K. J. (2016). *A comprehensive excitatory input map of the striatum reveals novel functional organization. September 2017*. https://doi.org/10.7554/eLife.19103

I Carannante, Y Johansson, G Silberberg, & J Hellgren Kotaleski. (2022). Data-Driven Model of Postsynaptic Currents Mediated by NMDA or AMPA Receptors in Striatal Neurons. *Frontiers in Computational Neuroscience*, *16*. https://doi.org/10.3389/fncom.2022.806086

Ibáñez-Sandoval, O., Tecuapetla, F., Unal, B., Shah, F., Koós, T., & Tepper, J. M. (2011). A novel functionally distinct subtype of striatal neuropeptide Y interneuron. *Journal of Neuroscience*, *31*(46), 16757–16769. https://doi.org/10.1523/JNEUROSCI.2628-11.2011

Izhikevich, E. M., Desai, N. S., Walcott, E. C., & Hoppensteadt, F. C. (2003). Bursts as a unit of neural information: Selective communication via resonance. In *Trends in Neurosciences* (Vol. 26, Issue 3, pp. 161–167). Elsevier Ltd. https://doi.org/10.1016/S0166-2236(03)00034-1

Jin, X., Tecuapetla, F., & Costa, R. M. (2014). Basal ganglia subcircuits distinctively encode the parsing and concatenation of action sequences. *Nature Neuroscience*, *17*(3), 423–430. https://doi.org/10.1038/nn.3632

Jing, M., Li, Y., Zeng, J., Huang, P., Skirzewski, M., Kljakic, O., Peng, W., Qian, T., Tan, K., Zou, J., Trinh, S., Wu, R., Zhang, S., Pan, S., Hires, S. A., Xu, M., Li, H., Saksida, L. M., Prado, V. F., … Li, Y. (2020). An optimized acetylcholine sensor for monitoring in vivo cholinergic activity. *Nature Methods*, *17*(11), 1139–1146. https://doi.org/10.1038/s41592-020-0953-2

JJJ Hjorth, J Hellgren-Kotaleski, & A Kozlov. (2021). Predicting Synaptic Connectivity for Large-Scale Microcircuit Simulations Using Snudda. *Neuroinformatics*, *19*(4), 685–701. https://doi.org/10.1007/s12021-021-09531-w/Published

Johansson, Y., & Silberberg, G. (2020a). The Functional Organization of Cortical and Thalamic Inputs onto Five Types of Striatal Neurons Is Determined by Source and Target Cell Identities. *Cell Reports*, *30*(4), 1178-1194.e3. https://doi.org/10.1016/j.celrep.2019.12.095

Johansson, Y., & Silberberg, G. (2020b). The Functional Organization of Cortical and Thalamic Inputs onto Five Types of Striatal Neurons Is Determined by Source and Target Cell Identities. *Cell Reports*, *30*(4), 1178-1194.e3. https://doi.org/10.1016/j.celrep.2019.12.095

Jones, E. G. (1999). Golgi, Cajal and the neuron doctrine. In *Journal of the History of the Neurosciences* (Vol. 8, Issue 2, pp. 170–178). Swets en Zeitlinger B.V. https://doi.org/10.1076/jhin.8.2.170.1838

Joshua, M., Adler, A., Mitelman, R., Vaadia, E., & Bergman, H. (2008). Midbrain dopaminergic neurons and striatal cholinergic interneurons encode the difference between reward and aversive events at different epochs of probabilistic classical conditioning trials. *Journal of Neuroscience*, *28*(45), 11673–11684. https://doi.org/10.1523/JNEUROSCI.3839-08.2008

Kandel, E. R., Jessell, T. M., Schwartz, J. H., Siegelbaum, S. A., & Hudspeth, A. J. (2012). *Principles of Neural Science. Fifth Edition.* . McGraw-Hill.

Kawaguchi, Y. (1992). Large aspiny cells in the matrix of the rat neostriatum in vitro: physiological identification, relation to the compartments and excitatory postsynaptic currents. *Journal of Neurophysiology*, *67*(6), 1669–1682. https://doi.org/10.1152/jn.1992.67.6.1669

Kawaguchi, Y. (1993). Physiological, Morphological, and Histochemical Characterization of Three Classes of Interneurons in Rat Neostriatum. In *The Journal of Neuroscience* (Vol. 13, Issue 11).

Kim, D. M., & Nimigean, C. M. (2016). Voltage-gated potassium channels: A structural examination of selectivity and gating. *Cold Spring Harbor Perspectives in Biology*, *8*(5). https://doi.org/10.1101/cshperspect.a029231

Kimura, M., Rajkowski, J., & Evarts, E. (1984). Tonically discharging putamen neurons exhibit set-dependent responses. *Proceedings of the National Academy of Sciences of the United States of America*, *81*(15 I), 4998–5001. https://doi.org/10.1073/pnas.81.15.4998

Kincaid, A. E., Zheng, T., & Wilson, C. J. (1998). Connectivity and convergence of single corticostriatal axons. *Journal of Neuroscience*, *18*(12), 4722–4731. https://doi.org/10.1523/jneurosci.18-12-04722.1998

Kita, H., Kosaka, T., & Heizmann, C. W. (1990). Parvalbumin-immunoreactive neurons in the rat neostriatum: a light and electron microscopic study. In *Brain Research* (Vol. 536).

Klaus, A., Alves Da Silva, J., & Costa, R. M. (2019). *Annual Review of Neuroscience What, If, and When to Move: Basal Ganglia Circuits and Self-Paced Action Initiation*. https://doi.org/10.1146/annurev-neuro-072116

Klaus, A., Martins, G. J., Paixao, V. B., Zhou, P., Paninski, L., & Costa, R. M. (2017). The Spatiotemporal Organization of the Striatum Encodes Action Space. *Neuron*, *95*(5), 1171-1180.e7. https://doi.org/10.1016/j.neuron.2017.08.015

Klaus, A., & Plenz, D. (2016). A Low-Correlation Resting State of the Striatum during Cortical Avalanches and Its Role in Movement Suppression. *PLoS Biology*, *14*(12), 1–30. https://doi.org/10.1371/journal.pbio.1002582

Klug, J. R., Engelhardt, M. D., Cadman, C. N., Li, H., Smith, J. B., Ayala, S., Williams, E. W., Hoffman, H., & Jin, X. (1998). *Differential inputs to striatal cholinergic and parvalbumin interneurons imply functional distinctions*. https://doi.org/10.7554/eLife.35657.001

Koós, T., & Tepper, J. M. (2002). Dual cholinergic control of fast-spiking interneurons in the neostriatum. *Journal of Neuroscience*, *22*(2), 529–535. https://doi.org/10.1523/jneurosci.22-02-00529.2002

Koos, T., Tepper, J. M., & Wilson, C. J. (2004). Comparison of IPSCs evoked by spiny and fast-spiking neurons in the neostriatum. *Journal of Neuroscience*, *24*(36), 7916–7922. https://doi.org/10.1523/JNEUROSCI.2163-04.2004

Kress, G. J., Yamawaki, N., Wokosin, D. L., Wickersham, I. R., Shepherd, G. M. G., & Surmeier, D. J. (2013). Convergent cortical innervation of striatal projection neurons. *Nature Neuroscience*, *16*(6), 665–667. https://doi.org/10.1038/nn.3397

Lahiri, A. K., & Bevan, M. D. (2020). Dopaminergic Transmission Rapidly and Persistently Enhances Excitability of D1 Receptor-Expressing Striatal Projection Neurons. *Neuron*, *106*(2), 277-290.e6. https://doi.org/10.1016/j.neuron.2020.01.028

Lai, H. C., & Jan, L. Y. (2006). The distribution and targeting of neuronal voltage-gated ion channels. In *Nature Reviews Neuroscience* (Vol. 7, Issue 7, pp. 548–562). https://doi.org/10.1038/nrn1938

Lapper, S. R., & Bolam, J. P. (1992). Input from the frontal cortex and the parafascicular nucleus to cholinergic interneurons in the dorsal striatum of the rat. *Neuroscience*, *51*(3), 533–545. https://doi.org/10.1016/0306-4522(92)90293-B

Le Moine, C., & Bloch, B. (1995). D1 and D2 dopamine receptor gene expression in the rat striatum: Sensitive cRNA probes demonstrate prominent segregation of D1 and D2 mRNAS in distinct neuronal populations of the dorsal and ventral striatum. *Journal of Comparative Neurology*, *355*(3), 418–426. https://doi.org/https://doi.org/10.1002/cne.903550308

Leopold, A. V., Shcherbakova, D. M., & Verkhusha, V. V. (2019). Fluorescent Biosensors for Neurotransmission and Neuromodulation: Engineering and Applications. In *Frontiers in Cellular Neuroscience* (Vol. 13). Frontiers Media S.A. https://doi.org/10.3389/fncel.2019.00474

Liljeholm, M., & O'Doherty, J. P. (2012). Contributions of the striatum to learning, motivation, and performance: An associative account. In *Trends in Cognitive Sciences* (Vol. 16, Issue 9, pp. 467–475). Elsevier Ltd. https://doi.org/10.1016/j.tics.2012.07.007

Lim, S. A. O., Kang, U. J., & McGehee, D. S. (2014). Striatal cholinergic interneuron regulation and circuit effects. *Frontiers in Synaptic Neuroscience*, *6*(SEP), 785907. https://doi.org/10.3389/fnsyn.2014.00022

Lindroos, R., Dorst, M. C., Du, K., Filipović, M., Keller, D., Ketzef, M., Kozlov, A. K., Kumar, A., Lindahl, M., Nair, A. G., Pérez-Fernández, J., Grillner, S., Silberberg, G., & Kotaleski, J. H. (2018). Basal ganglia neuromodulation over multiple temporal and structural scales—simulations of direct pathway MSNs investigate the fast onset of dopaminergic effects and predict the role of Kv4.2. *Frontiers in Neural Circuits*, *12*(February), 1–23. https://doi.org/10.3389/fncir.2018.00003

Lindroos, R., & Hellgren Kotaleski, J. (2021). Predicting complex spikes in striatal projection neurons of the direct pathway following neuromodulation by acetylcholine and dopamine. *European Journal of Neuroscience*, *53*(7), 2117–2134. https://doi.org/https://doi.org/10.1111/ejn.14891

Luo, R., Janssen, M. J., Partridge, J. G., & Vicini, S. (2013). Direct and GABA-mediated indirect effects of nicotinic ACh receptor agonists on striatal neurones. *The Journal of Physiology*, *591*(Pt 1). https://doi.org/10.1113/jphysiol.2012.241786

Ma, L., Day-Cooney, J., Benavides, O. J., Muniak, M. A., Qin, M., Ding, J. B., Mao, T., & Zhong, H. (2022). Locomotion activates PKA through dopamine and adenosine in striatal neurons. *Nature*, *611*(7937), 762–768. https://doi.org/10.1038/s41586-022-05407-4

Mallet, N., Leblois, A., Maurice, N., & Beurrier, C. (2019). Striatal cholinergic interneurons: How to elucidate their function in health and disease. *Frontiers in Pharmacology*, *10*(December), 1–7. https://doi.org/10.3389/fphar.2019.01488

Mallet, N., Schmidt, R., Leventhal, D., Chen, F., Amer, N., Boraud, T., & Berke, J. D. (2016). Arkypallidal Cells Send a Stop Signal to Striatum. *Neuron*, *89*(2), 308–316. https://doi.org/https://doi.org/10.1016/j.neuron.2015.12.017

Mandelbaum, G., Taranda, J., Haynes, T. M., Hochbaum, D. R., Huang, K. W., Hyun, M., Umadevi Venkataraju, K., Straub, C., Wang, W., Robertson, K., Osten, P., & Sabatini, B. L. (2019). Distinct Cortical-Thalamic-Striatal Circuits through the Parafascicular Nucleus. *Neuron*, *102*(3), 636-652.e7. https://doi.org/10.1016/j.neuron.2019.02.035

Markowitz, J. E., Gillis, W. F., Beron, C. C., Neufeld, S. Q., Robertson, K., Bhagat, N. D., Peterson, R. E., Peterson, E., Hyun, M., Linderman, S. W., Sabatini, B. L., & Datta, S. R. (2018). The Striatum Organizes 3D Behavior via Moment-to-Moment Action Selection. *Cell*, *174*(1), 44-58.e17. https://doi.org/10.1016/j.cell.2018.04.019

Markram, H., Muller, E., Ramaswamy, S., Reimann, M. W., Abdellah, M., Sanchez, C. A., Ailamaki, A., Alonso-Nanclares, L., Antille, N., Arsever, S., Kahou, G. A. A., Berger, T. K., Bilgili, A., Buncic, N., Chalimourda, A., Chindemi, G., Courcol, J.-D., Delalondre, F., Delattre, V., … Schürmann, F. (2015). Reconstruction and Simulation of Neocortical Microcircuitry. *Cell*, *163*(2), 456–492. https://doi.org/10.1016/j.cell.2015.09.029

Mathur, B., & Lovinger, D. (2012). Serotonergic action on dorsal striatal function. *Parkinsonism & Related Disorders*, *18*, S129–S131. https://doi.org/https://doi.org/10.1016/S1353-8020(11)70040-2

Matsuda, W., Furuta, T., Nakamura, K. C., Hioki, H., Fujiyama, F., Arai, R., & Kaneko, T. (2009). Single nigrostriatal dopaminergic neurons form widely spread and highly dense axonal arborizations in the neostriatum. *Journal of Neuroscience*, *29*(2), 444–453. https://doi.org/10.1523/JNEUROSCI.4029-08.2009

Maurice, N., Liberge, M., Jaouen, F., Ztaou, S., Hanini, M., Camon, J., Deisseroth, K., Amalric, M., Kerkerian-Le Goff, L., & Beurrier, C. (2015). Striatal Cholinergic Interneurons Control Motor Behavior and Basal Ganglia Function in Experimental Parkinsonism. *Cell Reports*, *13*(4), 657–666. https://doi.org/10.1016/j.celrep.2015.09.034

Maurice, N., Mercer, J., Chan, C. S., Hernandez-Lopez, S., Held, J., Tkatch, T., & Surmeier, D. J. (2004). D2 Dopamine Receptor-Mediated Modulation of Voltage-Dependent Na+ Channels Reduces Autonomous Activity in Striatal Cholinergic Interneurons. *Journal of Neuroscience*, *24*(46), 10289–10301. https://doi.org/10.1523/JNEUROSCI.2155-04.2004

McCoy, A. N., & Tan, S. Y. ong. (2014). Otto Loewi (1873-1961): Dreamer and Nobel laureate. *Singapore Medical Journal*, *55*(1), 3–4. https://doi.org/10.11622/smedj.2014002

McElvain, L. E., Chen, Y., Moore, J. D., Brigidi, G. S., Bloodgood, B. L., Lim, B. K., Costa, R. M., & Kleinfeld, D. (2021). Specific populations of basal ganglia output neurons target distinct brain stem areas while collateralizing throughout the diencephalon. *Neuron*, *109*(10), 1721-1738.e4. https://doi.org/10.1016/j.neuron.2021.03.017

McGregor, M. M., McKinsey, G. L., Girasole, A. E., Bair-Marshall, C. J., Rubenstein, J. L. R., & Nelson, A. B. (2019). Functionally Distinct Connectivity of Developmentally Targeted Striosome Neurons. *Cell Reports*, *29*(6), 1419-1428.e5. https://doi.org/10.1016/j.celrep.2019.09.076

Melendez-Zaidi, A. E., Lakshminarasimhah, H., & Surmeier, D. J. (2019). Cholinergic modulation of striatal nitric oxide-producing interneurons. *European Journal of Neuroscience*, *50*(11), 3713–3731. https://doi.org/10.1111/ejn.14528

Milardi, D., Quartarone, A., Bramanti, A., Anastasi, G., Bertino, S., Basile, G. A., Buonasera, P., Pilone, G., Celeste, G., Rizzo, G., Bruschetta, D., & Cacciola, A. (2019). The Cortico-Basal Ganglia-Cerebellar Network: Past, Present and Future Perspectives. In *Frontiers in Systems Neuroscience* (Vol. 13). Frontiers Media S.A. https://doi.org/10.3389/fnsys.2019.00061

Minagar, A., Ragheb, J., & Kelley, R. E. (2003). The Edwin Smith surgical papyrus: description and analysis of the earliest case of aphasia. *SAGE Publications Journal of Medical Biography*, *11*(2), 114–117.

Morris, G., Arkadir, D., Nevet, A., Vaadia, E., & Bergman, H. (2004). Coincident but Distinct Messages of Midbrain Dopamine and Striatal Tonically Active Neurons. *Neuron*, *43*, 133–143. https://doi.org/10.1016/j.neuron.2004.06.012

Muñoz-Castañeda, R., Zingg, B., Matho, K. S., Chen, X., Wang, Q., Foster, N. N., Li, A., Narasimhan, A., Hirokawa, K. E., Huo, B., Bannerjee, S., Korobkova, L., Park, C. S., Park, Y. G., Bienkowski, M. S., Chon, U., Wheeler, D. W., Li, X., Wang, Y., … Dong, H. W. (2021). Cellular anatomy of the mouse primary motor cortex. *Nature*, *598*(7879), 159–166. https://doi.org/10.1038/s41586-021-03970-w

Muñoz-Manchado, A. B., Foldi, C., Szydlowski, S., Sjulson, L., Farries, M., Wilson, C., Silberberg, G., & Hjerling-Leffler, J. (2016). Novel Striatal GABAergic Interneuron Populations Labeled in the 5HT3aEGFP Mouse. *Cerebral Cortex*, *26*(1), 96–105. https://doi.org/10.1093/cercor/bhu179

Nadim, F., & Bucher, D. (2014). Neuromodulation of neurons and synapses. *Current Opinion in Neurobiology*, *29*, 48–56. https://doi.org/10.1016/j.conb.2014.05.003

Nair, A. G., Gutierrez-Arenas, O., Eriksson, O., Vincent, P., & Kotaleski, J. H. (2015). Sensing positive versus negative reward signals through adenylyl cyclase-coupled GPCRs in direct and indirect pathway striatal medium spiny neurons. *Journal of Neuroscience*, *35*(41), 14017–14030. https://doi.org/10.1523/JNEUROSCI.0730-15.2015

Nambu, A., Tokuno, H., Hamada, I., Kita, H., Imanishi, M., Akazawa, T., Ikeuchi, Y., Hasegawa, N., & Hasegawa Excitatory, N. (2000). *Excitatory Cortical Inputs to Pallidal Neurons Via the Subthalamic Nucleus in the Monkey*. www.jn.physiology.org

Nambu, A., Tokuno, H., & Takada, M. (2002). Functional significance of the cortico-subthalamo-pallidal "hyper direct" pathway. *Neuroscience Research*, *43*, 111–117. www.elsevier.com/locate/neures

Napier, T. C., Simson, P. E., & Givens, B. S. (1991). Dopamine electrophysiology of ventral pallidal/substantia innominata neurons: comparison with the dorsal globus pallidus. *Journal of Pharmacology and Experimental Therapeutics*, *258*(1), 249. http://jpet.aspetjournals.org/content/258/1/249.abstract

NEHER, E., & SAKMANN, B. (1976). Single-channel currents recorded from membrane of denervated frog muscle fibres. *Nature*, *260*(5554), 799–802. https://doi.org/10.1038/260799a0

Nisenbaum, E. S., Xu, Z. C., & Wilson, C. J. (1994). Contribution of a Slowly Inactivating Potassium Current to the Transition to Firing of Neostriatal Spiny Projection Neurons. *Journal of Neurophysiology*, *7*(3).

Ondracek, J. M., Dec, A., Hoque, K. E., Lim, S. A. O., Rasouli, G., Indorkar, R. P., Linardakis, J., Klika, B., Mukherji, S. J., Burnazi, M., Threlfell, S., Sammut, S., & West, A. R. (2008). Feed-forward excitation of striatal neuron activity by frontal cortical activation of nitric oxide signaling in vivo. *European Journal of Neuroscience*, *27*(7), 1739–1754. https://doi.org/10.1111/j.1460-9568.2008.06157.x

Ovallath, S., & Sulthana, B. (2017). Levodopa: History and therapeutic applications. *Annals of Indian Academy of Neurology*, *20*(3), 185–189. https://doi.org/10.4103/aian.AIAN_241_17

Parent, A. (2012). The History of the Basal Ganglia: The Contribution of Karl Friedrich Burdach. *Neuroscience and Medicine*, *03*(04), 374–379. https://doi.org/10.4236/nm.2012.34046

Parent, A., Sato, F., Wu, Y., Gauthier, J., Levesque, M., & Parent, M. (2000). Organization of the basal ganglia: the importance of axonal collateralization. In *Trends Neurosci* (Vol. 23, Issue 10).

Parker, J. G., Marshall, J. D., Ahanonu, B., Wu, Y. W., Kim, T. H., Grewe, B. F., Zhang, Y., Li, J. Z., Ding, J. B., Ehlers, M. D., & Schnitzer, M. J. (2018). Diametric neural ensemble dynamics in parkinsonian and dyskinetic states. In *Nature* (Vol. 557, Issue 7704). https://doi.org/10.1038/s41586-018-0090-6

Parkinson, J. (1817). *An essay on the shaking palsy*. https://wellcomecollection.org

Patriarchi, T., Cho, J. R., Merten, K., Howe, M. W., Marley, A., Xiong, W. H., Folk, R. W., Broussard, G. J., Liang, R., Jang, M. J., Zhong, H., Dombeck, D., von Zastrow, M., Nimmerjahn, A., Gradinaru, V., Williams, J. T., & Tian, L. (2018). Ultrafast neuronal imaging of dopamine dynamics with designed genetically encoded sensors. *Science*, *360*(6396). https://doi.org/10.1126/science.aat4422

Paulus, W., & Rothwell, J. C. (2016). Membrane resistance and shunting inhibition: Where biophysics meets state-dependent human neurophysiology. *Journal of Physiology*, *594*(10), 2719–2728. https://doi.org/10.1113/JP271452

Piccolino, M. (1998). Animal electricity and the birth of electrophysiology: The legacy of Luigi Galvani. *Brain Research Bulletin*, *46*(5), 381–407. https://doi.org/https://doi.org/10.1016/s0361-9230(98)00026-4

Planert, H., Szydlowski, S. N., Hjorth, J. J. J., Grillner, S., & Silberberg, G. (2010). Dynamics of synaptic transmission between fast-spiking interneurons and striatal projection neurons of the direct and indirect pathways. *Journal of Neuroscience*, *30*(9), 3499–3507. https://doi.org/10.1523/JNEUROSCI.5139-09.2010

Plata, V., Duhne, M., Pérez-Ortega, J., Hernández-Martinez, R., Rueda-Orozco, P., Galarraga, E., Drucker-Colín, R., & Bargas, J. (2013). Global actions of nicotine on the striatal microcircuit. *Frontiers in Systems Neuroscience*, *7*(November), 1–13. https://doi.org/10.3389/fnsys.2013.00078

Plenz, D., & Kitai, S. T. (1998). *Up and Down States in Striatal Medium Spiny Neurons Simultaneously Recorded with Spontaneous Activity in Fast-Spiking Interneurons Studied in Cortex-Striatum-Substantia Nigra Organotypic Cultures*.

Plotkin, J. L., Day, M., & Surmeier, D. J. (2011). Synaptically driven state transitions in distal dendrites of striatal spiny neurons. *Nature Neuroscience*, *14*(7), 881–888. https://doi.org/10.1038/nn.2848

Rafalovich, I. V., Melendez, A. E., Plotkin, J. L., Tanimura, A., Zhai, S., & Surmeier, D. J. (2015). Interneuronal Nitric Oxide Signaling Mediates Post-synaptic Long-Term Depression of Striatal Glutamatergic Synapses. *Cell Reports*. https://doi.org/10.1016/j.celrep.2015.10.015

Rall, W., Burke, R. E., Smith, T. G., Nelson, P. G., & Frank, K. (1967). Dendritic location of synapses and possible mechanisms for the monosynaptic EPSP in motoneurons. *Journal of Neurophysiology*, *30*(5), 1169–1193. https://doi.org/10.1152/jn.1967.30.5.1169

Ravel, S., Sardo, P., Legallet, E., & Apicella, P. (2006). Influence of spatial information on responses of tonically active neurons in the monkey striatum. *Journal of Neurophysiology*, *95*(5), 2975–2986. https://doi.org/10.1152/jn.01113.2005

Reig, R., & Silberberg, G. (2014). Multisensory Integration in the Mouse Striatum. *Neuron*, *83*(5), 1200–1212. https://doi.org/10.1016/j.neuron.2014.07.033

Reynolds, J. N. J., Hyland, B. I., & Wickens, J. R. (2004). Modulation of an afterhyperpolarization by the substantia nigra induces pauses in the tonic firing of striatal cholinergic interneurons. *Journal of Neuroscience*, *24*(44), 9870–9877. https://doi.org/10.1523/JNEUROSCI.3225-04.2004

Reynolds, J. N. J., & Wickens, J. R. (2004). The corticostriatal input to giant aspiny interneurons in the rat: A candidate pathway for synchronising the response to reward-related cues. *Brain Research*, *1011*(1), 115–128. https://doi.org/10.1016/j.brainres.2004.03.026

Rice, M. E., & Cragg, S. J. (2004). Nicotine amplifies reward-related dopamine signals in striatum. *Nature Neuroscience*, *7*(6), 583–584. https://doi.org/10.1038/nn1244

Rice, M. E., Patel, J. C., & Cragg, S. J. (2011). Dopamine release in the basal ganglia. *Neuroscience*, *198*, 112–137. https://doi.org/10.1016/j.neuroscience.2011.08.066

Rommelfanger, K. S., & Wichmann, T. (2010). Extrastriatal dopaminergic circuits of the basal ganglia. In *Frontiers in Neuroanatomy* (Issue OCT). https://doi.org/10.3389/fnana.2010.00139

Rosenbaum, D. M., Rasmussen, S. G. F., & Kobilka, B. K. (2009). The structure and function of G-protein-coupled receptors. In *Nature* (Vol. 459, Issue 7245, pp. 356–363). https://doi.org/10.1038/nature08144

Rudkin, T. M., & Sadikot, A. F. (1999). Thalamic input to parvalbumin-immunoreactive GABAergic interneurons: Organization in normal striatum and effect of neonatal decortication. *Neuroscience*, *88*(4), 1165–1175. https://doi.org/10.1016/S0306-4522(98)00265-6

Sadeghi, S., Ghaffari, F., Heydarirad, G., & Alizadeh, M. (2020). Galen's place in Avicenna's The Canon of Medicine: Respect, confirmation and criticism. In *Journal of Integrative Medicine* (Vol. 18, Issue 1, pp. 21–25). Elsevier (Singapore) Pte Ltd. https://doi.org/10.1016/j.joim.2019.11.002

Sammut, S., Dec, A., Mitchell, D., Linardakis, J., Ortiguela, M., & West, A. R. (2006). Phasic dopaminergic transmission increases NO efflux in the rat dorsal striatum via a neuronal NOS and a dopamine D1/5 receptor-dependent mechanism. *Neuropsychopharmacology*, *31*(3), 493–505. https://doi.org/10.1038/sj.npp.1300826

Sammut, S., Park, D. J., & West, A. R. (2007). Frontal cortical afferents facilitate striatal nitric oxide transmission in vivo via a NMDA receptor and neuronal NOS-dependent mechanism. *Journal of Neurochemistry*, *103*(3), 1145–1156. https://doi.org/10.1111/j.1471-4159.2007.04811.x

Sandberg, A., & Bostrom, N. (2008). Whole Brain Emulation: A Roadmap. Technical Report No. 2008-3. *Future of Humanity Institute, Oxford University, Oxford.*

Schultz, W. (1998). Predictive Reward Signal of Dopamine Neurons. *Journal of Neurophysiology*, *80*(1), 1–27. https://doi.org/10.1152/jn.1998.80.1.1

Scurlock, J., & Andersen, B. R. (2005). *Ancient Sources, Translations, and Modern Medical Analyses*. University of Illinois Press. http://www.jstor.org/stable/10.5406/j.ctt2ttfm5

Sharott, A., Doig, N. M., Mallet, N., & Magill, P. J. (2012). Relationships between the firing of identified striatal interneurons and spontaneous and driven cortical activities in vivo. *Journal of Neuroscience*, *32*(38), 13221–13236. https://doi.org/10.1523/JNEUROSCI.2440-12.2012

Shen, W., Tian, X., Day, M., Ulrich, S., Tkatch, T., Nathanson, N. M., & Surmeier, D. J. (2007). Cholinergic modulation of Kir2 channels selectively elevates dendritic excitability in striatopallidal neurons. *Nature Neuroscience*, *10*(11), 1458–1466. https://doi.org/10.1038/nn1972

Smith, J. B., Smith, Y., Venance, L., & Watson, G. D. R. (2022). Editorial: Thalamic Interactions With the Basal Ganglia: Thalamostriatal System and Beyond. In *Frontiers in Systems Neuroscience* (Vol. 16). Frontiers Media S.A. https://doi.org/10.3389/fnsys.2022.883094

Somogyi, P., Bolam, J. P., & Smith, A. D. (1981). Monosynaptic cortical input and local axon collaterals of identified striatonigral neurons. A light and electron microscopic study using the golgi-peroxidase transport-degeneration procedure. *Journal of Comparative Neurology*, *195*(4), 567–584. https://doi.org/https://doi.org/10.1002/cne.901950403

Song, W. J., Tkatch, T., Baranauskas, G., Ichinohe, N., Kitai, S. T., & Surmeier, D. J. (1998). Somatodendritic depolarization-activated potassium currents in rat neostriatal cholinergic interneurons are predominantly of the a type and attributable to coexpression of Kv4.2 and Kv4.1 subunits. *Journal of Neuroscience*, *18*(9), 3124–3137. https://doi.org/10.1523/jneurosci.18-09-03124.1998

Steiner, H., & Tseng, K. (2016). *Handbook of Basal Ganglia Structure and Function (2nd edition)* (H. Steiner & K. Tseng, Eds.). Elsevier.

Stern, G. (1989). Did Parkinsonism occur before 1817? *Journal of Neurology, Neurosurgery and Psychiatry*, *52*(SUPPL), 11–12. https://doi.org/10.1136/jnnp.52.Suppl.11

Sterratt, D., Graham, B., Gillies, A., & Willshaw, D. (2011). *Principles of Computational Modelling in Neuroscience*. Cambridge University Press. https://doi.org/DOI: 10.1017/CBO9780511975899

Stiefel, M., Shaner, A., & Schaefer, S. D. (2006). The Edwin Smith Papyrus: The birth of analytical thinking in medicine and otolaryngology. *Laryngoscope*, *116*(2), 182–188. https://doi.org/10.1097/01.mlg.0000191461.08542.a3

Straub, C., Saulnier, J. L., Bègue, A., Feng, D. D., Huang, K. W., & Sabatini, B. L. (2016). Principles of Synaptic Organization of GABAergic Interneurons in the Striatum. *Neuron*, *92*(1), 84–92. https://doi.org/10.1016/j.neuron.2016.09.007

Sullivan, M. A., Chen, H., & Morikawa, H. (2008). Recurrent inhibitory network among striatal cholinergic interneurons. *Journal of Neuroscience*, *28*(35), 8682–8690. https://doi.org/10.1523/JNEUROSCI.2411-08.2008

Surmeier, D. J., Graves, S. M., & Shen, W. (2014). Dopaminergic modulation of striatal networks in health and Parkinson's disease. *Current Opinion in Neurobiology*, *29*, 109–117. https://doi.org/10.1016/j.conb.2014.07.008

Suzuki, T., Miura, M., Nishimura, K., & Aosaki, T. (2001). Dopamine-dependent synaptic plasticity in the striatal cholinergic interneurons. *The Journal of Neuroscience : The Official Journal of the Society for Neuroscience*, *21*(17), 6492–6501. https://doi.org/21/17/6492 [pii]

Szydlowski, S. N., Pollak Dorocic, I., Planert, H., Carlén, M., Meletis, K., & Silberberg, G. (2013). Target selectivity of feedforward inhibition by striatal fast-spiking interneurons. *Journal of Neuroscience*, *33*(4), 1678–1683. https://doi.org/10.1523/JNEUROSCI.3572-12.2013

Tecuapetla, F., Jin, X., Lima, S. Q., & Costa, R. M. (2016). Complementary Contributions of Striatal Projection Pathways to Action Initiation and Execution. *Cell*, *166*(3). https://doi.org/10.1016/j.cell.2016.06.032

Tepper, J. M., Koós, T., Ibanez-Sandoval, O., Tecuapetla, F., Faust, T. W., & Assous, M. (2018). Heterogeneity and diversity of striatal GABAergic interneurons: Update 2018. *Frontiers in Neuroanatomy*, *12*(November), 1–14. https://doi.org/10.3389/fnana.2018.00091

Tepper, J. M., Tecuapetla, F., Koós, T., & Ibáñez-Sandoval, O. (2010). Heterogeneity and diversity of striatal GABAergic interneurons. In *Frontiers in Neuroanatomy* (Issue DEC). https://doi.org/10.3389/fnana.2010.00150

Threlfell, S., & Cragg, S. J. (2011). Dopamine signaling in dorsal versus ventral striatum: The dynamic role of cholinergic interneurons. *Frontiers in Systems Neuroscience*, *5*(MARCH 2011), 1–10. https://doi.org/10.3389/fnsys.2011.00011

Tokarska, A., & Silberberg, G. (2022). GABAergic interneurons expressing the α2 nicotinic receptor subunit are functionally integrated in the striatal microcircuit. *Cell reports*, *39*(8), 110842. https://doi.org/10.1016/j.celrep.2022.110842

Toledo-Rodriguez, M., El Manira, A., Wallén, P., Svirskis, G., & Hounsgaard, J. (2005). Cellular signalling properties in microcircuits. In *Trends in Neurosciences* (Vol. 28, Issue 10, pp. 534–540). https://doi.org/10.1016/j.tins.2005.08.001

Tozzi, A., De Iure, A., Di Filippo, M., Tantucci, M., Costa, C., Borsini, F., Ghiglieri, V., Giampà, C., Fusco, F. R., Picconi, B., & Calabresi, P. (2011). The distinct role of medium spiny neurons and cholinergic interneurons in the D2/A2A receptor interaction in the striatum: Implications for Parkinson's disease. *Journal of Neuroscience*, *31*(5), 1850–1862. https://doi.org/10.1523/JNEUROSCI.4082-10.2011

Tsodyks, M. V, & Markram, H. (1997). *The neural code between neocortical pyramidal neurons depends on neurotransmitter release probability* (Vol. 94). www.pnas.org.

Uchimura, N., Cherubini, E., & North, R. A. (1989). *Inward Rectification in Rat Nucleus Accumbens Neurons* (Vol. 62, Issue 6).

Undieh, A. S. (2010). Pharmacology of signaling induced by dopamine D1-like receptor activation. In *Pharmacology and Therapeutics* (Vol. 128, Issue 1, pp. 37–60). https://doi.org/10.1016/j.pharmthera.2010.05.003

Van Geit, W., Gevaert, M., Chindemi, G., Rössert, C., Courcol, J. D., Muller, E. B., Schürmann, F., Segev, I., & Markram, H. (2016a). BluePyOpt: Leveraging open source software and cloud infrastructure to optimise model parameters in neuroscience. *Frontiers in Neuroinformatics*, *10*(JUNE), 1–18. https://doi.org/10.3389/fninf.2016.00017

Van Geit, W., Gevaert, M., Chindemi, G., Rössert, C., Courcol, J. D., Muller, E. B., Schürmann, F., Segev, I., & Markram, H. (2016b). BluePyOpt: Leveraging open source software and cloud infrastructure to optimise model parameters in neuroscience. *Frontiers in Neuroinformatics*, *10*(JUNE). https://doi.org/10.3389/fninf.2016.00017

Verkhratsky, A., Krishtal, O. A., & Petersen, O. H. (2006). From Galvani to patch clamp: The development of electrophysiology. *Pflugers Archiv European Journal of Physiology*, *453*(3), 233–247. https://doi.org/10.1007/s00424-006-0169-z

Virk, M. S., Sagi, Y., Medrihan, L., Leung, J., Kaplitt, M. G., & Greengard, P. (2016). Opposing roles for serotonin in cholinergic neurons of the ventral and dorsal striatum. *Proceedings of the National Academy of Sciences of the United States of America*, *113*(3), 734–739. https://doi.org/10.1073/pnas.1524183113

Wang, Z., Kai, L., Day, M., Ronesi, J., Yin, H. H., Ding, J., Tkatch, T., Lovinger, D. M., & Surmeier, D. J. (2006). Dopaminergic Control of Corticostriatal Long-Term Synaptic Depression in Medium Spiny Neurons Is Mediated by Cholinergic Interneurons. *Neuron*, *50*(3), 443–452. https://doi.org/10.1016/j.neuron.2006.04.010

Wickens, A. P. (2014). *A History of the Brain: From Stone Age surgery to modern neuroscience* (1st ed.). Psychology Press.

Wilson, C. J. (1992). Chapter 6 - Dendritic Morphology, Inward Rectification, and the Functional Properties of Neostriatal Neurons. In T. MCKENNA, J. DAVIS, & S. F. ZORNETZER (Eds.), *Single Neuron Computation* (pp. 141–171). Academic Press. https://doi.org/https://doi.org/10.1016/B978-0-12-484815-3.50012-8

Wilson, C. J. (1995). Dynamic Modification of Dendritic Cable Properties and Synaptic Transmission by Voltage-Gated Potassium Channels. In *Journal of Computational Neuroscience* (Vol. 2). Kluwer Academic Publishers.

Wilson, C. J., & Goldberg, J. A. (2006). Origin of the slow afterhyperpolarization and slow rhythmic bursting in striatal cholinergic interneurons. *Journal of Neurophysiology*, *95*(1), 196–204. https://doi.org/10.1152/jn.00630.2005

Wilson, C. J., & Groves, P. M. (1980). Fine structure and synaptic connections of the common spiny neuron of the rat neostriatum: A study employing intracellular injection of horseradish peroxidase. *Journal of Comparative Neurology*, *194*(3), 599–615. https://doi.org/https://doi.org/10.1002/cne.901940308

Wu, Y. W., Kim, J. I., Tawfik, V. L., Lalchandani, R. R., Scherrer, G., & Ding, J. B. (2015). Input- and cell-type-specific endocannabinoid-dependent LTD in the striatum. *Cell Reports*, *10*(1), 75–87. https://doi.org/10.1016/j.celrep.2014.12.005

Yan, Z., Flores-Hernandez, J., & Surmeier, D. J. (2001). Coordinated expression of muscarinic receptor messenger RNAs in striatal medium spiny neurons. *Neuroscience*, *103*(4), 1017–1024. https://doi.org/10.1016/S0306-4522(01)00039-2

Yin, H. H., Knowlton, B. J., & Balleine, B. W. (2004). Lesions of dorsolateral striatum preserve outcome expectancy but disrupt habit formation in instrumental learning. *European Journal of Neuroscience*, *19*(1), 181–189. https://doi.org/https://doi.org/10.1111/j.1460-9568.2004.03095.x

Yin, H. H., Knowlton, B. J., & Balleine, B. W. (2006). Inactivation of the dorsolateral striatum enhances sensitivity to changes in the action-outcome contingency in instrumental conditioning. *Behavioural Brain Research*, *166*(2), 189–196. https://doi.org/10.1016/j.bbr.2005.07.012

Yin, H. H., Ostlund, S. B., Knowlton, B. J., & Balleine, B. W. (2005). The role of the dorsomedial striatum in instrumental conditioning. *European Journal of Neuroscience*, *22*(2), 513–523. https://doi.org/10.1111/j.1460-9568.2005.04218.x

Yttri, E. A., & Dudman, J. T. (2016). Opponent and bidirectional control of movement velocity in the basal ganglia. *Nature*, *533*(7603). https://doi.org/10.1038/nature17639

Yuste, R., & Tank, D. W. (1996). Dendritic Integration Review in Mammalian Neurons, a Century after Cajal. In *Neuron* (Vol. 16).

Zamponi, G. W., Striessnig, J., Koschak, A., & Dolphin, A. C. (2015). The physiology, pathology, and pharmacology of voltage-gated calcium channels and their future therapeutic potential. *Pharmacological Reviews*, *67*(4), 821–870. https://doi.org/10.1124/pr.114.009654

Zhang, Y. F., & Cragg, S. J. (2017). Pauses in striatal cholinergic interneurons: What is revealed by their common themes and variations? *Frontiers in Systems Neuroscience*, *11*(October), 1–8. https://doi.org/10.3389/fnsys.2017.00080

Zucca, S., Zucca, A., Nakano, T., Aoki, S., & Wickens, J. (2018). Pauses in cholinergic interneuron firing exert an inhibitory control on striatal output in vivo. *ELife*, *7*, 1–20. https://doi.org/10.7554/eLife.32510

# I rörelse

*Den mätta dagen, den är aldrig störst.*
*Den bästa dagen är en dag av törst.*

*Nog finns det mål och mening I vår färd –*
*men det är vägen, som är mödan värd.*

*Det bästa målet är en nattlång rast,*
*där elden tänds och brödet bryts I hast.*

*På ställen, där man sover blott en gång,*
*blir sömnen trygg och drömmen full av sång.*

*Bryt upp, bryt upp! Den nya dagen gryr.*
*Oändligt är vårt stora äventyr.*

av Karin Boye